THE UNIVERSITY *of* EDINBURGH

THE IN-PLANE FAILURE OF BRICKWORK

BY

W. SAMARASINGHE

(B.Sc. ENG)

DOCTOR OF PHILOSOPHY

UNIVERSITY OF EDINBURGH

1980

PREFACE

This thesis is the result of a three-year research work for the degree of doctor of philosophy in the Department of Civil Engineering and Building Science, University of Edinburgh since October 1977.

During this period three papers have been accepted for publication. The titles are as follows:

1. "The In-plane Failure of Masonry - An Overview" Co-authors A.W. Page and A.W. Hendry, A paper to be presented for the "Seventh International Symposium on Load Bearing Brickwork", November 1980.

2. "Strength of Brickwork Under Biaxial Stresses" Co-author A.W. Hendry, A paper to be presented for the "Seventh International Symposium on Load Bearing Brickwork", November 1980.

3. "On the Failure of Masonry Shear Walls" Co-authors A.W. Page and A.W. Hendry, International Journal of Masonry Construction, June 1980, Vol. 1, No. 2.

It is declared that the thesis has been composed by the author himself, and all the work and results in the thesis have been carried out and achieved solely by him under the supervision of Professor A.W. Hendry, unless otherwise stated.

Edinburgh, September 1980

W. Samarasinghe

ABSTRACT

This thesis presents the results of an experimental investigation into the strength of brickwork under biaxial tension-compression. Since there is insufficient experimental evidence available on the strength of brickwork under biaxial stress to explain the behaviour of brick masonry walls under in-plane loads, experiments were carried out on one-sixth scale model brickwork panels under uniform stress conditions. An idealized failure surface is suggested based on experimental results, and the effect of shear bond strength and tensile bond strength on the results is discussed.

An iterative plane stress finite element computer programme incorporating the above information is used to simulate the in-plane behaviour of brickwork. Brickwork is treated as an elastic, isotropic material with limited capacity when stressed in a state of biaxial tension-compression. The model reproduces the non-linear behaviour of masonry produced by progressive cracking. Shear wall tests have been used to test the validity of the analytical model. Sensitivity analysis of the elastic constants used in the model are performed to illustrate their influence on the calculated stresses.

The influence of the stress distribution on shear wall behaviour, and the derivation of a failure criterion for local failure in masonry shear walls, are described. This criterion, in terms of the vertical stress and shear stress at a point, has been derived for particular values of horizontal stress from the three dimensional surface mentioned above. The effect of the shape of the specimen, testing technique, and boundary conditions on the shear strength of masonry panels is discussed.

ACKNOWLEDGEMENT

The author is gratefully indebted to a number of persons and parties who have helped, criticised, financed, encouraged and typed during the three years of this project.

In particular, the author is grateful to the British Council (Technical Coorporation Training Department) and members of his family for their financial support and encouragement during the period of this research. Thanks are also due to the authorities in the University of Moratuwa, Sri-Lanka, for granting leave to continue this study. Special thanks are due to Professor D.S. Wijeyesekara, Dean of the Faculty of Engineering and Architecture, University of Moratuwa, Sri-Lanka, for his warm encouragement and understanding throughout the whole period of work.

To Professor A.W. Hendry, Head of the Department of Civil Engineering and Building Science, University of Edinburgh, the author owes very special thanks for his kindness, generosity, encouragement and invaluable advice on every occasion.

Dr. S.R. Davies (University of Edinburgh) and Dr. A.W. Page (University of Newcastle, Australia) are gratefully acknowledged for their constructive advice, suggestions and interest during the period of developing the computer model.

Within the Department of Civil Engineering and Building Science at the University of Edinburgh the author wishes to thank the technical staff for their help with the experiments and photography. Thanks are also due to Dr. B.P. Sinha and Dr. R. Royles and the past and present fellow post-graduate students for their help

on several occasions.

The British Ceramic Research Association is thanked for providing model bricks for the experimental programme.

Mrs. E. Wagner and Mr. and Mrs. W.H.R. Laird are deeply appreciated for reading the typed manuscript, and for their generosity, hospitality, kindness and encouragement during the author's stay in Edinburgh.

Finally the author is thankful to Miss Gillian Erskine and Mrs. Liz Paterson who turned tangled notes into a tidy typescript in a short time.

CONTENTS

LIST OF FIGURES

LIST OF TABLES

NOTATIONS

Each symbol used in the text is explained where it first appears. However, a summary of frequently used symbols is also presented below for convenience.

Note: (1) The following general terminology has been adopted:

{ } denotes a column vector

[ ] denotes a row vector, or rectangular or square matrix

$[\ ]^T$ denotes the transpose of a matrix or a column vector.

(2) The notation adopted in the computer programme is listed in Appendix C.

σ_1	Major principal stress
σ_2	Minor principal stress
σ_t	Principal tensile stress at failure
σ_n	Average compressive stress at the brick-mortar interface
σ_N	Stress normal to the brick-mortar interface
σ_{NB}	Normal stress at the bed joints
σ_{NP}	Normal stress at the perpend joints
σ_x, σ_y	Local stresses parallel to x and y directions (parallel to bed joints and perpendicular to bed joints respectively)
τ_o	Initial shear bond strength at the brick-mortar interface
τ	Local shear stress
τ_{av}	Average shear stress at the brick-mortar interface
t_o	Tensile bond strength at the brick-mortar interface
θ	Direction of σ_1 relative to the bed joint direction
f_c	Principal compressive stress
f_t	Principal tensile stress
f_m	Compressive strength of masonry
f_{td}	Diagonal tensile strength of brickwork
f_{bt}	Flexural tensile strength of brick unit

μ	Coefficient of friction
$\bar{X}$	mean
S.D.	Standard deviation
C. of V.	Coefficient of variation
u, v,	Displacements in x and y directions
2a,2b	Rectangular element length and height respectively
{c}	Displacement function coefficients
{t}	Element displacements
[Z]	Transformation relating displacement function coefficients to element displacements
$[Z_n]$	Transformation relating nodal displacement function coefficients
{n}	Nodal displacements for an element
[P]	Transformation relating nodal and element displacements
$\{\varepsilon\}$	Element strains
$\varepsilon_x, \varepsilon_y, \varepsilon_{xy}$	Strain in x and y directions and shear strain
[s]	Transformation relating element strains to element displacements
[B]	Transformation relating strains and nodal displacements
[D]	Constitute strain-stress matrix
E	Elastic Modulus
ν	Poisson's Ratio
$\{\sigma\}$	Element stress
{f}	Nodal forces
[K]	Element stiffness matrix
[k]	Structure stiffness matrix
W	Load applied normal to the bed joints for shear walls
P	Shearing load applied for shear walls
α	$\tan^{-1}(W/P)$

CHAPTER ONE : INTRODUCTION

Although masonry structures have a long history, masonry has not kept pace with the development of the structural use of other building materials which are being used today. It is only recently that masonry structures have been designed using engineering principles. In the early days of man, the design criterion was stability rather than the strength of the masonry, especially for walls resisting lateral loads. With this concept of structural design, the wall thickness became the critical parameter of a load bearing wall. However, recent development of structural use of brickwork has effectively exploited shear wall action to resist lateral loads and thereby the strength and deformation characteristics of brickwork have become much more significant.

There has been increasing interest during the last few decades in load bearing brickwork for non-framed multistorey construction, and for infill walls in steel or reinforced concrete frames to reduce side sway in tall structures. In the former, the mass of the walls and the weight of the floors they carry is not always sufficient to ensure stability against horizontal wind loading normal to the wall face. Hence, when the main load bearing walls of a constructional layout are disposed primarily in one direction, current practice is to provide secondary walls at right angles to the main walls, so that the resistance to wind loading in any direction can be made dependent on the shearing strength of some walls rather than on the bending strength which is relatively

weaker. When a structural frame with brickwork infill is subjected to loading in the direction of the plane of the frame, the shear strength of the brickwork makes an important contribution to the stiffness and the strength of the composite assembly. Therefore, the in-plane strength of brickwork subjected to multiaxial stresses plays an important role on the overall stability of a structure.

The in-plane strength of brick masonry can be categorized into specific cases such as compressive strength, tensile strength, shear strength, etc. Existing information has been obtained usually by a series of tests on brick assemblages arranged and loaded in a way appropriate to the particular aspect of behaviour under investigation. Failure theories have been proposed for individual aspects without any relation to each other. The principal aim of previous research has been to produce suitable design information for the formulation of codes of practice to allow prediction of wall capacities when considered as a complete unit, either acting as a load bearing element, or in conjunction with a structural frame. However, very little emphasis has been placed on the development of a fundamental theory of failure for brick masonry which could be applied to any case of in-plane loading.

A considerable proportion of previous research has been devoted to studies of the in-plane behaviour of brick masonry, with particular emphasis on the behaviour of shear walls which are frequently designed to withstand horizontal forces from wind loading in their own planes. These horizontal forces are accompanied by vertical forces (dead loads, etc) of different magnitudes. In a masonry building, walls loaded in this manner are also affected by surrounding structural elements. Hence, these assemblages

will be under normal stresses parallel and perpendicular to the bed joints as well as shearing stresses along the joints. In other words a state of biaxial stress is common.

Most experimental determinations of the strengths of material are based on uniaxial stress states. However, the general practical problem involves at least a biaxial if not a triaxial state of stress. It is known that strength in one direction is to some extent affected by the stress in the perpendicular direction. Therefore, for better understanding of the material behaviour, biaxial or triaxial strength is required.

The state of stress at any point within a solid can be specified in terms of three principal stresses: $\sigma_1, \sigma_2, \sigma_3$, where $\sigma_1 > \sigma_2 > \sigma_3$; i.e. maximum, intermediate, and least stresses, respectively. As far as in-plane behaviour is concerned the effect of σ_3 can be ignored. Therefore, the set of σ_1 and σ_2 values at which failure occurs in an element of a material can be represented by a point in σ_1, σ_2 space, and the totality of these points describes the failure curve.

$$f(\sigma_1, \sigma_2) = 0 \qquad (1.1)$$

Such a relation is called a criterion of failure. Essentially, experimental measurements under different conditions should provide the form of this curve.

Because masonry is an anisotropic material, the elastic properties and strength characteristics will vary with the stress orientation relative to the bed and perpend joints planes. Therefore failure theories for isotropic materials, used currently for masonry[6 68 80 82], are not applicable since the direction of

stress has no significance on the strength properties of isotropic material.

The development of a failure criterion for brickwork is thus made more difficult by the presence of mortar joints acting as planes of weakness. The failure of brick masonry cannot be defined simply in terms of principal stresses at any point. The influence of a third variable, the bed joint orientation relative to the principal stresses, must also be considered. Thus, completely to define masonry failure a three dimensional failure surface in terms of the principal stresses σ_1 and σ_2, and their respective orientations to the bed joint θ and $90 + \theta$ is required. Hence, the stress state at a local failure point of a masonry wall subjected to any sort of in-plane loads would represent a particular point on this $(\sigma_1, \sigma_2, \theta)$ surface.

Information about the variation of the strength and deformation characteristics of brick masonry with the variation of the stress orientation is not yet documented in the masonry literature, in order to define a general failure surface. The present investigation is an attempt to define this surface under the conditions that will be stated. This will enable one to predict the initiation of failure of brick panels subjected to in-plane loads.

Brick walls subjected to in-plane loads are mostly under a stress state of biaxial tension-compression and/or biaxial compression-compression, whereas biaxial tension-tension stress state may not occur in a general practical problem. Brickwork is generally regarded as a brittle material. Brittle materials are usually

weaker in biaxial tension-compression stress state than in biaxial compression-compression. Therefore initiation of failure of an assemblage is always created in an area where the biaxial tension-compression stress state dominates, unless the whole wall is under biaxial compression. Hence, the present investigation is confined to defining a failure surface for brick masonry in terms of principal tensile stress (σ_1), principal compressive stress (σ_2), and the inclination of σ_1 relative to the bed joint direction (θ).

To start with, a series of tests were performed on brickwork panels (150 mm wide x 150 mm high x 18 mm thick) manufactured from one-sixth scale clay bricks and 1:0.25:3 (cement:sand:lime) mortar. A uniform biaxial stress field was induced in the panels by applying compressive and tensile loads in two normal directions. The angle between the bed joint and the principal tensile stress was varied by sawing large test samples, at the required orientation. Tests were performed for varying ratios of principal stresses and values of θ of 0^o, 22.5^o, 45^o, 67.5^o and 90^o. An idealized surface was derived from the experimental results and the influence of shear bond strength and tensile bond strength on the shape of the failure surface is discussed.

The adequacy of the failure surface obtained under uniform biaxial stress field to predict the failure of a brick wall subjected to non-uniform biaxial tension-compression stress field was verified using shear walls. The biaxial failure surface is incorporated into an iterative finite element computer program. The theoretical model developed is capable of simulating the non-

linearity due to progressive cracking but, the non-linearity in the constitutive laws are ignored. The analytical results have been verified with shear wall tests. The shear walls were manufactured with the same brick and mortar and the test condition was designed to give rise to different biaxial stress fields under varying combinations of shear and compressive loads. Sensitivity analysis of the elastic constants used in theoretical model have also been carried out in relation to the verification tests.

The analytical model is used to study the parameters influencing shear strength of brick masonry. Usually, shear wall test results are presented as a relationship between the average shear stress and the average vertical compressive stress at the bed joints at failure, and it is implicitly assumed that the failure load is not sensitive to the local stress distribution. In this investigation it will be shown that this can be misleading if account is not taken of the influence of local stresses in initial failure in critical regions of the panel. The stress state in these regions can be markedly influenced by the method of load application, the wall geometry and the support conditions at the boundaries of the panel.

A summary of the thesis is as follows:

(i) A review of previous research on brick masonry with particular emphasis on areas significant to this study (Chapter 2)

(ii) Experimental Study: on the material properties, biaxial strength (tension-compression) of brickwork under uniform biaxial stress field, and on the shear walls (Chapters 3 and 4).

(iii) The development of a suitable analytical model and the comparison of shear wall test results, with the theoretical results (Chapter 5).

(iv) A study of the shear wall behaviour with particular emphasis to the influence of local stress distribution on the shear strength (Chapter 6).

(v) Summary and conclusions (Chapter 7).

CHAPTER TWO : REVIEW OF IN-PLANE BEHAVIOUR OF BRICKWORK

2.1 INTRODUCTION

In recent years there has been a marked increase in structural masonry research. Variables affecting brick masonry strength are numerous and have been studied to a great extent. A considerable portion of this research has taken place in the area of in-plane behaviour of masonry, on complete wall panels at full or model scale or, in tests on small samples of masonry to simulate the local stress state in large panels.

The main aim of this research has been to produce suitable design guidance for the codes of practice, based on empirical relationships. For example, a large amount of research has been carried out on shear walls subjected to varying combinations of shear and compressive loads, and the failure envelope is presented as a relationship between average shear stress and average normal stress acting at the bed joints. However, a large scatter of results has been observed among different investigators. Therefore, fairly high safety factors have been used in formulating the design codes. However, all these results should lie on one general failure surface which takes into account all the possible variables. Very little emphasis has been placed, up to date, on the development of a fundamental theory of failure of masonry which could be applied to any case of in-plane loading.

A general failure surface which can be used to predict the failure of brick masonry under biaxial tension-compression stress state, in terms of principal stresses and their inclination to the bed joints has been presented in this investigation. This chapter summarizes previous research on the in-plane failure of masonry which could be related to the above generalized failure surface. The discussion is confined to in-plane failure, with particular emphasis on the compressive strength, tensile strength and shear strength of masonry.

2.2 ANISOTROPIC NATURE OF BRICKWORK

Masonry exhibits distinct directional properties due to the influence of the mortar joints. Depending upon the orientation of the joints to the applied stresses, failure can occur in the joints alone, or in some form of combined mechanism involving the mortar and the masonry unit.

Researchers have long been aware of the significance of the bed joint angle to the applied load. In 1963, Johnson and Thompson [31] carried out diametral compression tests on brick masonry discs to produce indirect tensile stresses on joints inclined at various angles to the vertical compressive load. Differences in failure patterns and strength of the specimens were evident with the discs bed joints at various angles. The highest strength of the masonry was observed when the compressive load was perpendicular to the bed joints or when the principal tensile stress at the

centre of the disc was parallel to the bed joints, the failure occurring through birkcs and perpend joints. The lowest strength was observed when the compressive load was parallel to the bed joints or when the principal tensile stress at the centre of the disc was perpendicular to the bed joints. In this case fracture occurred along the interface of brick and mortar joint. Similar tests have been recently reported by Drysdale et al.[14] on hexagonal masonry discs.

The influence of bed joint orientation on the strength of masonry has also been illustrated by many investigors [1 4 7 15 47 50 56 82] by tests carried out on samples under uniaxial compression. The uniaxial compressive loads were typically applied to prisms or piers of masonry with the bed joints oriented at varying angles to the applied load. The load carrying capacity, and the failure mode, were critically dependent upon this angle.

Therefore, the anisotropic characteristic of masonry material is evident. Hence, failure theories for isotropic materials, used currently for masonry [6 68 82], are not applicable.

2.3 FAILURE OF MASONRY IN TERMS OF PRINCIPAL STRESSES

There have been few attempts to obtain a general failure criterion for masonry subjected to in-plane loads due to the difficulty in developing a representative biaxial tests and the large number of tests required. However, the problem has been quantitatively discussed by some research workers.

In 1971, in an attempt to explain the behaviour of shear walls, Chinwah [7] hypothesised that the diagonal tensile failure through brick and mortar is due to critical combinations of biaxial stresses (tension-compression). This was examined by plotting the stress path for the loading history of the wall up to failure using elastic finite element analysis. The principal tensile stress was plotted against the principal compressive stress using a computer plotter for different points on the wall which was referred to as the tensile stress path. It was observed that the critical principal tensile stress value (σ_t) varies with the precompression applied normal to the bed joints (σ_n). An increase in σ_t with increase in σ_n has been reported. A probable strength envelope was obtained by drawing a line through critical stress points, tangential to the stress paths for three different precompression values, and a general relationship was established between the principal tensile strength at failure (σ_t) and the corresponding normal stress at the bed joints. This can be expressed in the form:

$$\sigma_t = K \sigma_n + \sigma_{to} \qquad (2.1)$$

where K is a constant and σ_{to} is the value of the principal tensile stress at failure when $\sigma_n = 0$. A similar relationship has been reported by Schneider et al [60] from shear wall tests.

In 1976, Yokel and Fattal [82] investigated the applicability of a biaxial failure criterion to propose a failure hypothesis for brick masonry under combined stresses. The investigation

was carried out with reference to in-plane tests on brick panels subjected to combined shear and compression. A biaxial stress failure criterion for the stress range of tension-compression was uniquely defined by two points; one corresponding to the state of stress at failure under vertical compressive load ($\sigma_1 = 0$, $\sigma_2 = f_m$, f_m = uniaxial compressive strength) and the other corresponding to the state of stress at failure under a diagonal load as shown in Figure 2.1. A linear strength envelope was assumed and the tensile strength was defined as the apparent major stress at failure when the principal compressive was zero. Mohr's theory of failure for isotropic materials was considered in their investigation.

They found that reasonable prediction of the splitting type failure was obtained from a criterion based on a critical combination of normal principal stresses although the direction of the principal stresses made with the bed joint direction has been ignored in the failure criterion. Within the same range, load capacity was overestimated by the hypothesis that failure occurs when the critical principal tensile stress is exceeded, and underestimated by the hypothesis that failure occurs at a critical value of tensile strain. However, the authors stated that for a more general application of their hypothesis, the directional variation of the splitting strength should be considered,so that

$$\sigma_1 = f(\sigma_2, \theta) \qquad (2.2)$$

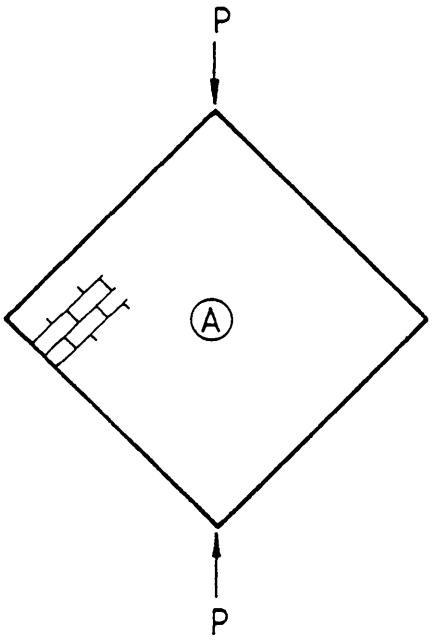

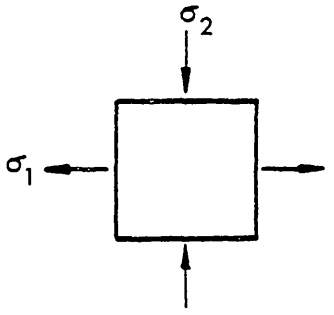

Stresses on Element A

$\sigma_1 = 0.7336\ \bar{\tau}$

$\sigma_2 = 2.380\ \bar{\tau}$

$\bar{\tau} = 0.707\ P/A$

A = sectional area of wall parallel to bed joints

DIAGONAL TENSION TEST

FIGURE 2.1

where σ_1 and σ_2 are the principal stresses (tensile and compressive respectively) at failure, and θ is the angle between the principal tensile stress and the bed joint.

The importance of a biaxial failure envelope to predict the strength of shear walls subjected to combined compression and racking shear was discussed qualititatively by Hendry [27] in 1978. Due to insufficient information available to define the failure surface, he extended the relationship obtained by Chinwah [7] and Schneider [60] to predict the shear strengths of brick masonry, which will be discussed later in this chapter.

A failure surface for brick masonry in the tension-tension principal stress region has been recently derived by Page [52] using an analytical approach. Biaxial tests were simulated, using an iterative finite element computer program which modelled bricks and joints separately and was capable of simulating a collapse mechanism after the progressive failure of a number of joints. The shear bond strength and tensile bond strength of the brickwork studied were 0.24 N/mm^2 and 0.29 N/mm^2 respectively. The theoretical model used in this investigation will be briefly described in Chapter 5. The resulting surface, shown in Figure 2.2 is a function of the principal stress ratio at any point and the inclination of the principal stresses to the bed jointing plane. The author has concluded that the failure surface is critically dependent upon the relationship between the shear and tensile bond strength of the masonry assemblage, and its influence must be considered in deriving a general failure surface since this

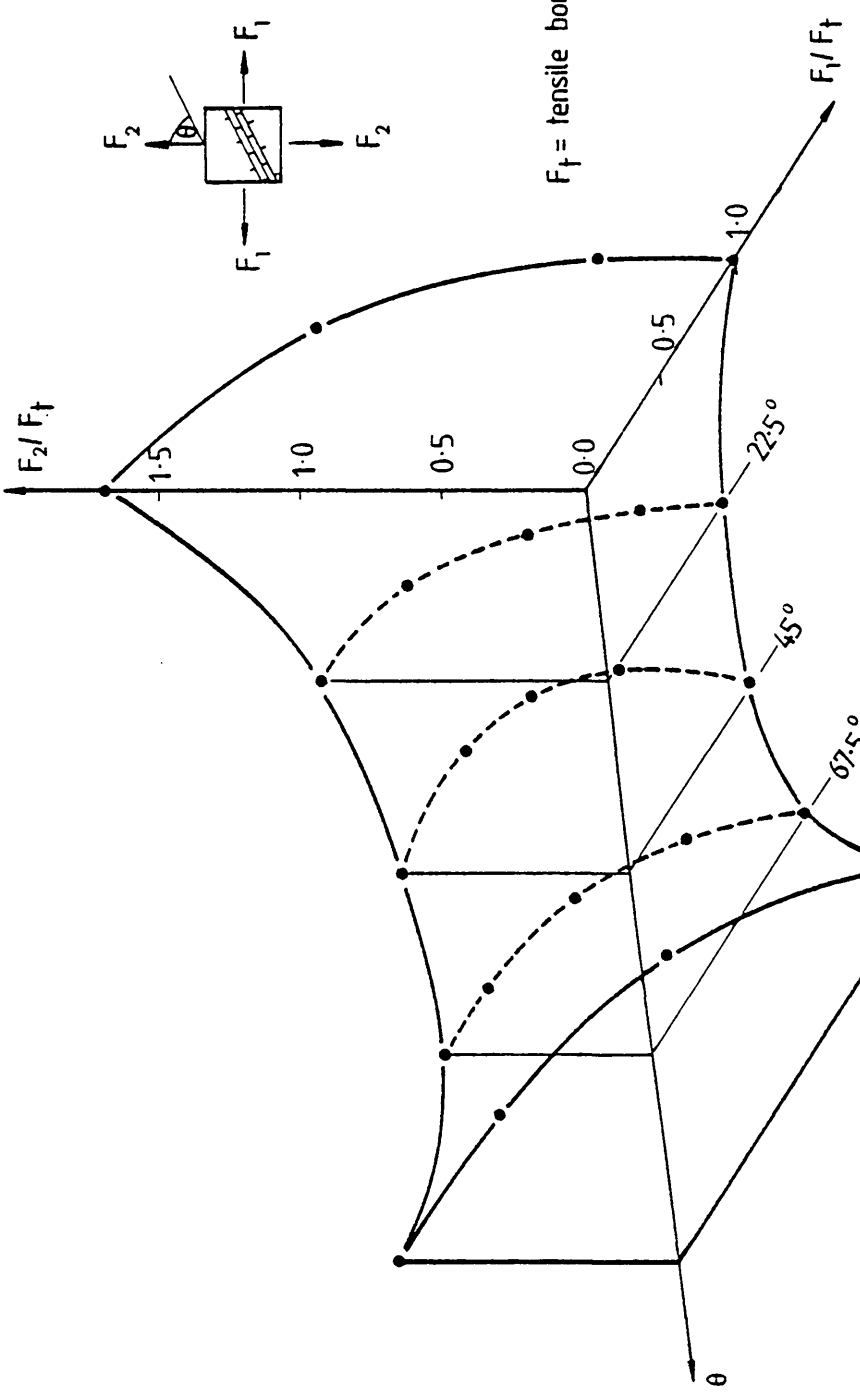

BIAXIAL (TENSION-TENSION) FAILURE CRITERION

FIGURE 2.2

relationship varies with different brick-mortar combination. However, this approach could not be extended to derive a failure surface for the tension-compression range and compression-compression ragne since the model was not capable of predicting brick failure.

No experimental or theoretical investigations of the compression-compression principal stress range have been reported, despite the fact that this region can play a significant role in masonry failure.

2.4 SPECIFIC CASES COVERED BY A BIAXIAL STRENGTH ENVELOPE

2.4.1 Failure of masonry under uniaxial load normal to the bed joint

The behaviour of brickwork under uniaxial compression is obviously influenced by the properties of its components. Despite the fact that the bricks and mortar have different deformation characteristics, brickwork properties are usually described in terms of the average behaviour of the composite material.

The tensile splitting of masonry assemblages under uniaxial compression is caused by the differing strain characteristics of the brick and mortar. Generally the brick unit is stiffer than mortar and hence free lateral expansion of mortar under compression is greater than that of brick. Because the masonry unit at the mortar interface must undergo the same lateral expansion as the mortar, due to friction, bond, etc., the lateral expansion of mortar is restrained, producing a triaxial compressive stress

state in the mortar and a biaxial tensile stress and vertical compressive stress in the brick. The lateral tensile stress produced will eventually cause failure in the brittle brick.

Analytical attempts have been made by Hilsdorf [29] and Francis et al [16] to describe and predict this behaviour by considering the interaction of the strength properties of brick and mortar in appropriate complex stress states. The lack of failure criterion for brick and mortar under this triaxial stress state was one of the major difficulties encountered in these investigations. Later, Khoo and Hendry [34 35] extended this work for brick masonry by experimentally evaluating the strength properties of brick and mortar under the relevent conditions of applied stresses.

The parameters influencing the strength of masonry such as brick and mortar properties, dimensional variations and slenderness ratio have been comprehensively reviewed [16 19 37 56]. Multiple wythe masonry is said to be somewhat weaker than single wythe masonry [19]. It has been analytically and experimentally shown [16 20 34] that increasing joint thickness is accompanied by a decrease in brickwork strength. Francis et al. [16] have observed a greater loss of strength with increase in joint thickness for perforated bricks compared with solid bricks. This has been explained as the greater weakness in lateral tensile strength in the perforated bricks caused by the presence of holes.

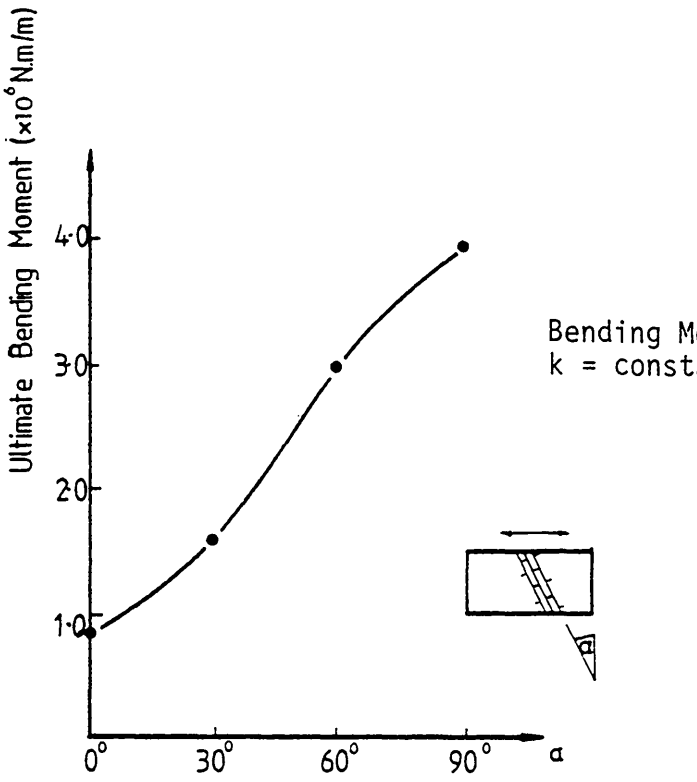

VARIATION OF FLEXURAL STRENGTH (f_b) WITH BED JOINT ANGLE

FIGURE 2.3

2.4.2 Tensile strength of brickwork

The tensile strength of brickwork, although not as extensively studied as the compressive strength test, is equally important. One of the major difficulties faced by the investigators is the development of test techniques that determine properties appropriate for the analysis of larger wall elements that fail in tension.

A large number of investigations [4] [48] [55] [63] [64] have been carried out to determine the tensile bond strength between brick and mortar using brick-mortar complets. It has been shown that the moisture content of the brick at the time of laying for a given type of mortar and brick, has a great influence on the tensile bond strength [7] [64].

Tests on full scale brickwork panel beams have been carried out by Losberg and Johansson [38] to study the influence of the bed joint direction to the spanning direction on the flexural tensile strength. The panels were simply supported and loaded at the one-quarter points. An increase in tensile strength with increasing α (see Figure 2.3) has been observed and the results are summarized in Figure 2.3. A similar trend has been reported by McKeague [41] as well. Although this is not the in-plane tensile strength of brickwork, it gives some indication about the influence of bed joint angle on the tensile strength.

Because of its significance for the structural behaviour, numerous studies on the diagonal tensile strength of masonry have been carried out. Few investigators [8] [68] [80] have considered the diagonal tension capacity, f_{td}, to be a constant

value directly proportional to the square root of the compressive strength of masonry, f_m, as follows:

$$f_{td} = R \sqrt{f_m} \qquad (2.3)$$

Square panels and circular discs have been tested to establish, experimentally, the proportional constant, R; for brickwork, R values ranging from 2.5 to 4.5 have been reported [8]. Based on a linear finite element analysis of the circular masonry disc used in the diametral test procedure, for the case of the bed joint at 45^{o} degrees to the line of load application, Stafford Smith et al.[73] concluded that the diagonal tensile strength of brickwork is approximately equal to the tensile strength of the mortar or the tensile strength of the brick, whichever is lesser.

In both diagonally loaded circular discs and square panels the failure takes place along the loaded diagonal. According to the elastic analysis, most of the area of the specimen is under a state of biaxial tension-compression, and at the centre $\sigma_1:\sigma_2 = 1:3$. Therefore the diagonal tensile strength obtained under this condition gives one point on the $(\sigma_1,\sigma_2,\theta)$ general failure surface but, does not give the overall diagonal tensile strength of brickwork.

2.4.3 Failure of masonry shear walls

Many investigations have been carried out on shear wall behaviour, and a large number of these have been full or model scale tests on wall panels [4 7 8 18 26 28 40 42 46 54 59 60 61 62 68 80 83]. A criterion for shear failure of a joint has been

reported in terms of average normal stress and average shear stress at the brick-mortar interface. It assumes that the joint resistance is attributed to the initial bond strength between the mortar and the masonry units and to the frictional resistance which is said to be proportional to the compressive stress normal to the bed joint. This criterion can be formulated as:

$$\tau_{av} = \tau_o + \mu\sigma_n \qquad (2.4)$$

where τ = the average shear stress at failure

τ_o = the average shear stress at failure when $\sigma_n = 0$

σ_n = the average compressive stress normal to the bed joint

and μ = a coefficient attributed to friction.

Since this criterion has been formulated in average stresses, it is implicitly assumed that the failure load is not sensitive to the shear stress distribution. Also, it is not contemplated that this formulation would be applicable to failure modes other than mortar joint failure.

The values of τ_o and μ vary considerably and are influenced by such things as the properties of the components and the form of the test. Typical values are summarized by Sahlin [56], Hendry [27], Schneider [60] and Grimm [19]. It has been reported [73], that the values of μ appear to decrease for similar brick and mortar specimens with increasing normal compressive stresses. Hence, in order to support the friction theory, it has been necessary to adopt an average value of μ. However the equation (2.4) has been used, as an empirical expression, to

predict the shear strength in brick masonry panels reasonably well, where the failure is predominant in masonry joints. This corresponds to the practical range of compression found in shear walls, up to, say, 2.0 N/mm^2. Stafford Smith et al. [73] questioned this criterion of failure and has suggested that shear failure may be due to tensile failure in the mortar.

As the degree of compression increases, the failure mode changes from joint failure to brick-joint failure. Yorulmaz and Atan [83] obtained the average shear and normal stress envelope for the whole range of compressive stress up to uniaxial compressive strength using racking tests on half scale walls. Theories for predicting failure in this region have been postulated by Yokel and Fattal [82] and Mann and Muller [40]. Yokel and Fattal have assumed that there is no redistribution of stresses before the failure, in shear walls, and that the most critical condition always occurs at or near the centre of the panel. Their theoretical results tallied with experimental results obtained on square panels but, the applicability of those conditions to rectangular panels with different wall lengths is questionable. Mann and Muller assumed that there is no shear transfer through perpend joints, but this is a matter of speculation.

An alternative method of predicting failure of brickwork to that based on the Coulomb type of relationship, has been proposed by Hendry [27] as an extension of the work of Turnsek and Cacovic [80], Chinwah [7], and Schneider et al [60]. He found that a wide variety of tests on brickwork loaded in combined

shear and compression were consistent with the relationship

$$\frac{\tau_{av}}{\sigma_t} = \sqrt{1 + \frac{\sigma_n}{\sigma_t}} \qquad (2.5)$$

where σ_t = principal tensile stress at failure.

From the results obtained by Chinwah and Schneider et al., he proposed that the principal tensile strength at failure was a function of average normal stress at the bed joints (σ_n), in the form:

$$\sigma_t = \sigma_{to} + 0.05\ \sigma_n \qquad (2.6)$$

where σ_{to} is the value of σ_t at failure when $\sigma_n = 0$, this being equal to the ultimate shear stress, τ_o, in a pure shear condition. From equations (2.5) and (2.6) the following empirical expression for shear strength has been proposed.

$$\tau_{av}^2 = (\tau_o^2 + 1.1\ \tau_o\ \sigma_n + 0.053\ \sigma_n) \qquad (2.7)$$

The advantage of this relationship in practice is that it requires knowledge of only one parameter, τ_o, the shear strength at zero compression. The author pointed out that this could be determined by a simple brickwork triplet test, which is cheap and easy to make, thus avoiding the need of elaborate testing apparatus.

2.5 CONCLUSIONS

This chapter summarizes the previous research on brickwork subjected to in-plane loads, with particular emphasis on the compressive strength, tensile strength and shear strength of masonry. It can be seen that there are many areas in which knowledge is lacking, particularly with regard to the fundamental behaviour of brickwork. Most previous research has been directed towards the study of average wall behaviour and the estimation of ultimate loads to allow the preparation of suitable design codes.

Masonry exhibits distinct directional properties due to the influence of mortar joints acting as planes of weakness. To completely define its in-plane failure, a surface in terms of the principal stresses and their inclination to the bed joints is required. Failure of masonry under uniaxial loading or a combination of shear and compressive load, or under a diagonal load represents particular points on this general failure surface.

CHAPTER THREE : EXPERIMENTAL STUDY : MATERIAL PROPERTIES

3.1 INTRODUCTION

The existence of a masonry structure depends not only on the form of the structure but ultimately on the properties of individual units and jointing material. It is therefore, necessary to determine the characteristics of the materials involved before considering the structural behaviour of the material in a structural element.

The properties of brickwork are influenced by variables such as type and physical properties of bricks, type of mortar, physical properties of the sand and lime used for the mortar, state of the bricks before laying, curing, workmanship etc. In order to keep the scope of this investigation within reasonable limits, the materials used were kept constant, and the properties of the component masonry materials are documented in this Chapter.

3.2 PROPERTIES OF BRICKS

The bricks employed in this investigation were one-sixth scale model clay bricks produced by the British Ceramic Research Association, Stoke-on-Trent. The dimensions of the bricks used are given in Table 3.1 and, to scale are in accordance with B.S. 3921.

3.2.1 Compressive Strength of Bricks

There is no universally accepted method of testing the brick units to determine the compressive strength of material as an

Parameter	Brick Dimension			No of bricks used
	$\bar{x}$(mm)	S.D.	C. of V.	
Length	37.50	0.005	0.013	12
Breadth	18.04	0.003	0.016	12
Depth	12.51	0.004	0.032	12

$\bar{x}$ = mean, S.D. = standard deviation, C. of V. = coefficient of variation

Table 3.1: Dimensions of Bricks

absolute value. The recommended methods available provide only a measure or a 'standard' indicator for the compressive strength which is useful for quality control. To obtain the true uniaxial compressive strength more elaborate testing technique such as 'brush platens' [36,48,78] can be used to overcome the effect of geometry of the specimen and the problem of end restraint.

The compressive strength quoted in Table 3.2 were evaluated using the standard code[87] procedure. This involved loading a sixth scale brick in compression with the brick located between the testing machine platens in the same manner as in a wall.

3.2.2 Tensile Strength of Bricks

Since brick is a brittle material, the stress field developed by different test techniques is very sensitive to the ultimate tensile strength. Apparently, there is no universal method or standard test available to determine the brick tensile strength. In this investigation, two different techniques were adopted. The detailed results of the tests are given in Appendix A.

Physical Property	$\bar{x}$	S.D.	C. of V.	No of bricks used
Compressive Strength (N/mm^2)	30.5	1.53	5.01	10
Tensile Strength (N/mm^2) (Axial Tension)	2.2	0.18	8.1	10
Tensile Strength (N/mm^2) (Flexural Tension)	6.27	0.5	8.0	10

$\bar{x}$ = mean, S.D. = standard deviation, C. of V. = coefficient of variation

Water Absorption of Bricks

% by weight after 24 hrs. immersion = 12.5

% by weight after 5 hrs. boiling = 13.0

saturation coefficient = 0.96

Table 3.2: Physical Properties of Bricks

(a) Axial Tension

The brick units were tested in axial tension using the Instron machine as shown in Figure 3.1(a). The brick unit glued with Rapid Hardening Araldite to the steel platens through which tensile load was applied. The test results are shown in Table 3.2.

(b) Flexural Tension

The tensile strength of the brick was determined by a flexural

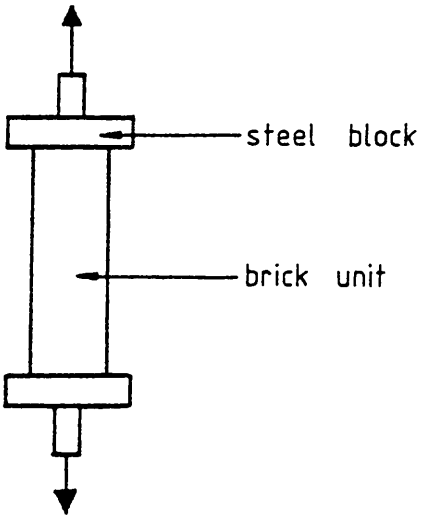

(a) A brick unit under axial tension

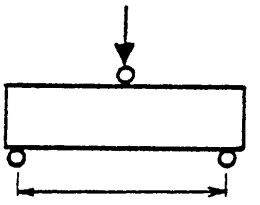

(b) A brick unit under flexural tension

TESTING OF BRICKS IN TENSION

FIGURE 3.1

test carried out on single brick with a line load applied perpendicular to the bedding planes as shown in Figure 3.1(b). The flexural tensile strength (f_{bt}) was calculated using the expression:

$$f_{bt} = 1.5 \frac{WL}{bd^2} \qquad (3.1)$$

The test results are given in Table 3.2.

3.2.3 Water Absorption of Bricks

The strength of brickwork is greatly influenced by the water absorption of bricks. Therefore a knowledge of brick suction is essential in choosing a suitable brick-mortar combination.

The percentages of absorption were calculated by immersing oven dried bricks in water for different time intervals. The relationship between the water absorption and the immersion time is illustrated in graphical form in Figure 3.2. The 5 hours boiling test results are given in Table 3.2.

3.3 MORTAR PROPERTIES

A mortar mix of 1:¼:3 (cement:lime:sand) was used throughout this investigation.

CEMENT : Ordinary Portland cement

LIME : White powdered hydrated lime

SAND : Finely graded sand suitable for scaled mortar joints. The grading of the sand used is illustrated in Appendix A.

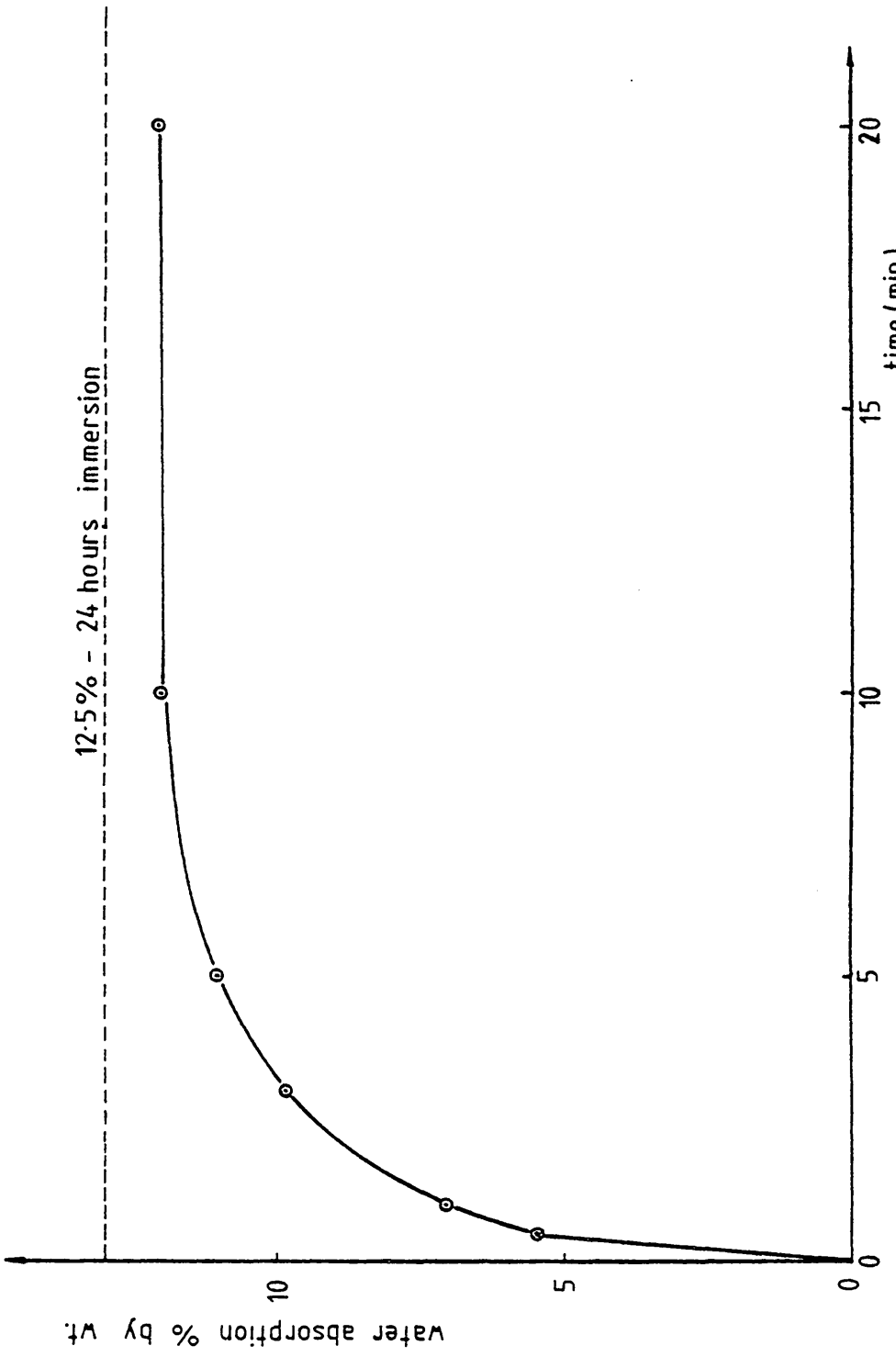

WATER ABSORPTION OF BRICKS

FIGURE 3.2

The water/cement ratio for the mortar mix was 0.90, and it was decided by the bricklayer so that it was workable enough for the model brickwork construction.

3.3.1 Compressive Strength of Mortar

Crushing strength, mainly for quality control purposes, was determined by 25 mm cube compression tests.

crushing strength of mortar	=	9.6 N/mm^2
standard deviation	=	0.3
number of cubes tested	=	12
coefficient of variation	=	3.1

3.4 PROPERTIES OF BRICKWORK

All the brick masonary walls for the test programme were constructed by an experienced bricklayer and the details of construction will be discussed in Chapter 4.

3.4.1 Scale Effect of Model Brickwork

The preparation and handling of specimens for biaxial tests is rather difficult with full scale specimens. Sixth scale brickwork has been adopted throughout this investigation to allow significant reductions in both the overall size of brickwork panels and the magnitude of the ultimate loads. Consequently, all tests required to define a suitable failure criterion can be performed in the Instron machine with a small test rig to apply the compressive load to the test specimen.

A large number of investigations[25,43,46,48,64] have been carried out to investigate the scale effects in model walls. Murthy[43] in 1964 used $^1/_3$ and $^1/_6$ scale model brickwork to study the behaviour of piers, couplets and more complex masonry structures. He found it was possible to reproduce the strength of full size brickwork for given strengths of brick and mortar, provided the thickness of mortar joints was scaled down, and the strength of 25 mm cubes of mortar was adopted in place of the 70 mm cubes used in full scale tests.

However, any differences due to scale effects will certainly be no more significant than the random effects of material variability, and the variations in workmanship.

3.4.2 Elastic Properties of Brickwork

The elastic modulus and Poisson's Ratio for brickwork were obtained from uniaxial compression tests on square panels. The aim of these tests was to determine the influence of the inclination of bedding planes to the direction of loading on the elastic properties of brickwork. The typical loading condition is shown in Figure 3.3.

Five wall panels with different bed joint orientation to the loading direction {$(90-\theta) = 0^o$, 22.5^o, 45^o, 67.5^o and 90^o} were selected for this investigation. The panels were typically 150 mm high x 150 mm wide x 18 mm thick.

The panels were uniaxially loaded in the Instron machine at 28 days after construction. Longitudinal and lateral strains were measured on a central 50 mm gauge length using a 50 mm demec gauge on both sides of the panel. These readings were averaged to eliminate bending effects.

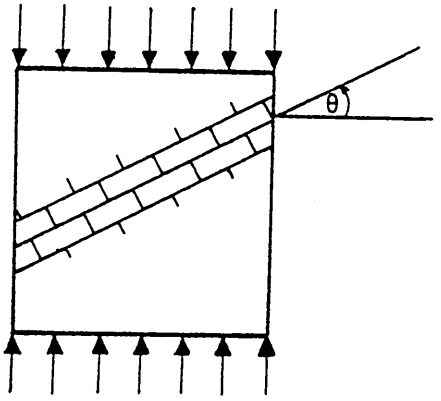

UNIAXIAL COMPRESSION TEST

ON BRICKWORK PANELS

FIGURE 3.3

The mean stress-strain curve obtained for each set of panels (by averaging the strain readings at each stress level) is shown in Figure 3.4. Detailed results may be found in Appendix A. The curves for each bed joint orientation is non-linear in nature characetised by a linear portion at the start. It is evident that the bed joint orientation to the applied load has a marked effect on the elastic properties of brickwork.

A plot of longitudinal versus lateral strain for the panels is shown in Figure 3.5. Each curve represents average results of two tests. The detailed results are available in Appendix A. If the slope of the curves are taken as Poisson's Ratio, it can be seen that its value increases with stress level. The Poisson's Ratio varies with the bed joint angle relative to the direction of the applied load. At very low stress levels, it appears that it is approximately the same for both $\theta = 0^{o}$ and 90^{o}.

The Poisson's Ratio values were calculated at zero vertical stress level for each bed joint orientation and tabulated in Table 3.3. The modules of elasticity (tanget modulus) for each panel obtained at the zero stress level is also presented in Table 3.3. A large scatter of results is evident.

Chinwah[7] carried out similar tests to find out the influence of the direction of bedding planes to the applied load on the elastic properties of brickwork. The strain measurements were taken on sixth scale brick masonry panels using wire strain gauges. His results are given in Table 3.4. It appears that the elastic modulus is insensitive to the bed joint direction and this seems to conflict with the author's results. However, the wire strain gauges cannot be used to measure strains in sixth scale model brickwork successfully because, the

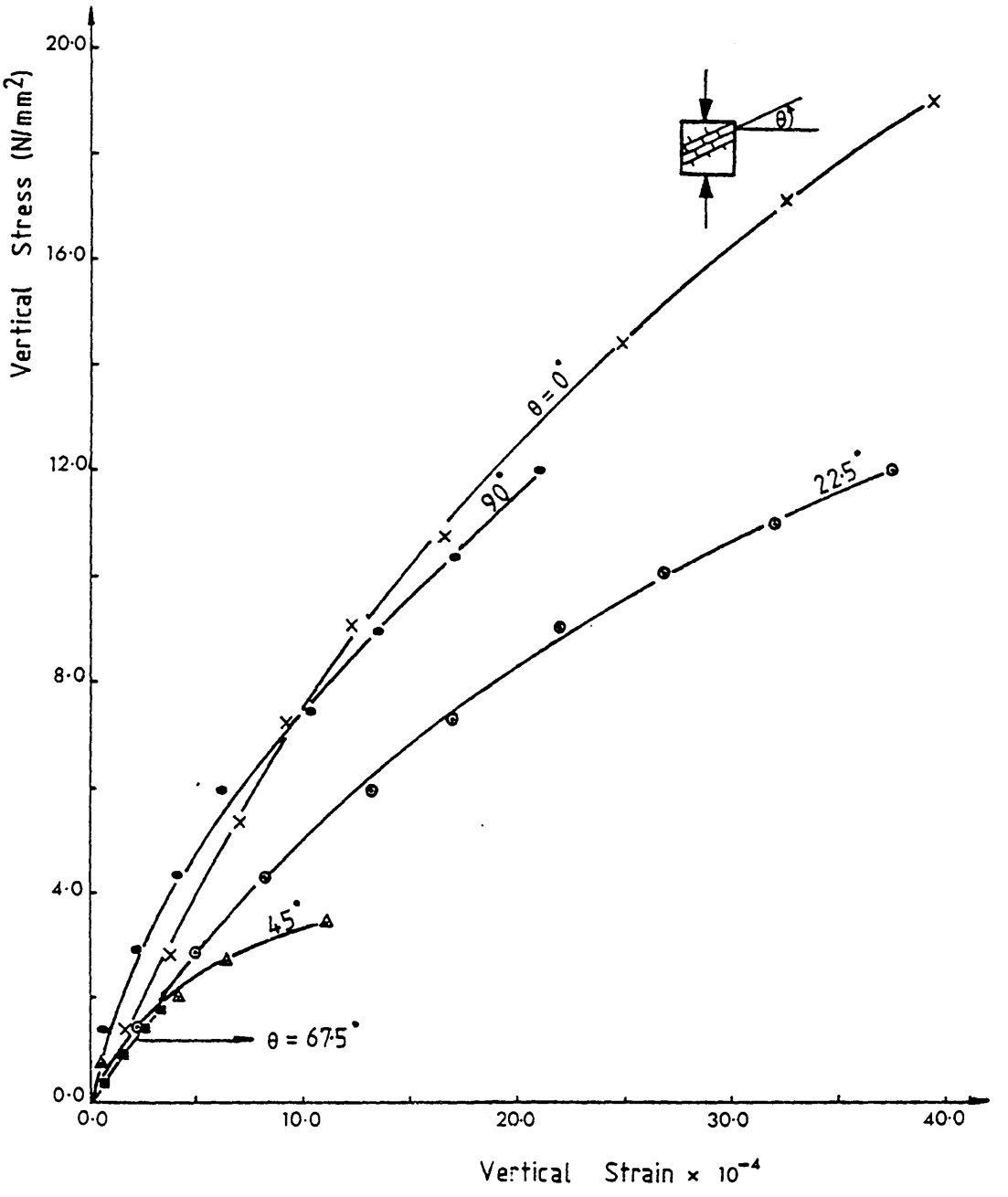

STRESS - STRAIN CURVES IN COMPRESSION
FOR PANELS WITH VARYING BED JOINT ANGLES

FIGURE 3.4

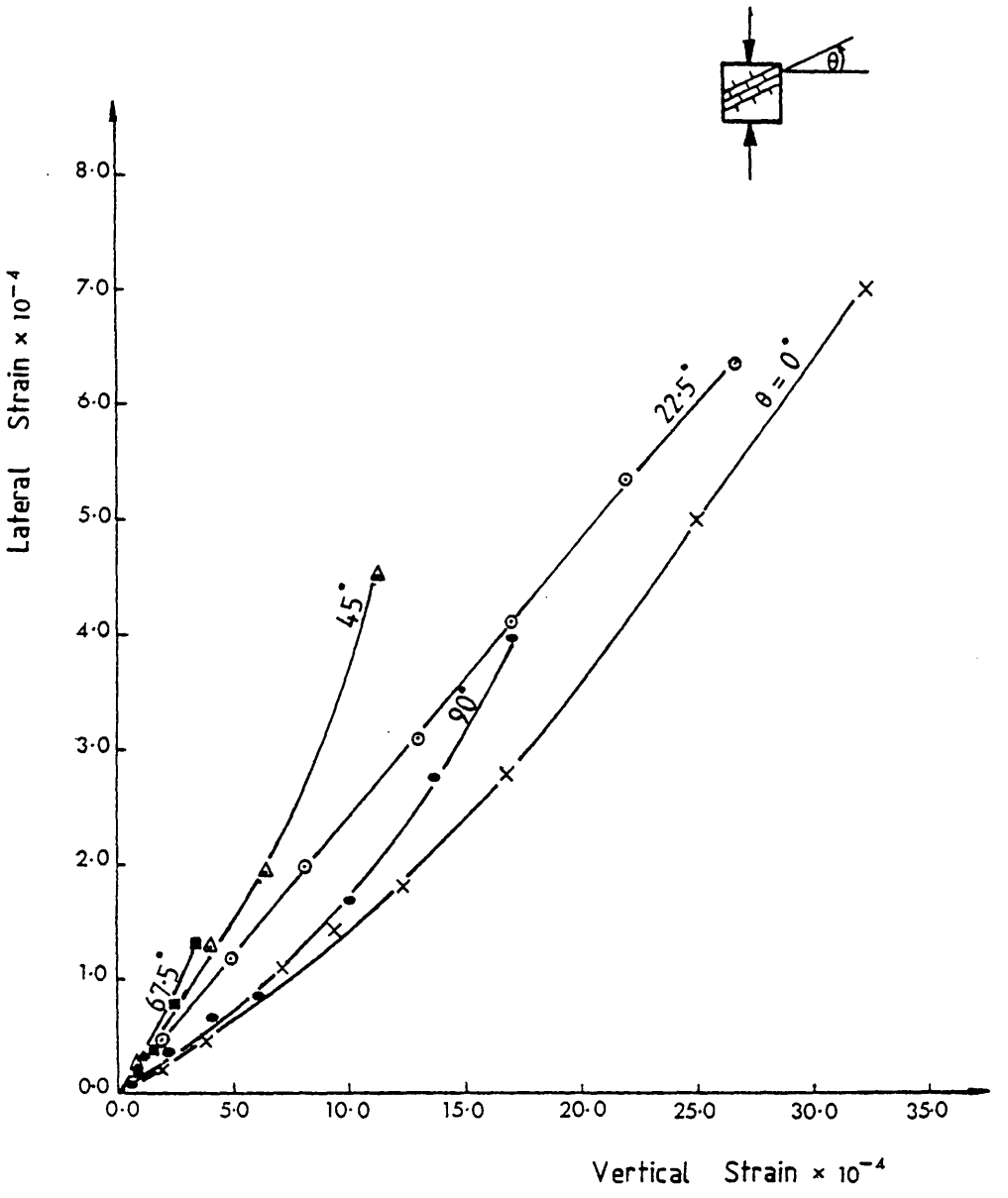

HORIZONTAL - VERTICAL STRAIN CURVES IN COMPRESSION FOR PANELS WITH VARYING BED JOINT ANGLES

FIGURE 3.5

brackets of the gauges cover a relatively large area of the wall and in turn reinforce the brickwork. Therefore apparent deformations may be restrained and are not allowed to reflect the influence of the bed joint direction on the elastic properties.

Property	$\theta = 0^o$	22.5^o	45^o	67.5^o	90^o
Elastic Modules (N/mm^2)	9120.0	6800.0	7900.0	6580.0	15866.0
Poisson's Ratio	0.14	0.24	0.28	0.28	0.14

Table 3.3: Elastic Modulus and Poisson's Ratio for Brickwork

θ	Elastic Modulus (N/mm^2)	Poisson's Ratio
0^o	6828.0	0.011
30^o	7241.0	0.103
90^o	7103.0	0.022

Table 3.4: Elastic Modulus and Poisson's Ratio for Brickwork (Chinwah's Results)

Sinha[71] carried out tests on one third scale model brickwork wallettes under uniform axial compression in either direction to obtain the moduli of elasticity normal (E_y) and parallel (E_x) to the

bedding plane. The strains were measured by means of 63.5 mm vibrating wire gauges. The results clearly exhibited the amisotropy of the material and the average orthotropic ratio (E_x/E_y) was found to be 1.4.

However, more comprehensive testing would be required before accurate estimates of elastic modulus and Poisson's Ratio could be made. The values of 7000.0 N/mm^2 and 0.2 were assumed as reasonable values for elastic modulus and Poisson's Ratio respectively for this investigation. The influence of these elastic constants on the stress distribution of brickwork will be discussed in Chapter 5.

3.5 CONCLUSIONS

In this Chapter the material properties of brick and mortar used in this investigation are presented. Information about the deformation characteristics of brickwork, which will be used in the succeeding chapter are also presented.

It is interesting to note that the coefficient of variation for compressive strength of the brick unit was relatively low. However, a fairly high coefficient of variation was observed in the test results obtained for tensile strength of brick units. This would have been caused by unavoidable variation in the test conditions.

Brickwork exhibited non-linear stress-strain characteristics. The direction of the bed joints to the applied compressive load, in the uniaxial compressive stress tests on brickwork, has a pronounced effect on the deformation characteristics.

CHAPTER FOUR : EXPERIMENTAL STUDY : BRICKWORK UNDER BIAXIAL STRESSES

4.1 INTRODUCTION

Biaxially stressed brickwork occurs in almost all walls subjected to complex systems of in-plane loads; for example shear walls, infilled walls, walls supported on elastic foundations and beams, in the shear region of flexural members etc. Experimental investigation into the strength of brickwork in a state of biaxial stress is therefore very important. Unfortunately, due to the complexities of biaxial testing, few experiments have been carried out in the past and hence very little documented literature is available on the problem. Previous research has been summarized in Chapter 2.

Failure of an isotropic material in a state of biaxial stress can be defined in terms of principal stresses σ_1 and σ_2. The interaction of principal stresses at failure or in other words the failure envelope can be obtained from biaxial tests together with uniaxial compression and tension tests.

Concrete has been regarded as an isotropic material although it exhibits anisotropic characteristics due to the non-uniformity of material. Since the turn of the century many investigators have carried out experimental investigations with regard to the behaviour of concrete under biaxial stresses. Such investigations can be categorized into three groups depending on the type of specimens

used and the method of load application.

(a) Concrete cubes or plates subjected to direct principal stresses, σ_1 and σ_2.

(b) Cylindrical specimens subjected to radial stresses ($\sigma_1 = \sigma_2$).

(c) Hollow cylinders subjected to either torsion and axial compression or to internal hydraulic pressure and axial compression.

A more detailed review of previous investigations has shown[36], that square concrete plates subjected to in-plane loading appear to be suitable specimens to determine the biaxial strength of concrete over the entire range of biaxial stress combinations. Perhaps the most representative of these was performed by Kupfer, Hilsdorf and Rusch[36], using brush platens in conjunction with an elaborate biaxial testing machine. The failure envelope obtained by them is shown in Figure 4.1(a), and it is typical for a homogeneous, brittle material.

A strength envelope obtained by Khoo and Hendry[35] for clay brick material based on biaxial tests on 25mm square x 76 mm specimens is shown in Figure 4.1(b). The Khoo-Hendry interaction curve does not reflect the effect of the mortar in the brick masonry since the specimens were cut from a brick unit. It would appear initially that a similar technique which can predict the behaviour of an isotropic material can be expected to apply equally well to brickwork to obtain a failure envelope under biaxial stresses. However, brickwork is anisotropic, two phase material consisting of linearly

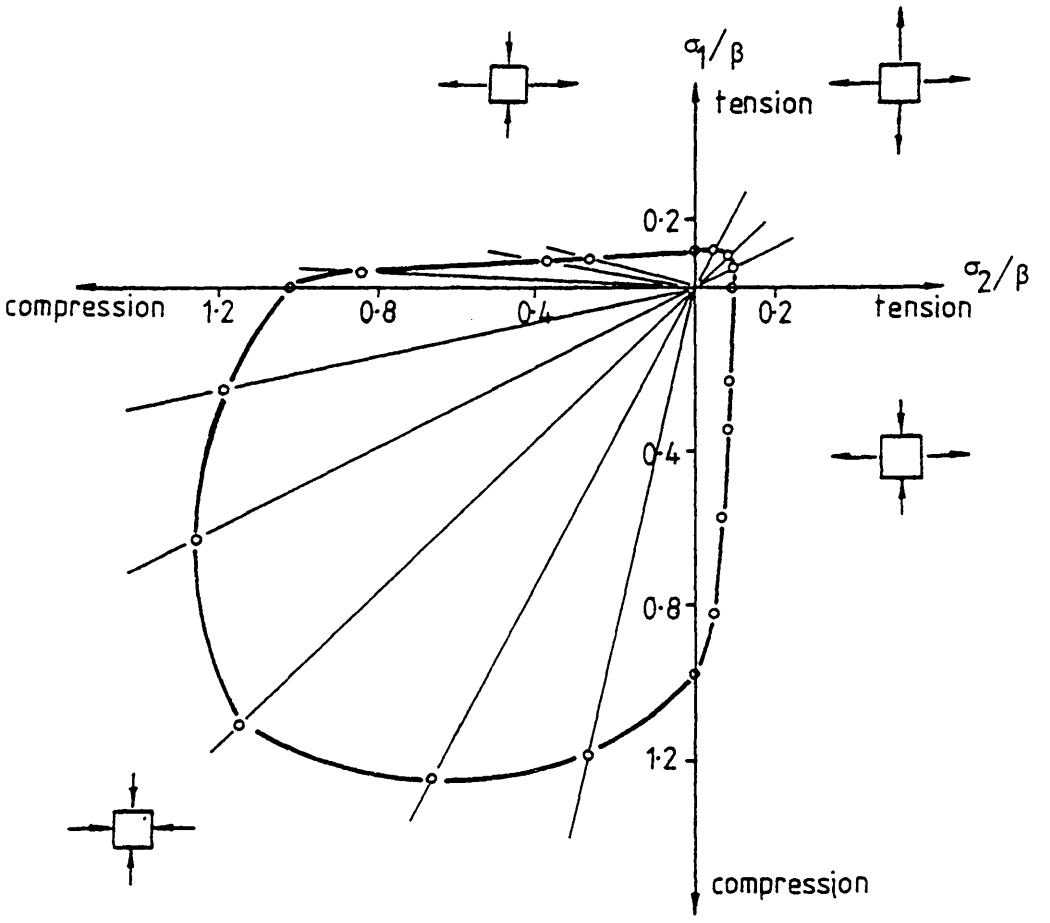

$\beta = 30{\cdot}6$ N/mm^2 (unconfined uniaxial compressive strength)

TYPICAL FAILURE ENVELOPE FOR THE BIAXIAL STRENGTH OF CONCRETE

FIGURE 4.1.(a)

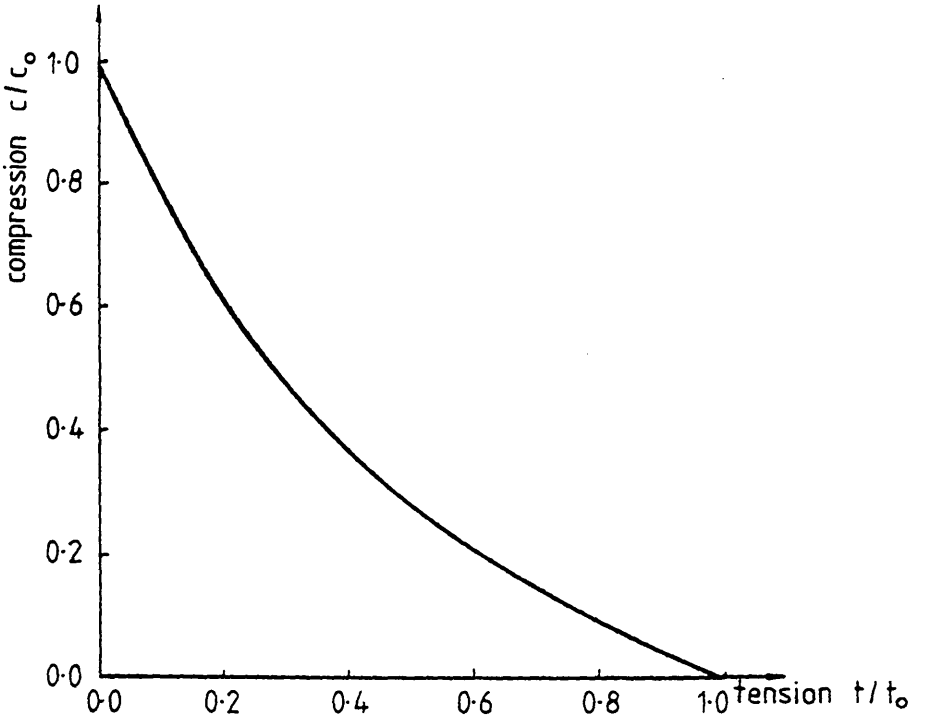

KHOO-HENDRY BIAXIAL STRENGTH ENVELOPE FOR BRICK

FIGURE 4.1(b)

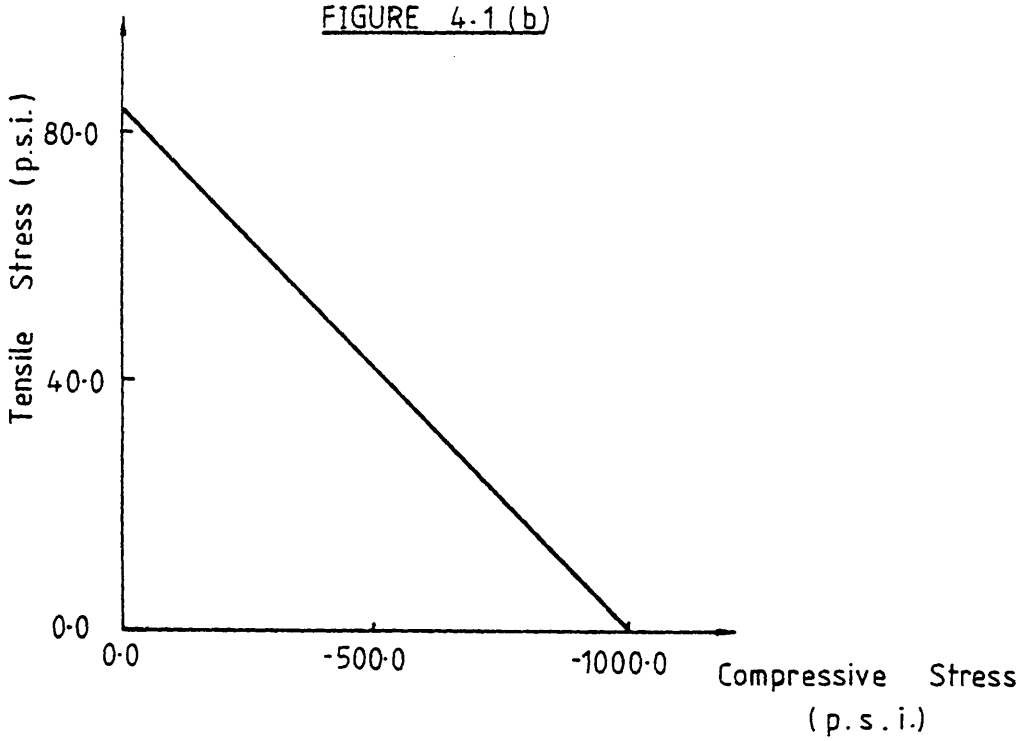

BIAXIAL STRENGTH ENVELOPE FOR GROUTED CONCRETE MASONRY

FIGURE 4.1(c)

elastic bricks embedded in thin layers of non-linearly elastic mortar. The mortar joints usually act as planes of weakness. Therefore, a criterion based solely on principal stresses cannot be postulated without reference to the effect of a third variable, the bed joint orientation. Hence, to completely define masonry failure, a three dimensional failure surface is required in terms of the principal stresses, and their respective directions relative to the bed joint.

Biaxial tests on full scale panels under monotonic and cyclic stress histories were first carried out by Hegmier et al.[24] for grouted concrete masonry in 1978. According to those results the influence of joint orientation seems to be less significant for grouted conrete masonry. The resulting failure surface was very similar to concrete and is shown in Figure 4.1(c). The authors point out that this isotropic behaviour would not necessarily be found for all block and grout combinations.

In order to define the complete behaviour of brickwork under biaxial stresses, a sufficient number of tests must be carried out to cover the following combination of stresses.

(i) Biaxial tension - tension
(ii) Biaxial compression - compression
(iii) Biaxial tension - compression

Due to the very poor inherent tensile strength characteristics of brickwork very sophisticated and sensitive load application and measuring instruments would be required to obtain a failure surface in the tension-tension region, and it would be extremely difficult. Moreover, a study of the behaviour of brickwork in this range is not

so important from the practical view point apart from the case where panels are subjected to loads normal to the plane of the wall in which case the failure might be predicted at the tensile face of the panel. This case has, however been investigated analytically by Page.[52]

In practice both compression-compression and tension-compression principal stresses are equally likely to occur when a brick wall is subjected to in-plane loads. The pattern of the distribution of these two systems of stresses over the area of the wall depends solely on the nature of the externally applied loads and boundary conditions, the wall is subjected to. Therefore, both compression-compression and tension-compression stress regions are equally important as far as their occurrence is concerned. However, the author realises, the relatively low tensile strength characteristics of brickwork over its compressive strength characteristics make tension-compression stress region more significant in predicting the initiation of failure. Nevertheless, as will be shown, in order to explain the ultimate behaviour completely, knowledge of biaxial compression stress region is also necessary. In view of the difficulties of carrying out experiments to cover the full range of stresses in a biaxial stress field, the present tests were confined to define the dominating range for the initiation of failure, i.e. biaxial tension-compression stress region.

The experimental techniques that can be applied in brickwork for biaxial tests are very limited due to the difficulty of forming test specimens. For example, the solid and hollow cylindrical specimens adopted in concrete are impracticable in brickwork. However, since square specimens have been suggested as most suitable specimens for concrete, square brick panels subjected to direct biaxial stresses were proposed for the biaxial test programme.

4.2 TESTS ON BRICKWORK UNDER UNIFORM BIAXIAL STRESS FIELD

4.2.1 Construction of the Walls for the Preparation of Test Specimens

To reduce the required capacity of test rigs, brickwork panels were built using one-sixth scale fired clay model bricks. The properties of the bricks have been discussed in Chapter 3.

A standard mortar mix 1:¼:3 (cement:sand:lime) by volume was adopted and used throughout. The properties of mortar have been discussed in Chapter 3. The water cement ratio for the mortar mix was decided by the bricklayer in order to achieve a workable mix, and it was found to be 0.90. Bulk density variations in materials were eliminated by weighing measured volumes of fresh materials and thereafter batching by weight.

Before construction of wall panels, the suction rate of the bricks was adjusted by immersion in water with a view to attaining a constant, although not necessarily an optimum value. Bricks were immersed in water for ten minutes and spread on an aluminium tray until the external surfaces were fairly dry.

One of the major variables in brickwork construction is the standard of workmanship and in order to reduce the variability in workmanship an experienced bricklayer was employed to build the specimens throughout the experimental programme.

Brick walls were constructed in standard stretcher bond against a vertical, oiled plywood sheet to ensure plane-ness of the specimens and consistency of joint thickness. Single leaf walls were built which represented 108 mm walls at full scale. Constant thickness of joints

of about 2 mm was maintained throughout. The common malpractices in bricklaying such as insufficient filling of joints, excessive variations in joint thickness, excessive raking of completed joints and excessive tapping of the bricks during placement were avoided to a great extent in the model wall construction.

Two sizes of walls were built in order to prepare the biaxial test specimens. These were typically 150 mm high x 150 mm wide x 18 mm thick, and 230 mm high x 240 mm wide x 18 mm thick, constructed to one-sixth scale using the standard manufacturing technique. The resulting panels were 11 courses high x 4 bricks wide and 16 courses high x 6 bricks wide. These walls represent 0.9 m x 0.9 m and 1.4 m x 1.44 m wall panels in full scale. Usually building of a wall was completed within 30 to 60 minutes.

4.2.2 Curing

Walls were covered with a polythene sheet for twenty four hours after construction and subsequently air cured under laboratory conditions.

4.2.3 Control Specimens

4.2.3.1 Mortar Cubes

With each wall constructed, three 25 mm mortar cubes were cast for control specimens[43]. These were made from the same 1:¼:3 (cement:sand:lime) mortar used for building the brick walls. Specimens were cast in 25 mm x 25 mm x 25 mm steel moulds. All specimens were compacted by hand. The mortar cubes were air cured for twenty four hours, and then water cured until the time of testing.

4.2.3.2 Brick-Mortar Cubes

Two brick-mortar cubes were built with each wall for the determination of tensile bond strength at the interface between brick and mortar. The typical shape of the cube adopted is shown in Figure 4.2. Although, initially brick-mortar couplets were adopted, due to the low tensile bond strength between brick and mortar a sufficient measureable force could not be achieved, and hence brick-mortar cubes were chosen for this investigation. Both brick and mortar were of similar condition to those used in the wall construction. They were air cured until the time of testing.

4.2.4 Preparation of Test Specimens

All the biaxial test specimens were 150 mm x 150 mm in size. At the age of fourteen days the larger wall panels (230 mm x 240 mm) were reduced to the correct shape and size of the test specimens.

First, a 150 mm square was drawn on the surface of the wall by a pencil at the appropriate orientation to achieve the correct lay-up angle as shown in Figure 4.3. The lay-up angle is defined as the angle between the direction of the bed joints and one of the edges of the finished test specimen. Therefore, bed joints run at oblique incidence to the edges of the finished saw-cut specimen. Five lay-up angles were selected for biaxial tests, such as, 0^{o}, $22\frac{1}{2}^{o}$, 45^{o}, 67.5^{o} and 90^{o}. For specimens in which the lay-up angle was 0^{o} or 90^{o}, 150 mm x 150 mm wall panels were used and no further preparations were required since they were of correct shape and size.

The other panels were cut to the required size and shape by a "Clipper" saw. The "Clipper" has the capacity to hold impregnated

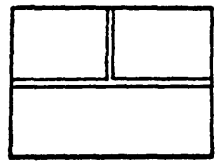

Front Elevation

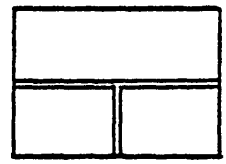

End Elevation

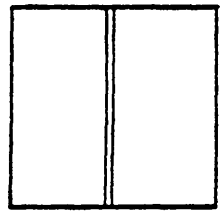

Plan

TYPICAL SHAPE OF BRICK-MORTAR CUBE

FIGURE 4.2

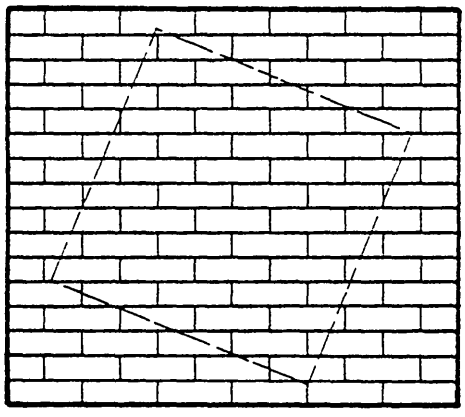

A WALL PANEL BEFORE SAW CUT

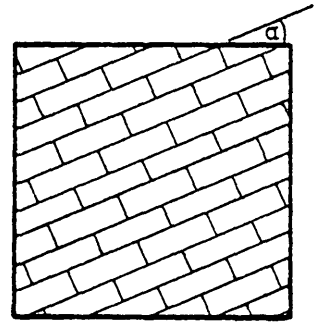

α = layup angle

SAW CUT SPECIMEN

FIGURE 4.3

diamond edge circular blades of varying thickness and diameters. The blade is driven by 5.5 h.p. motor at a constant speed of 3000 r.p.m. The blade of the machine can be moved manually in the vertical plane through a considerable range. The "Clipper" is provided with a mobile platform on which the specimens to be cut are placed.

Circular blades of different thickness were used on trial walls to find out the most suitable blade which gives a perfectly smooth cut without damaging the bonds of the wall. As the thickness of the blade becomes larger, more force is transmitted to the wall which causes bond failure. It was found that a 250 mm (10") diameter, 2 mm thick blade was suitable to cut one-sixth scale model brick walls.

About 25 mm thick polystyrene sheet was placed on the mobile platform and the wall was laid flat on top of the sheet. The wall was wetted for about one minute prior to cutting. A complete cut along a pencil line was undertaken in 6-7 steps. In each step not more than 3 mm cut was taken and a very smooth cut surface achieved.

Later, prepared specimens were kept in the laboratory under normal conditions until the age of 28 days. The specimens were usually tested 28-30 days after construction. Generally, two days prior to the date of testing, the "compressive edge" of the panel (the side on which the compressive force was going to be applied) was capped with 1:1 (cement:sand) mortar.

4.2.5 Friction Reduction Packing

4.2.5.1 Platen Restraint/

4.2.5.1 Platen Restraint

If a homogeneous isotropic material is tested in compression between platens or capping materials of higher elastic modulus than the test specimen, no tensile stresses are induced in the test piece. The higher the modulus of elasticity of the capping and higher the friction between the test piece and the platens, the greater the modification of the stress system in the specimen. This is the effect of platen restraint.[42] When platens or capping material of lower elastic modulus or stiffness than the test material are used, the test piece is subjected to tensile stresses arising from the greater lateral strains of the platen or capping. For brittle masonry materials which are substantially weaker in tension than in compression, this tensile splitting effect can lead to a considerable reduction in the load at failure. The effect of platen restraint gives an erroneously high estimate of masonry strength.

4.2.5.2 Techniques Adopted in Concrete to Eliminate Platen Effect

Biaxial test on concrete has been carried out for many decades on various forms of test specimens as has been discussed in section 4.1. It is believed that the discrepancies between the results from different investigators are often due to unintended differences in the stress states which have been developed in the test specimens. Introduction of different materials between the machine platen and the loading face of the specimen was the most common practice in concrete to eliminate or at least to minimize the platen effect. Effective minimization of platen

restraint on test specimens in biaxial tests on concrete was introduced by Kupfer, Hilsdorf and Rusch[36] by replacing the solid bearing platens of the conventional testing machine with "Brush bearing platens. These platens consisted of a series of closely spaced small steel bars flexible enough to follow the concrete deformations without generating an appreciable restraint on the test piece. The buckling stability of the filaments is sufficient to transmit the required compressive force into the specimen. Brush platens have been used to apply both tension and compression, and in the latter case filaments have been glued to the specimen.

Although brush platens have not been used for tests on brickwork to date, it has been successfully used by Thomas and O'Leary[78] and by Page[48] to determine the true compressive strength of brick units.

4.2.5.3 Adopted Technique to Minimize the Platen Effect

Brush platens cannot be used repeatedly. Therefore they are expensive and time consuming to use for a large number of biaxial tests in brickwork under biaxial stresses. In view of this, and to minimize the platen effect a technique adopted by Hughes and Bahramian[30] for concrete was used.

A thin layer of friction reduction packing known as 'M.G.A. pad' which consisted of a Melinex polyester film, gauge 100; Molyslip grease (containing 3% Molybdenum disulphide); and a hardened aluminium sheet 0.003 inches thick was used. The Molyslip grease was applied thinly to the aluminium sheet and the Melinex layer was placed on top of the grease. The aluminium

sheet was placed against the brickwork and Melinex film against the steel load spreader.

4.2.6 Test Rig and Instrumentation

One of the major problems in conducting tests on brickwork under uniform biaxial stress state is the difficulty of achieving a well defined and uniform stress state in the specimen. From the practical point of view, achieving a hundred percent uniformity of the stresses is impossible. Nevertheless, the following load application techniques were developed in an effort to produce a state of uniform stresses within the specimen.

4.2.6.1 Mechanism for Tensile Load Application and Setting Up of Specimens

Direct uniform tensile stress was applied to the test specimen by glueing four exactly similar steel blocks ("tensile blocks") to both "tensile edges" (sides on which tensile force is applied) and pulling them apart. These blocks were hinged to a simple pin joint mechanism as shown in Figure 4.4. This mechanism was designed to withstand the highest expected tensile strength of brickwork. The tensile force was applied externally using an Instron machine.

Care was taken when glueing the "tensile blocks" onto the specimen to ensure that they were equally spaced. In order to accomplish this, a special device was made which consisted of a steel plate having four 10 mm diameter, rigidly fixed pins at 37 mm intervals. Those pins were loosely fitted to the central holes of the "tensile blocks".

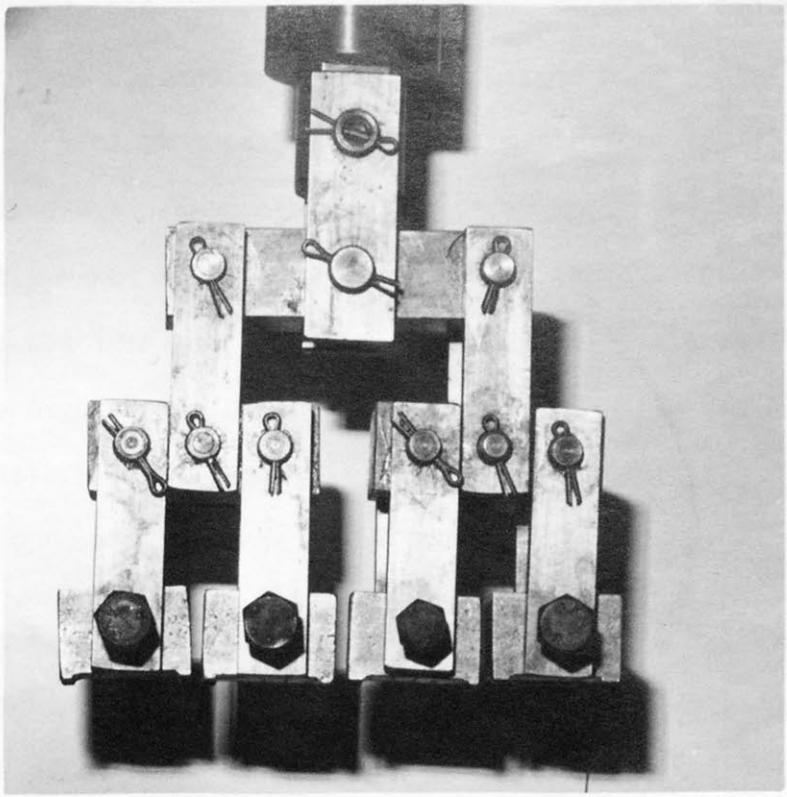

PIN JOINT MECHANISM FOR TENSILE LOAD APPLICATION

FIGURE 4.4

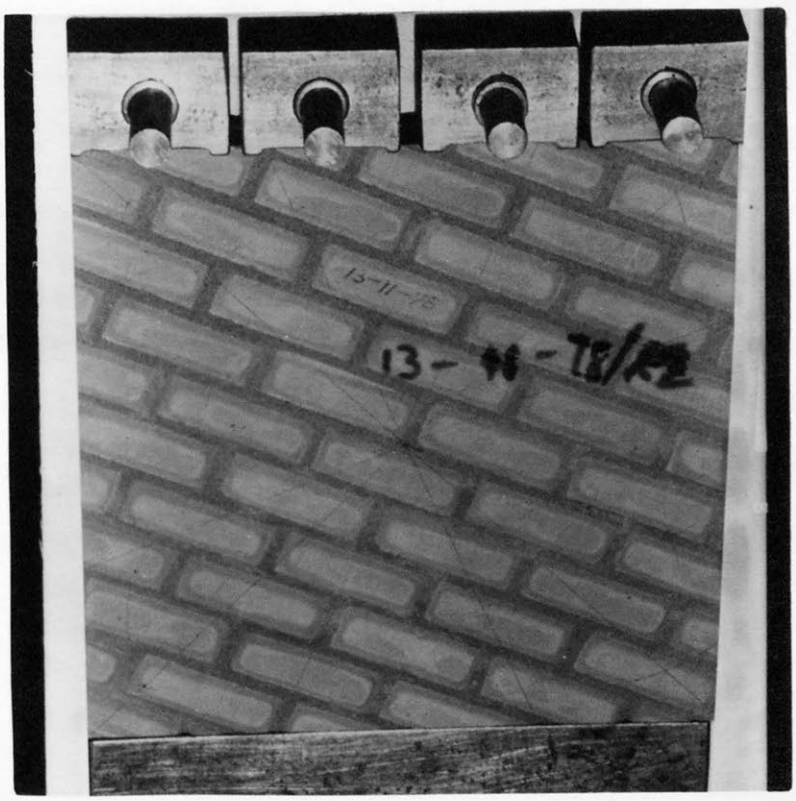

GLUEING THE TENSILE BLOCKS TO TEST SPECIMEN

FIGURE 4.5

Firstly, the "tensile edges" of the test specimen were cleaned and four cleaned tensile blocks were placed on the steel plate, so that each of them passed through a pin. Then, equal amounts of Araldite Rapid Hardener and Araldite Rapid Adhesive were thoroughly mixed and coated on one "tensile edge" of the specimen. Then the specimen was laid flat on the steel plate against the "tensile blocks" and glued to them. The adhesive was allowed to set undisturbed for about six hours before repeating the procedure for the opposite side.

The Figure 4.5 and Figure 4.6 illustrates the glueing of "tensile blocks" to the specimen and the typical arrangement of the test panel when it was ready to be subjected to tensile loads respectively.

4.2.6.2 Test Set up for the Application and Measurement of Compressive Load

The compressive force was applied by means of two 10 ton Hydraulic jacks which were fixed firmly to opposing sides of a steel frame as shown in Figure 4.7. The rig was mounted on an adjustable stand so that the hydraulic jacks could be centred easily on "compressive edges" (sides on which compressive force is going to be applied) of the specimen. The compressive force was transmitted to the wall through a 175 mm long spreader beam of 30 mm x 30 mm section. In order to achieve a truly perpendicular force to the sides of the test specimen the hydraulic jack heads acted through two spherical steel balls.

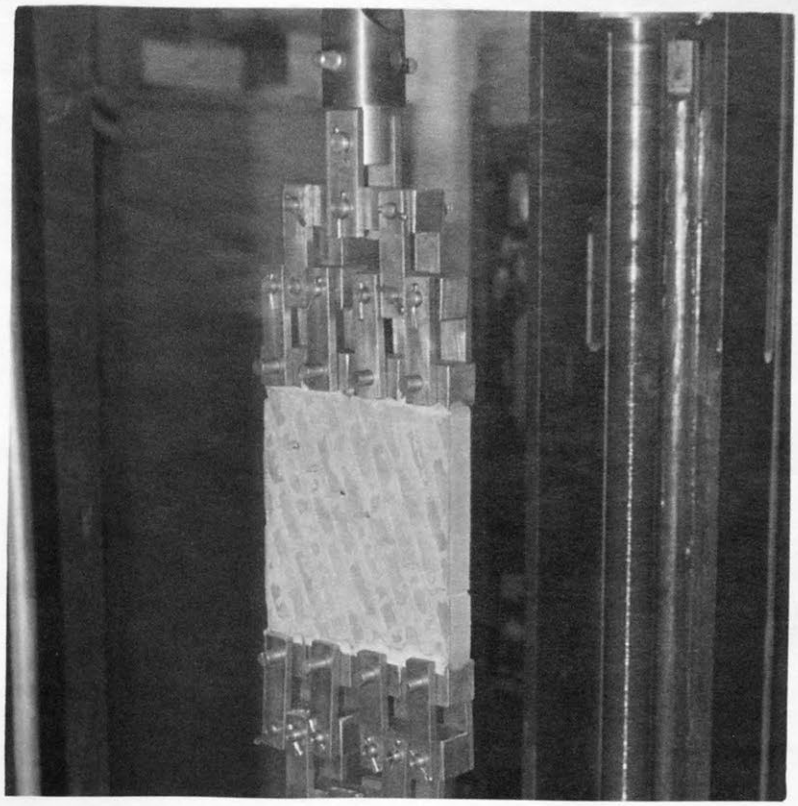

UNIAXIAL TENSION TEST ON BRICKWORK

FIGURE 4.6

TEST RIG FOR APPLICATION OF COMPRESSION ON SPECIMENS UNDER BIAXIAL STRESSES

FIGURE 4.7

The compressive force applied was measured by a pre-calibrated proving ring and its arrangement is also illustrated in Figure 4.7. Both hydraulic jacks and the one which was connected to the proving ring were controlled by the same hydraulic hand pump.

4.2.7 Uniaxial and Biaxial Tests

Three areas of in-plane behaviour have been investigated as shown in Figure 4.8.

(1) Panels loaded in uniaxial tension with load applied at varying angles(θ) to the bed joints.

(2) Panels loaded in biaxial tension and compression with different ratios of compression to tension for different bed joint orientations.

(3) Panels loaded in uniaxial compression with load applied at varying angles(Θ) to the bed joints.

In addition to these tests,control specimens built with each wall panel were tested.

4.2.7.1 Uniaxial Tension Test

The uniaxial tension test defines one of the points in the biaxial failure envelope for a particular bed joint orientation at which compressive force is zero.

The tensile load cell of the Instron machine was calibrated for the application of tensile load and the mechanisms for tensile load application were attached to it. Great care was taken when

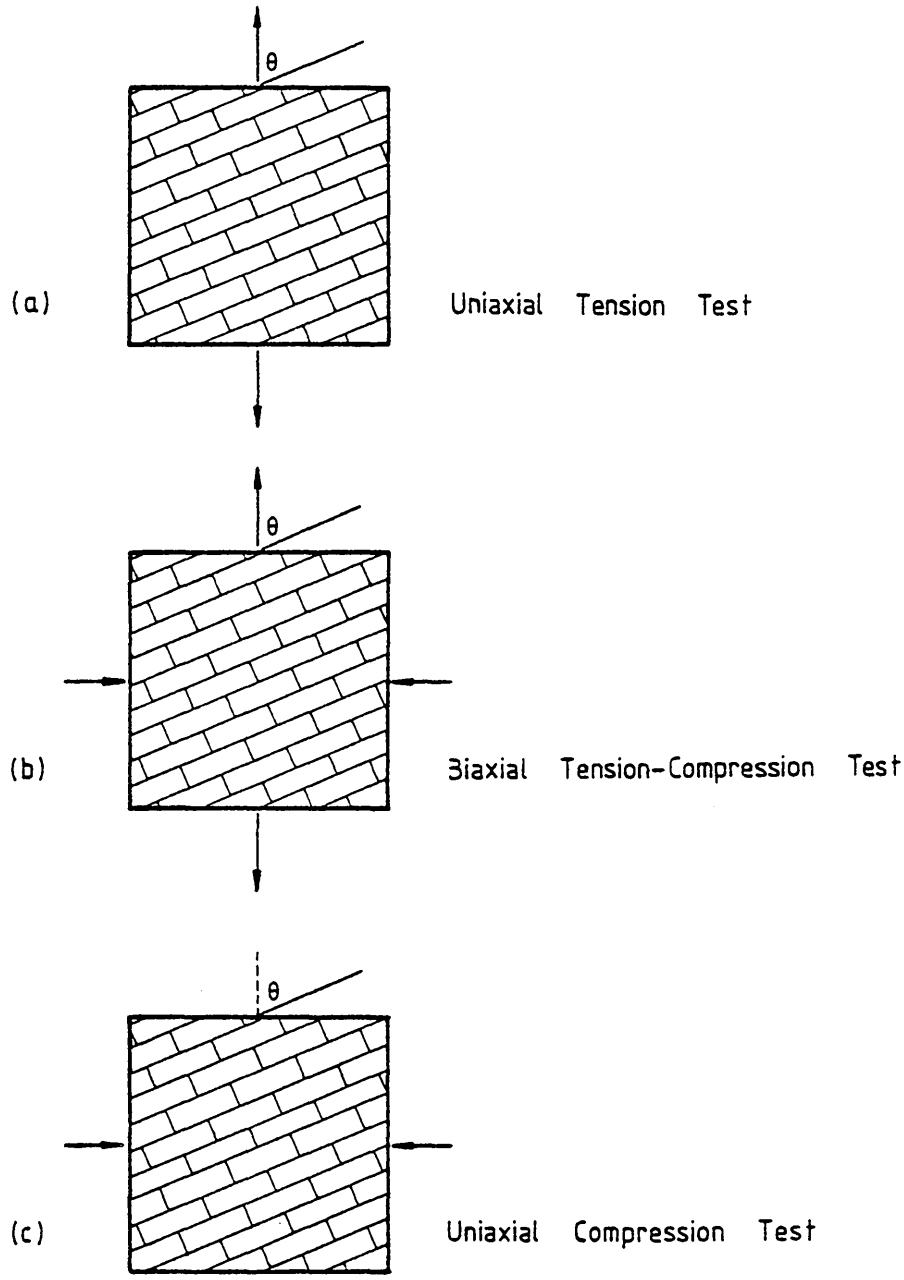

TESTS ON BRICKWORK WITH VARYING BED JOINT ORIENTAION

FIGURE 4.8

the test specimen was being connected to the pin-joint mechanism. Initially 2-3 kg was applied very slowly (0.005 cm extension per minute) to remove the slackness of the system and to straighten the specimen. After that, the tensile force was gradually increased up to failure at a rate of 0.02 cm elongation per minute. At least two tests were carried out for each bed joint orientation. Detailed results are in Appendix B .

4.2.7.2 Biaxial Tension-Compression Test

Tensile force was applied to the specimen using the Instron machine which was calibrated before use. Generally two types of load cells were used, either 50 kg or 500 kg capacity, depending on the typical strength of the specimen and the ratio of the biaxial stresses.

Although the ratio of the compressive force to the tensile force applied was controlled manually, it was maintained as far as possible, at a pre-determined value. The tensile force was applied at a rate of 0.02 cm extension per minute. The rate of increase of compressive force could not be controlled to a certain specific value, as the hydraulic pump was controlled manually. However, it was applied at a low rate. Tensile and compressive forces were applied to the specimen in increments. Each specimen was first loaded in tension to 2-3 kg, in order to remove the slackness of the pin-joint mechanism and straighten the specimen. After the initial increment, tensile and compressive forces were increased gradually up to failure. The failure was defined when both the compressive and tensile loads started to drop suddenly and

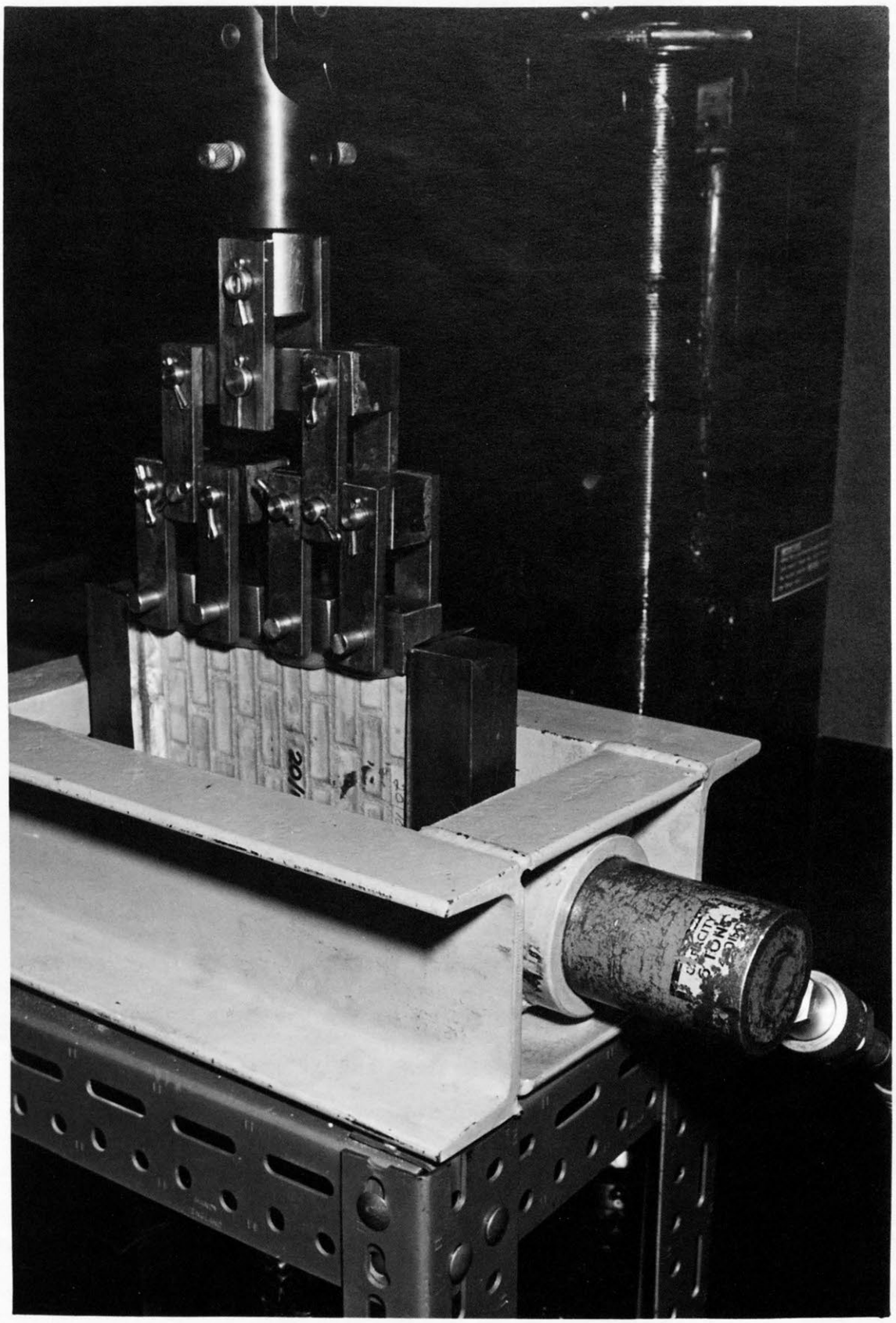

BIAXIAL TENSION-COMPRESSION TEST

FIGURE 4.9

simultaneously. Both the ultimate compressive and tensile loads were recorded. At least two experiments were carried out for similar specimens under similar conditions of loading. The detailed results of tests are shown in Appendix B.

4.2.7.3 Uniaxial Compression Test

As in the uniaxial tension case, a point on the principal compressive stress axis of the biaxial strength envelope for a particular bed joint angle is defined by uniaxial compressive strength.

Specimens were tested in the Instron machine. A 500 kg load cell was used to test the specimen having 67.5^{o} bed joint orientation whereas the rest of the specimens were tested using a 10,000 kg load cell. Longitudinal and lateral strains were measured on a central 50 mm gauge length using a demec gauge, on both sides of the specimens. These readings were averaged to eliminate bending effects. The detailed results of strain measurements are discussed in section 3.4.2 in Chapter 2.

Although in biaxial tests both the "compressive edges" were free to move, in the uniaxial tests one side was restrained. This was adopted to simplify the experiments and study the crack pattern at failure. However, it was assumed that the variation of the test results due to this effect was insignificant.

The detailed results of the experiments are shown in Appendix B.

4.2.7.4 Strain Measurement

A problem in a biaxial test of this sort on brickwork was the difficulty of measuring strains. The size of the specimen was small (150 mm x 150 mm) and the whole system was not rigid enough to take any strain measurements on the wall other than in the uniaxial compression test. Use of electrical strain gauges on brickwork has proved to be unsuccessful.[7] Vibrating wire strain gauges are also inapplicable for one-sixth scale brickwork, because the brackets for the gauges cover a considerable area of the wall and in turn strengthen the brickwork. It would be possible to measure the total deformation, longitudinally and laterally, and calculate mean strains in the respective directions. However, in view of the difficulties and the complication in setting up the test panels and the fact that the primary objective was to establish strength relationships, no strain measurements were undertaken in this test programme except in the uniaxial compression test.

4.2.8 Mode of Failure

When brickwork with varying bed joint orientations is subjected to uniform biaxial tensile and compressive stresses, the failure modes at the ultimate load level can be categorized mainly into three groups.

(1) Bond failure mostly along the bed joints.

(2) Zig-zag bond failure through perpendicular and bed joints.

(3) Tensile splitting failure through bricks and mortar joints.

The change in bed joint angle relative to the principal tensile stress direction and the various ratios of compressive stress to tensile stress produce different combinations of normal and shear stress along the joints. Therefore, depending on the strength of bricks relative to mortar strength, the bond strength at the brick-mortar interfaces, and the nature of stresses, the failure modes can be varied.

4.2.8.1 Mode of Failure of Uniaxial Tension Tests

Generally, in uniaxial tension tests, whatever the bed joint orientation, both bed and perpend joints are in tension normal to the brick-mortar interface.

All the specimens failed along the joints. When load was applied normal to the bed joint, or in other words when θ equalled 90^{o}, the tensile capacity of the specimen is purely dependent upon the tensile bond strength at the brick-mortar interface. All the specimens with 90^{o} bed joint angle failed in the same ideal tension mode with the failure plane passing through the horizontal bed joint. When the load was applied perpendicular to perpend joints ($\theta = 0^{o}$), a staggered joint failure pattern was induced by low bond strength between bricks and mortar compared to the high tensile strength of brick units.

For the cases where $0^{o}<\theta<90^{o}$, the mode of failure changed from zig-zag joint failure (along the bed and perpend joints) to bed joint failure as θ increased from 0^{o} to 90^{o}. This was quite evident from the failure modes illustrated in Appendix B. When $\theta>45^{o}$, the magnitude of the tensile-normal stress at the bed joint is higher

than the tensile-normal stress at the perpend joint, where as when $\theta<45^{o}$, the tensile-normal stress at the perpend joint is relatively higher. Although for specimens where $0^{o}<\theta<90^{o}$ the failure at joints is governed by mixed shear and tension, since both perpend and bed joints undergo equal shear stresses, the magnitude of tensile stress at brick-mortar interface dominates the failure. Therefore when $\theta>45^{o}$, failure takes place right along the bed joints. However, when $\theta<45^{o}$, although the failure initiated at perpend joints, it could not propagate through strong brick units and hence followed through bed and perpend joints resulting in a zig-zag pattern joint failure. The intensity of normal and shear stresses at the perpend and bed joints are equal for the case where θ equals 45^{o}, and therefore, the crack propagated along the weakest joint in the test specimen. The typical failure modes are shown in Appendix B.

4.2.8.2 Mode of Failure in Uniaxial Compression Test

In the uniaxial compression test for all the bed joint orientations, the normal stress at the perpend and bed joints are compressive.

The failure modes of the specimens varied with the ratio of shear stress to normal stress at the joints. For high ratios (low normal stress), failure occured as a bond failure in one of the bed joints with no sign of distress in the bricks. For low ratios (high normal stress), a combined brick-mortar failure occured. The higher load capacity of the specimens in the latter case can be attributed to the additional frictional resistance in the joint due to the compressive normal stress, and lateral tensile splitting was evident in the brick with some bond failure in the joints.

When the load acted perpendicular to the bed joints ($\theta = 0^{o}$) a typical splitting mode of failure through bricks and perpend joints induced by the differing strain characteristics of the weaker mortar and the strong bricks took place. Numerous micro-cracks parallel to the direction of applied load were formed. Complete collapse of the specimen was accompanied by a few major cracks. The specimens with bed joint angle 22.5^{o} and 45^{o} to the applied load (ie $\theta = 67.5^{o}$ and $\theta = 45^{o}$ respectively) exhibited a failure confined to the joints whereas the specimens with 67.5^{o} to the applied load (ie $\theta = 22.5^{o}$) exhibited a failure approaching that of uniaxial compression for the θ equals 0^{o} case. In the latter case partial bond failures in the joints were accompanied by brick splitting. When the load was applied normal to the perpend joints ($\theta = 90^{o}$) sudden splitting failure along the bed joints was expected. However, the specimen initially separated into indivdiual columns by splitting along the vertical bed joints. This phenomenon was initiated near to the free edges and gradually spread towards the centre of the panel. The ultimate failure took place due to lateral buckling of some of those separated individual brickwork columns. In both the cases, where bed joint angle was 0^{o} and 90^{o}, bricks and mortar particles spalled off from the surfaces of the specimens revealing the tri-axial state of stress existing in brickwork panels loaded in uni-axial compression. The typical failure modes are shown in Appendix B.

4.2.8.3 Mode of Failure in Biaxial Compression-Tension Test

The failure mode was greatly affected by the orientation of the bed joints relative to the direction of tensile load and the ratio of externally applied compressive stress to tensile stress

ratio, f_c/f_t, at failure.

In order to study the effect of (f_c/f_t) on the failure mode the stress distribution on a small element at the brick-mortar interface of bed and perpend joints of a brick panel subjected to uniform biaxial stresses [compression (f_c) and tension (f_t)] as shown in Figure 4.10 was considered.

It can be shown that at bed joints,

$$\sigma_N = f_t \sin^2\theta - f_c \cos^2\theta$$

ie, $$(\sigma_N/f_t) = \sin^2\theta - (f_c/f_t)\cos^2\theta \qquad (4.1)$$

and $$\tau = \frac{(f_c + f_t)}{2} \sin 2\theta \qquad (4.2)$$

Similarly at perpend joints

$$(\sigma_N/f_t) = \cos^2\theta - (f_c/f_t) \sin^2\theta \qquad (4.3)$$

$$\tau = -\frac{(f_c + f_t)}{2} \sin 2\theta$$

Tensile stress normal to the joint at the brick-mortar interface and the shear stress in a clockwise direction is taken as positive. Both f_c and f_t are taken as numerically positive.

The variation of the normal stress (σ_N) at the interface of bed and perpend joints with f_c and f_t can be obtained using equation (4.1) and (4.3). The graphicalinterpretation is illustrated in Figure 4.11 with reference to the axes (σ_N/f_t) and (f_c/f_t) for three bed joint orientations relative to the direction of f_t, viz 22.5^o and 45^o and 67.5^o.

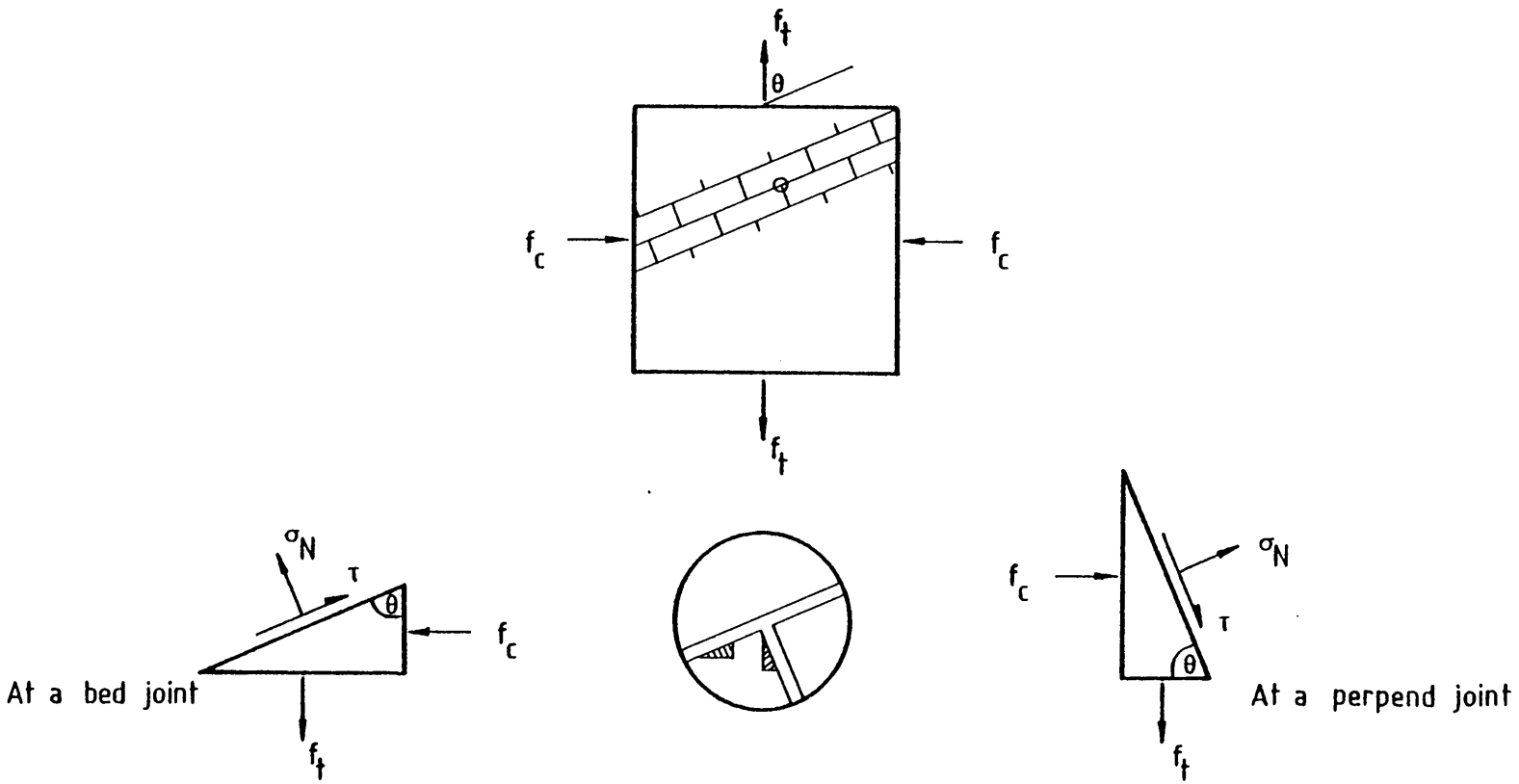

STRESSES ON AN ELEMENT ON BED AND PERPEND JOINTS

FIGURE 4.10

From Figure 4.11 it appears that as f_c to f_t ratio increases above a certain value the normal stress (σ_N) at the joints changes from tension to compression. This value is a function of bed joint orientation and it is given by equation (4.4).

$$\left(\frac{f_c}{f_t}\right)_{\sigma_{N=0}} = \begin{cases} \tan^2\theta \text{ (for bed joints)} \\ \cos^2\theta \text{ (for prepend joints)} \end{cases} \qquad (4.4)$$

The corresponding values which satisfy equation (4.4) for bed joints angles, such as $22.5^o, 45^o, 67.5^o$, are given in Table 4.1.

θ	$(f_c/f_t)_{\sigma_{NP=0}}$	$(f_c/f_t)_{\sigma_{NB}=0}$
22.5^o	5.85	0.17
45^o	1.0	1.0
67.5^o	0.17	5.85

σ_{NP} - normal stress at perpend joints

σ_{NB} - normal stress at bed joints

θ - bed joint orientation relative to the direction of f_t.

TABLE 4.1: THE VALUES OF (f_c/f_t) RATIOS AT WHICH THE NORMAL STRESS AT BED AND PERPEND JOINTS EQUAL TO ZERO

Therefore it is quite clear that both interfaces at bed and perpend joints are in compression when (f_c/f_t) becomes greater than 5.85, 1.0 and 5.85 for bed joint angles 22.5^o, 45^o and 67.5^o, respectively

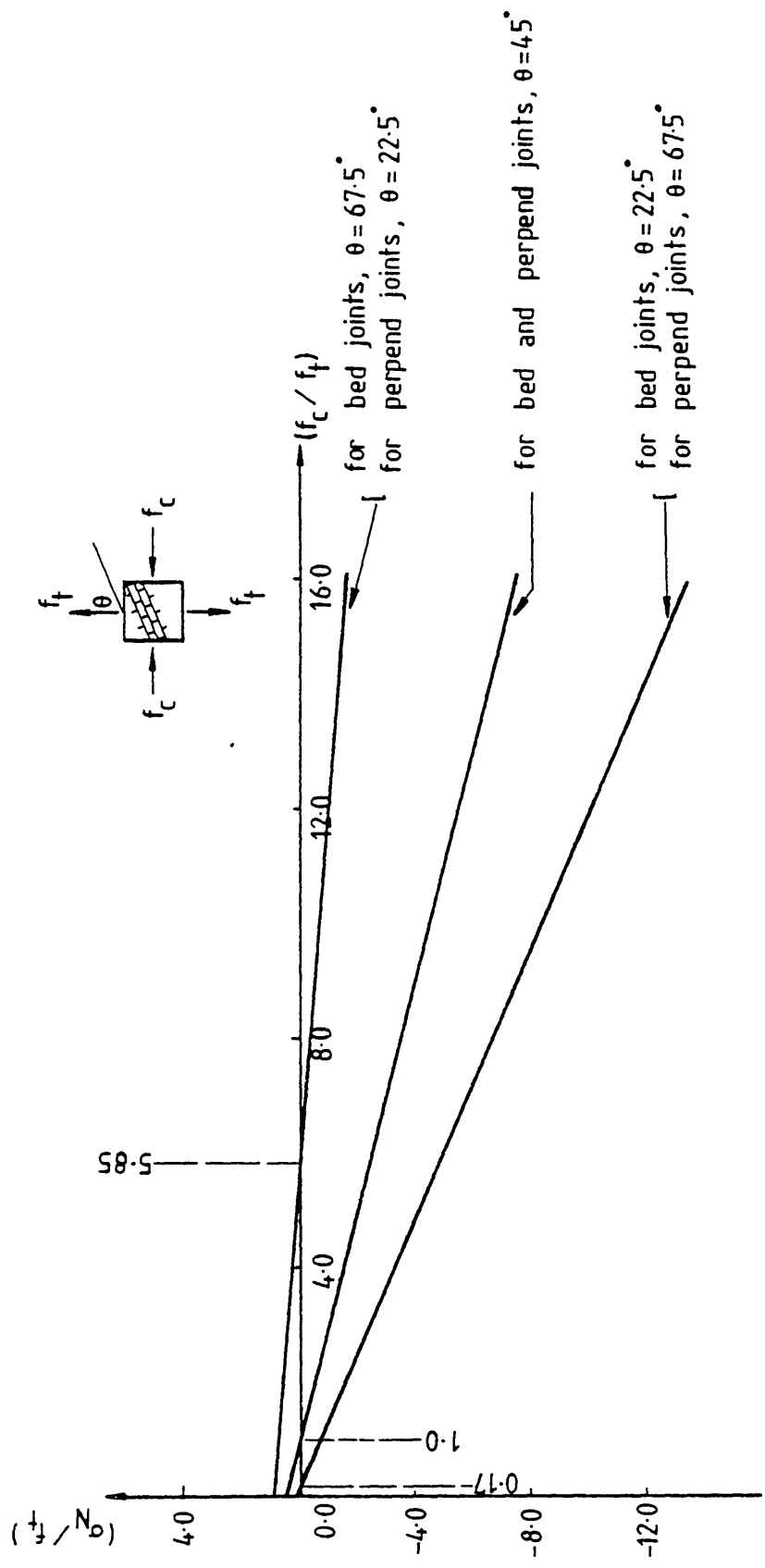

VARIATION OF NORMAL STRESS AT BED AND PERPEND JOINTS WITH VARYING (f_c / f_t) RATIO

FIGURE 4·11

When (f_c/f_t) is greater than the above values (high compression) the failure is governed either by shear-friction theory or by splitting tensile strength of the brickwork. When (f_c/f_t) is less than these values failure tends to initiate either at perpend or bed joints or at both simultaneously, this being governed by the interaction between shear stress and tensile stress.

From Figure 4.11, it appears that in specimens having 22.5^o bed joint orientation failure will always be initiated at perpend joints irrespective of the value of (f_c/f_t), because of either lower normal compressive stress or higher normal tensile stress at the perpend joints relative to the bed joints. If (f_c/f_t) is high enough to bring the brick units to their limiting strength under biaxial stresses f_c and f_t, then ultimate failure would take place through bricks and perpend joints - otherwise a zig-zag failure along bed and perpend joints would take place. The typical failure patterns for specimens with 22.5^o bed joint angle are illustrated in Appendix B.

Similarly, in specimens with 67.5^o bed joint orientation, whatever the value of (f_c/f_t), the failure is initiated at the bed joints because of higher normal tensile stress or lower compressive stress acting at the bed joints relative to the perpend joints. Therefore, for such specimens one could expect a failure line to pass entirely along the bed joints. Nevertheless, in the specimens tested, the failure occurred in some perpend joints, and this may be due to variability of the material properties and workmanship. The typical failure modes are shown in Appendix B.

According to Figure 4.11, for all the values of (f_c/f_t) the perpend and bed joints subject to similar stresses when θ is equal to 45^o. Therefore at the ultimate load level a crack can propagate either through perpend and bed joints or through a bed joint. The typical failure modes are illustrated in Appendix B.

The specimens with zero bed joint orientation subjected to biaxial stresses, always failed either in a staggered pattern or through the bricks and mortar. Usually, a failure through bricks and mortar was exhibited at high compression. The typical failure modes are shown in Appendix B.

No experiments were carried out for the state of uniform biaxial stress for specimens with 90^o bed joint orientation due to poor tensile strength of the specimens.

4.2.9 Tests on Control Specimens

Control specimens were tested along with the panel specimens. 25 mm mortar cubes were tested in the Instron machine placed between friction reduction packing. The brick-mortar cubes were tested in direct tension in a Hounsfield Tensometer. The cubes were glued to a pulling device and attached to the testing machine. The testing arrangement is shown in Figure 4.12(a).

The mortar cubes failed splitting vertically whereas brick-mortar cubes failed by a tensile bond failure at the brick-mortar interface as shown in Figure 4.12(b). The average ultimate compressive strength of mortar cubes was 9.2 N/mm^2 (standard deviation 0.82 N/mm^2, coefficient of variation 8.9%).. The

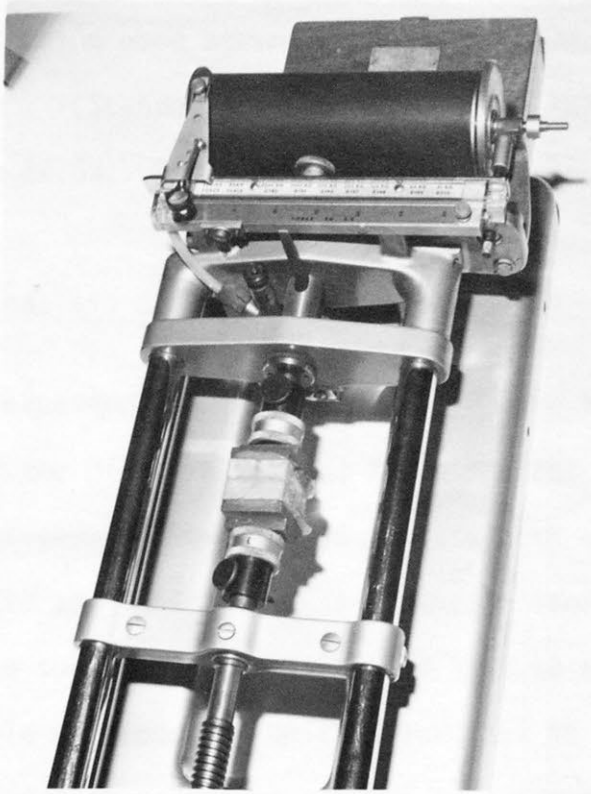

(a) TESTING ARRANGEMENT

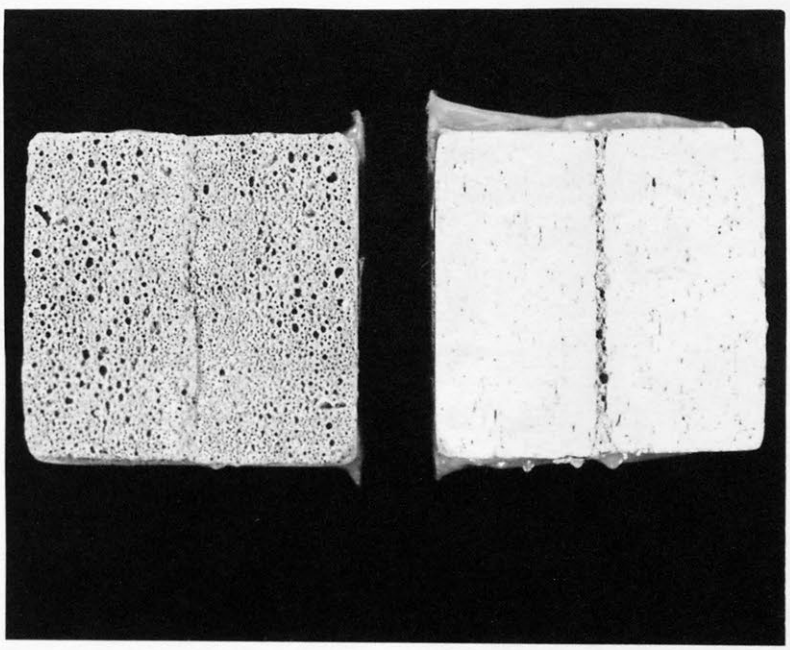

(b) TYPICAL FAILURE

TENSION TEST ON BRICK-MORTAR CUBES

FIGURE 4.12

average tensile bond strength of the brick-mortar cubes was 0.07 N/mm^2. (Standard deviation 1.6 x $10^{-2} N/mm^2$, coefficient of variation 22.8%). The detailed results are contained in Appendix B.

4.2.10 Analysis of Experimental Results

The experimental results recorded were tensile and compressive forces at the ultimate failure for different bed joint orientations. It was assumed, at the time of failure both externally applied compressive and tensile forces produce uniform biaxial stress field within the specimen. However, this is true only if loading fixtures are capable of producing uniform stresses at the sides of the panel and the friction reduction packing is sufficiently efficient to eliminate the shear stress which can be induced by different stiffness characteristics of the load spreader and the specimen.

The following equations were used to calculate the average stresses within the specimen at failure.

$$f_t = \frac{F_T}{A} \tag{4.5}$$

$$f_c = \frac{F_C}{A} \tag{4.6}$$

where F_T - tensile load at failure

F_C - compressive load at failure

A - cross-sectional area of the square brickwork panel.

All the ultimate stresses (f_c and f_t) at failure have been tabulated in Appendix B. The test results were plotted in Figure

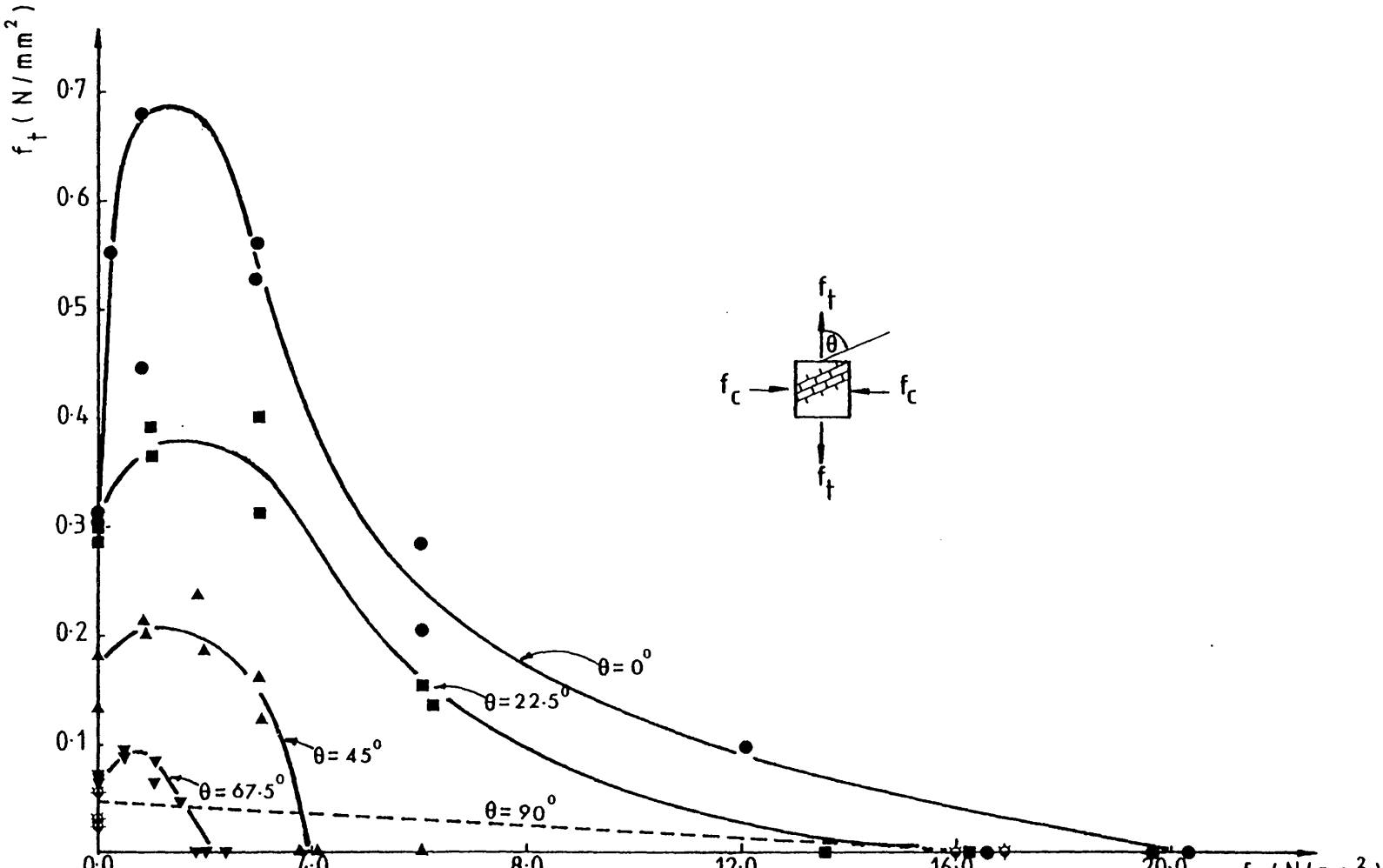

BIAXIAL STRENGTH CURVES FOR BRICK PANELS FOR DIFFERENT BED JOINT ORIENTATIONS

FIGURE 4·13

4.13 with reference to principal compressive stress (f_c) and principal tensile stress (f_t).

For each bed joint orientation the different combinations of biaxial stresses at failure followed a certain pattern. It is evident, that the direction of major principal stress relative to the bed joint has a marked influence on the biaxial strength of brickwork, as has been originally suggested by Johnson and Thompson.[31] Scatter of the results to a certain degree was observed. Usually brickwork tests exhibits greater variability than tests on most other engineering materials due to unavoidable variation in material properties resulting from their manufacture and the variation in standard of workmanship. For each bed joint angle, a best fit curve was drawn to obtain the strength characteristics of brickwork under different ratios of biaxial stresses. The failure envelope when the tensile load was perpendicular to the bed joints ($\theta = 90^o$) was not completed due to insufficient data.

The highest material strengths were achieved when the bed joints were parallel to the direction of the tensile load. The greater the bed joint angle (up to $\theta = 90^o$), the lower was the strength of the brickwork under a state of biaxial stress and each failure envelope exhibited a similar trend. At low compression, the tensile strength of brickwork increases with the compressive stress, up to a certain maximum.

Both the uniaxial compressive strength and the tensile strength decreased as the inclination of the bed joints relative to the principal tensile stress direction (θ) was increased. The test results reveal that the uniaxial compressive strength has been considerably

affected by the mode of failure. The specimens which failed through the joints were relatively weaker than the specimens which failed through the bricks and mortar. A considerable reduction in uniaxial compressive strength with increase of θ from 22.5^{c} to 45^{o} was caused by the change of failure mode. In the uniaxial tension test, although a change of failure mode was observed when the value of θ equals 45^{o} as discussed in section 4.2.8.1, there was no marked change in the rate of change of strength. The uniaxial tensile strength was found to be lower than the typical values for brick masonry. This was caused mainly by the high degree of saturation of brick which produced weaker tensile bond strength at the brick-mortar interface. When the specimens were pulled perpendicular to the bed joints at zero compression, the tensile bond strength was obtained, the average value being 0.07 N/mm^2.

4.2.11 The Influence of Shear Bond Strength to Tensile Bond Strength Ratio on the Shape of the Failure Envelope

In Figure 4.13 it is shown that an increase of strength occurs when the compressive force is increased up to a certain limit, at which brickwork is under a state of uniform biaxial stresses. Increase of principal tensile strength as the principal compressive stress is increased, is rather unusual for a brittle material. Although brickwork as a whole is treated as a brittle material, the presence of mortar joints influences the shape of the strength envelope to a certain degree. The strength of brickwork is greatly dependent on the bond strength between brick units and mortar. The bond strength is considerably affected by the degree of saturation of bricks at the time of laying,the consistency of mortar and the surface properties.

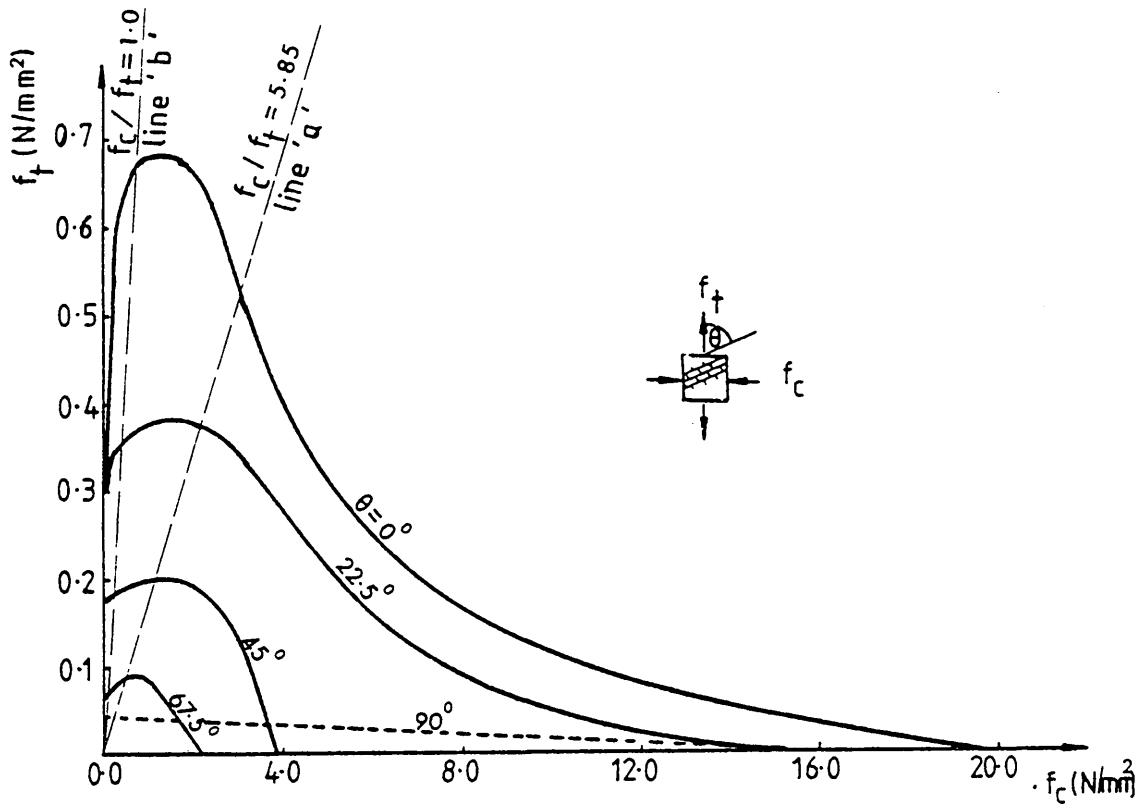

BIAXIAL STRENGTH CURVES

FIGURE 4.14

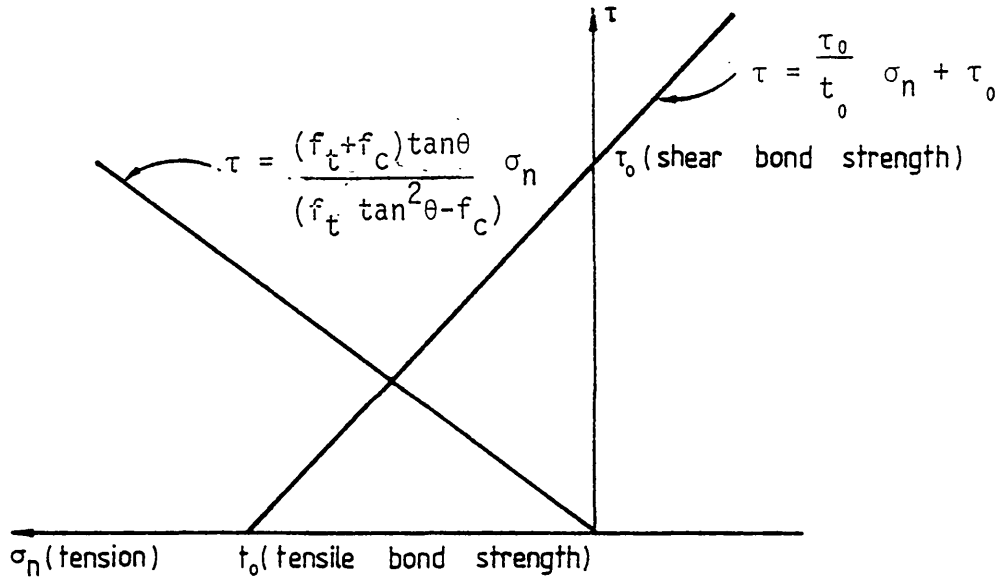

FAILURE CRITERION FOR JOINT FAILURE

FIGURE 4.15

However, it has been shown[64] that the effect of the degree of saturation of bricks on shear bond strength is insignificant in comparison with the effect on tensile bond strength.

The experimentally obtained biaxial failure curves have been redrawn and shown in Figure 4.14 to indicate the limiting values of (f_c/f_t) at which either perpend bed joints remain in tension (see Table 4.1) for θ equals 22.5^o, 45^o and 67.5^o. Obviously, when θ equals 0^o and 90^o, the perpend and bed joints remain in tension. The line 'a' in Figure 4.14 passes approximately through the peaks of 22.5^o and 67.5^o curves and line 'b' passes approximately through the peak of the 45^o curve. Therefore it can be seen that the apparent strength increase takes place when the joints are in tension and the initiation of failure under such condition is governed by the combined action of shear and tension.

As has been explained in section 4.2.8.3 when θ is greater than or equal to 45^o, the failure is initiated at the bed joints and constitute the ultimate failure of the wall. When θ is less than 45^o although failure initiates at the perpend joints, this may not constitute the ultimate failure of the wall panel which will occur after a collapse mechanism has been formed in the panel. Therefore, in order to study the effect of shear bond strength (τ_o) to tensile bond strength (t_o) ratio on the shape of the failure envelope, specimens with 45^o and 67.5^o bed joint orientations were selected. In this analysis for the sake of simplicity a linear relationship of the form:

$$\tau = \frac{\tau_o}{t_o} \sigma_n + \tau_o \qquad (4.7)$$

was assumed as the interaction of shear stress and normal tensile stress at the joint at failure (see Figure 4.15), with the typical shear bond strength being 0.3 N/mm^2.

The equations 4.1 and 4.2 in section 4.2.8.3 can be combined to yield,

$$\frac{\tau}{\sigma_n} = \frac{(f_t + f_c) \tan \theta}{(f_t \tan^2\theta - f_c)} \qquad (4.8)$$

The failure of the panel occurs when equations 4.7 and 4.8 intersect each other, as shown in Figure 4.15. By solving these equations f_t at failure can be obtained.

$$f_f(\text{failure}) = f_c \frac{(k - \tan \theta)}{(k \tan \theta + 1)} \tan\theta + \frac{2\tau_o}{\sin 2\theta (k \tan \theta + 1)}$$

$$\text{where} \quad k = \tau_o/t_o \qquad (4.9)$$

The ultimate tensile strength under biaxial stresses at low compression is therefore a function of applied compressive stress, shear bond strength, tensile bond strength and the bed joint angle. The typical variation of strength with different τ_o/t_o ratios are shown in Figure 4.16 and Figure 4.17 for two values of θ, such as 45^o and 67.5^o respectively. At low τ_o/t_o ratios (high tensile bond strength) the strength of the material decreases as the compressive stress increases similar to the brittle materials. For high τ_o/t_o ratios (low tensile bond strength) an increase of strength take place as the compressive stress increases. Although the foregoing analysis does not take into consideration the panels having bed joint orientations less than 45^o, it does indicate that the shape of the failure surface depends upon the relationship between shear and tensile bond strength.

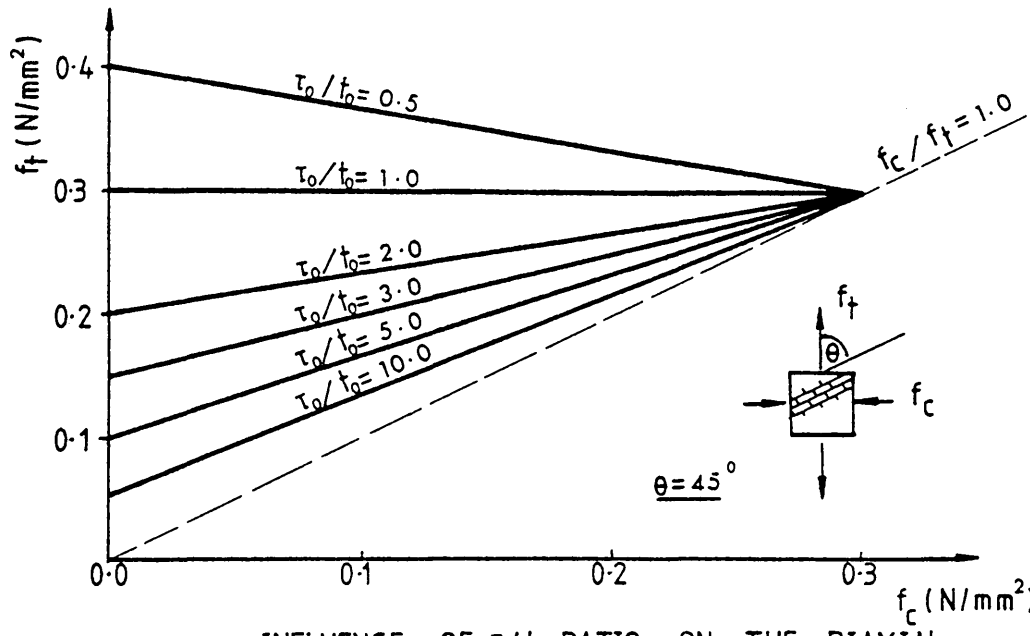

INFLUENCE OF τ_0/t_0 RATIO ON THE BIAXIAL STRENGTH AT LOW COMPRESSION

FIGURE 4·16

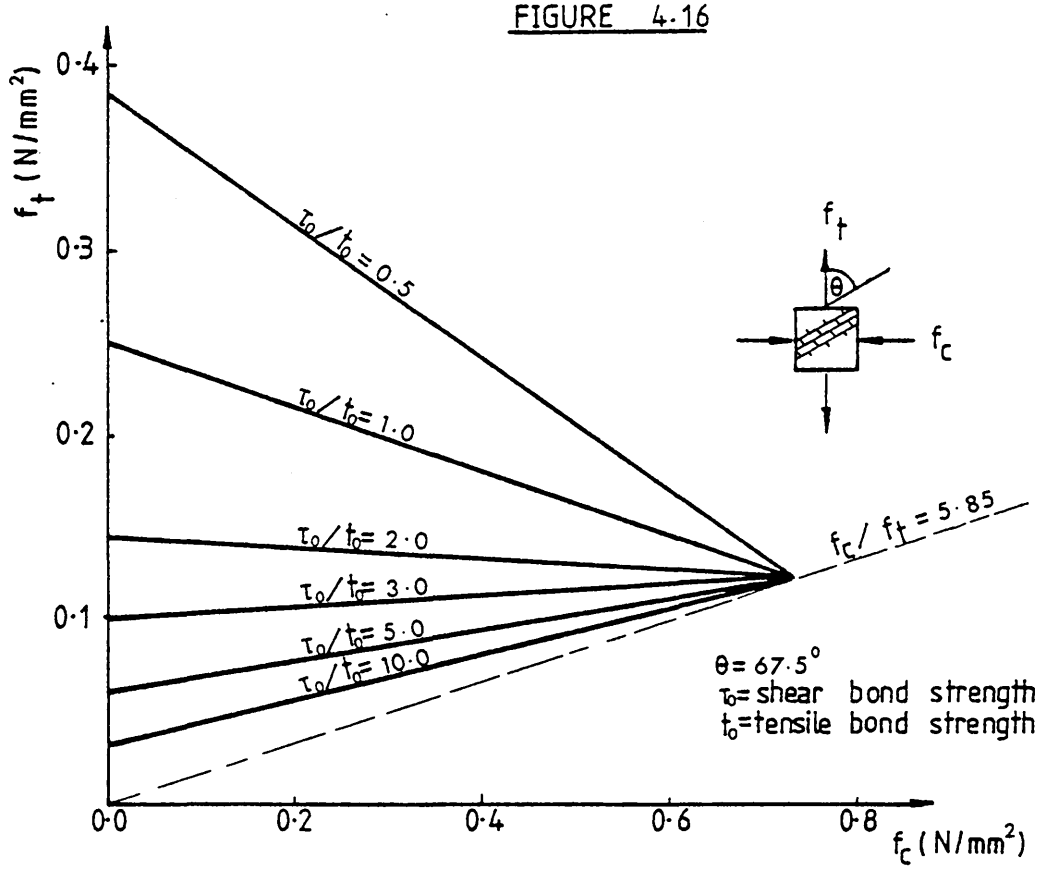

INFLUENCE OF τ_0/t_0 RATIO ON THE BIAXIAL STRENGTH AT LOW COMPRESSION

FIGURE 4·17

4.2.12 Generalizing the Failure Envelopes

As discussed in the preceding section, although the experimental curves have a positive gradient at very low compression, the theoretical gradient may be positive or negative, depending on the shear bond strength to tensile bond strength ratio in brick masonary. Many investigators have tried to establish a relationship between shear bond strength and tensile bond strength, in the past. Murthy[43] found in his experiments on model bricks and 1:3 cement mortar that bond shear was 2.3 times bond tension whereas Semenstov[64] suggested that it was 1.7 times bond tension. Polyakov[55] found that the ratio of bond shear to bond tension depends on the value of bond tension and give the relationship as follows:

$$\frac{\tau_o}{t_o} = 2.25 - 0.5\ t_o \text{ (units in kg/cm}^2\text{)}$$

where $\tau_o \leqslant 2.5$ kg/cm^2.

Sinha[64] suggested a relationship of the form

$$\tau_o = 8.8\ t_o^{0.5} \text{ (units in lbs/in}^2\text{)}$$

from the experiments carried out on one sixth scale model bricks for different degress of saturation of bricks. According to Page results[48] the tensile bond strength was higher than the shear bond strength, and his τ_o/t_o ratio was 0.83.

Therefore a standard relationship between shear bond strength to tensile bond strength is rather difficult to establish. As a result, in order to simplify and generalize the biaxial failure envelopes, a family of hyperbolic curves was derived from the exper-

imental curves. Four idealized curves were obtained for four bed joint orientations (θ) such as 0^o, 22.5^o, 45^o and 67.5^o. The suggested idealized envelopes are illustrated in Figure 4.18 and the equation of those curves are as follows:

$$f_t = 0.7e^{-0.14f_c} - C \qquad (4.10)$$

where C is a constant for a given value of θ. Thus,

θ =	0^o	22.5^o	45^o	67.5^o
C =	0.02	0.185	0.355	0.525

According to Figure 4.18 it appears that the tensile strength of brickwork decreases gradually as the compressive stress increases under a state of biaxial stress which is typical for a brittle material.

4.2.13 A General Failure Surface for Brickwork Under Uniform Biaxial Stresses

A three dimensional failure surface, from which failure at any point on a wall subjected to in-plane loads can be defined by the values of principal stresses (f_c and f_t) and inclination of the principal tensile stress to the bed joint direction, is usually more effective than a family of curves and a general failure surface is much easier to apply. Therefore an idealized failure surface was derived from the above set of curves for brickwork subjected uniform biaxial stresses. The surface equation can be written as:

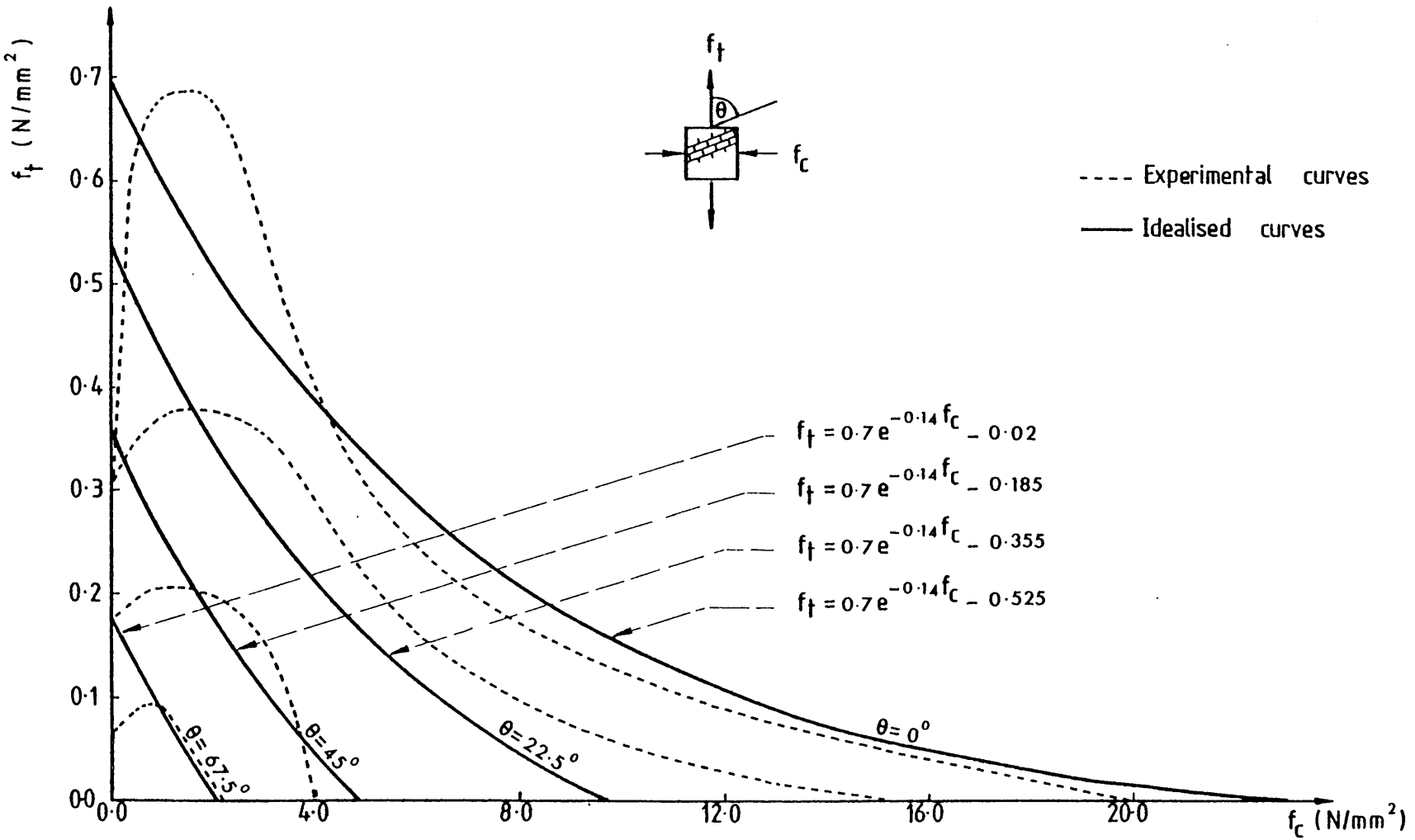

IDEALIZED BIAXIAL STRENGTH CURVES FOR BRICKWORK

FIGURE 4·18

$$f_t = 0.7e^{-0.14 f_c} - 1.34 \frac{\theta}{\pi} - 0.02 \qquad (4.11)$$

(units in N/mm^2)

f_t - principal tensile stress

f_c - principal compressive stress

θ - the angle between the direction of f_t and bed joints in radians.

This surface incorporates all the possible failure modes in biaxial tension-compression, namely joint failure, combined brick-joint failure and brickwork compression failure and has the form shown in Figure 4.19.

4.3 TESTS ON BRICKWORK UNDER NON-UNIFORM BIAXIAL STRESS FIELD

4.3.1 Introduction

In practice brick walls are not usually subjected to a uniform biaxial stress field. Therefore, in order to justify the applicability of the biaxial strength envelope obtained under uniform stress condition in a non-uniform stress field, a series of verification tests were carried out on shear walls. Shear walls are usually designed to withstand in-plane lateral loads which arise from wind loads or in seismic areas of the world from earthquakes. Many experimental and theoretical investigations have been undertaken in the past to explain the behaviour of shear walls when they are subjected to various combinations of shear and compressive loads , and it has been accepted that walls under such conditions are usually in a non-uniform, complex biaxial stress field.

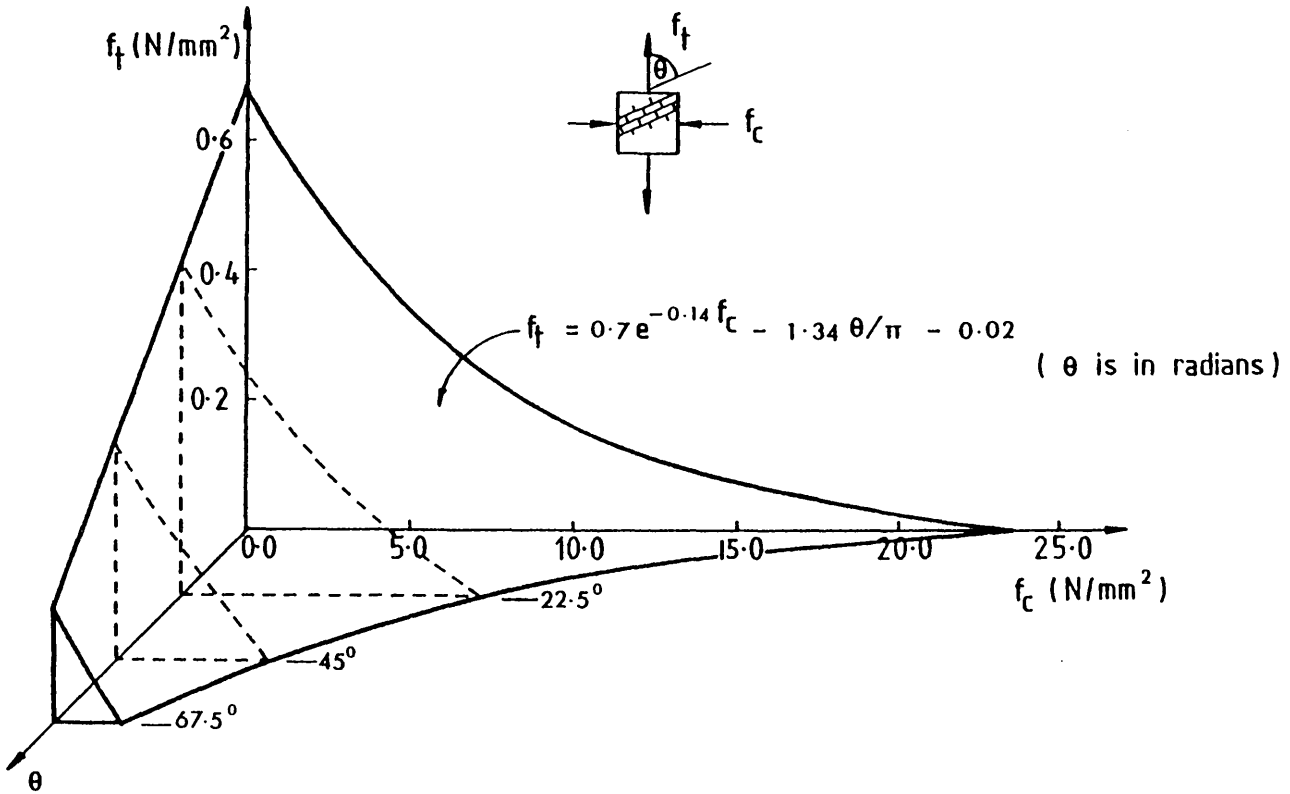

FAILURE SURFACE FOR BRICKWORK UNDER BIAXIAL STRESSES

FIGURE 4·19

If a wall is subjected to increasing in-plane loads up to failure, the initial failure will occur due to a critical combination of biaxial stresses, which may be tension-tension, tension-compression or compression-compression. Thereafter, progressive failure takes place in the joints and bricks wherever critical until the wall collapse, and all these local failures should satisfy the criterion for failure. However, in view of the experimental difficulties of determining the magnitude of stresses at such local failure points on the wall, a computer model was developed (as will be discussed in Chapter 5) incorporating the suggested failure criterion to predict the load at which initial failure take place. The model was capable of redistributing the stresses after each local failure and thereby predicting the other failure points as well. Thus the trend of the crack formation could be predicted. Hence, in this test programme shear walls were tested and the investigation was mainly concerned with obtaining the following information.

1. The ultimate strength of the wall.
2. The crack pattern.

A generally accepted approach to the behaviour of structural masonry under wind loading is best obtained from some form of 'racking test' on a complete wall. A test of this kind in its simplest form is one in which a horizontal load is applied in the plane of the wall at an upper corner together with a compressive load acting on top of the wall whilst it is prevented from sliding or rotating.

Usually a masonry wall under the action of racking load and precompression is subjected to biaxial compressive-compressive and tensile-compressive stresses. As the compressive load to racking load ratio increases (high compression) larger areas of the wall are subjected to biaxial compressive-compressive stresses, whereas when the ratio decreases (high racking load) the field of biaxial tensile-compressive stresses increases. Therefore, in order to produce a larger field of tensile-compressive stress, higher racking load to compressive load ratios were maintained in the experiments. However, high racking load to compressive load ratio produce high overturning moments and the system becomes unstable. Therefore the shear arm (distance to the racking load from the base of the wall) was varied to maintain the equilibrium of the specimen.

4.3.2 Preparation of Specimens

The method of construction of the wall specimens was identical to that already described in section 4.2.1. Five panels were manufactured from one-sixth scale clay bricks and 1:¼:3 (cement:lime:sand) mortar. Walls were 320 mm wide x 245 mm high x 18 mm thick in size. All the wall specimens were cured under the same condition as the test panels for the biaxial test. Usually two days before the test was performed, all the sides of the walls were capped with 1:1 cement mortar and white-washed.

Three 25 mm mortar cubes and two brick-mortar cubes were built with each wall as control specimens and cured as described in section 4.2.3.1.

4.3.3 Method of Load Application and Measurement

The horizontal racking load was applied to the specimen by a ten ton jack. The jack was rigidly fixed to a self restraining rig which had sufficient room to accomodate the shear wall. The arrangement of the specimen inside the test rig is illustrated in Figure 4.20. The rig was so constructed that the jack could be placed in five pre-determined locations on the vertical channel section to which the jack was fixed. The racking load was applied over an area of 18 mm x 25 mm (2 brick course high). Sliding of the wall was prevented by a block of steel placed at the bottom corner of the wall over a length of 25 mm along the vertical side of the wall. The vertical load was applied to the specimen, uniformly along its top side by a 340 mm long spreader beam (25 mm wide x 50 mm high). The wall was vertically loaded using an Instron testing machine.

The applied racking load was measured by a proving ring and the vertical load measured by a 10,000 kg load cell provided with the Instron testing machine.

4.3.4 Test Procedure

The specimen was carefully set up as illustrated in Figure 4.20. Friction reduction packings were provided at the top and bottom sides of the wall in order to minimize the effect of friction. Before the application of load, the vertical centre line was aligned with the centre of the circular platen of the Instron.

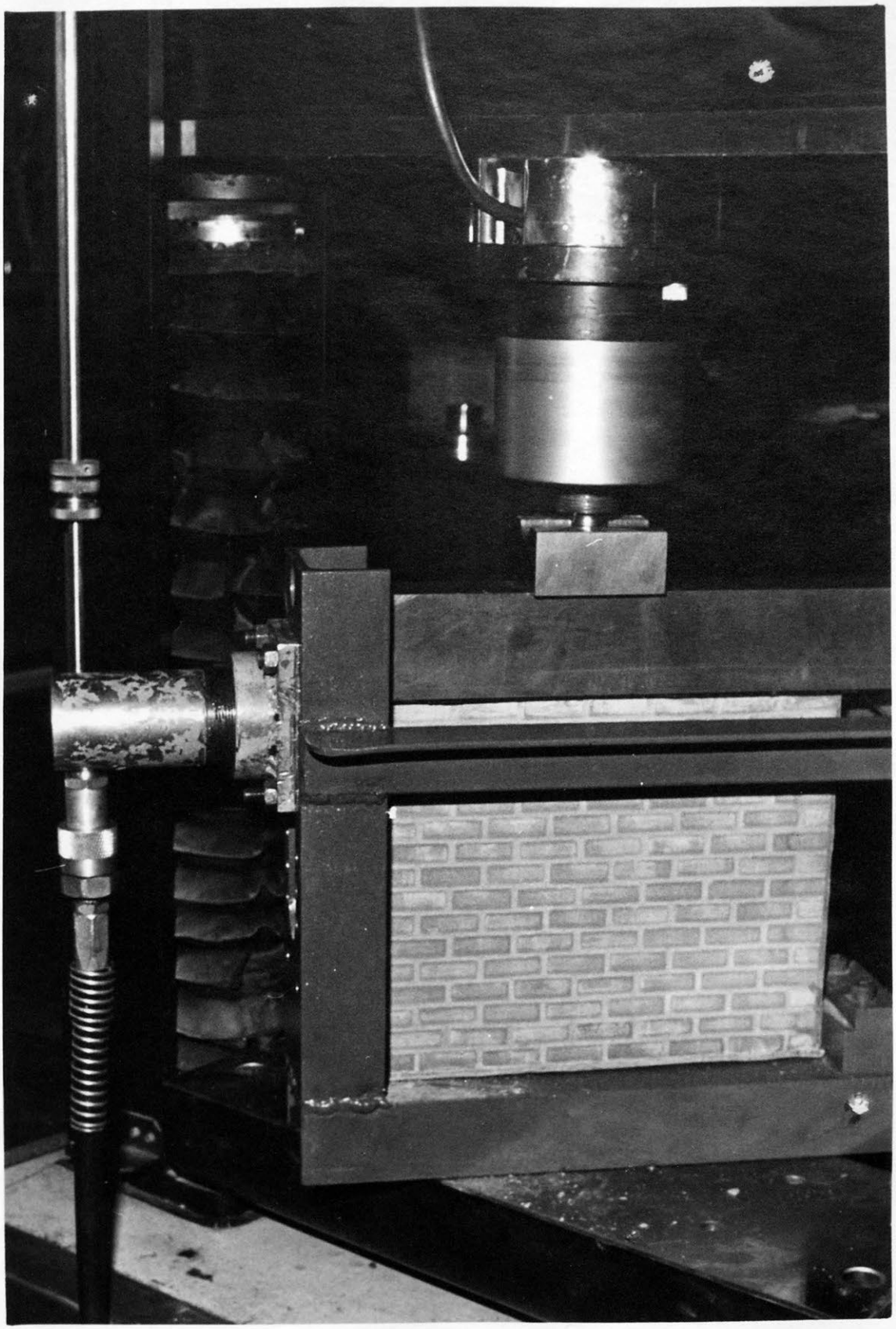

SHEAR WALL TEST

FIGURE 4.20

Both the compressive load and the racking load were gradually increased in increments up to failure whilst maintaining a constant loading ratio. In each load increment, the vertical load was applied prior to the racking load to maintain the stability of the wall and simulate the behaviour of shear walls in practice. The compressive load was applied at a rate of 0.02 mm/min. The racking load was applied very slowly and it was controlled manually. At the end of each load increment the wall was inspected to observe any formation and propagation of cracks.

Five specimens were tested. Five different ratios of vertical load (W) to lateral load (P) were selected ($W/P = \tan \alpha$) for testing the rectangular walls. For each case the position of the jack was different; 110 mm, 140 mm, 170 mm, 200 mm and 230 mm from the base of the wall when α equals 36^{o}, 43^{o}, 51^{o}, 56^{o} and 63^{o} respectively, thus producing shear arm/width ratios of 0.34, 0.44, 0.53, 0.63 and 0.72 respectively.

Control specimens were tested with each wall tested, as described in section 4.2.9.

4.3.5 Analysis of Results and Mode of Failure

The average vertical stress (σ_n) and the horizontal shear stress (τ_{av}) were computed using the following equations.

$$\sigma_n = W/A \qquad (4.12)$$

$$\tau_{av} = P/A \qquad (4.13)$$

where A is the bed joint area of the shear wall.

The average shearing stress at ultimate load (τ_{av}) was plotted against the corresponding average normal stress (σ_n) as shown in Figure 4.21, although the length of the wall to shear arm ratio has an important influence on ultimate strength capacity.[54] An increase of shear strength with an increase of compressive stress was observed.

The failure of walls was sudden and no visible cracks were shown beforehand. In general, the line of failure was inclined, stepping from one course to the next through the perpend joints. In some places, however, the failure crack was horizontal for some distance, specially at relatively high shear stress to normal stress ratios. The pronounced diagonal crack formed suddenly and extended from a zone at or near the horizontally loaded point to the lower corner of the wall adjacent to the stop. The load causing this crack was the maximum racking load corresponding to the applied normal stress to the bed joints. No cracks passed through brick units in any of the walls, with the failure in all cases being caused by the breakdown of bond between brick and mortar. This is due to the high shear stress/normal stress applied to the walls. The failure modes of all the walls are embodied in Appendix B.

For the sake of comparison of the results, the author has plotted some shear wall results obtained by Sinha-Hendry[26,28,64] and Chinwah[7] on one-sixth scale model structures, and shown in Figure 4.21. The results are seen to be in reasonable agreement although many factors which affect the shear strength of walls, such as, the shape of the walls, the shear arm/length of the wall, properties of the bricks at the time of building, were not the same in all tests.

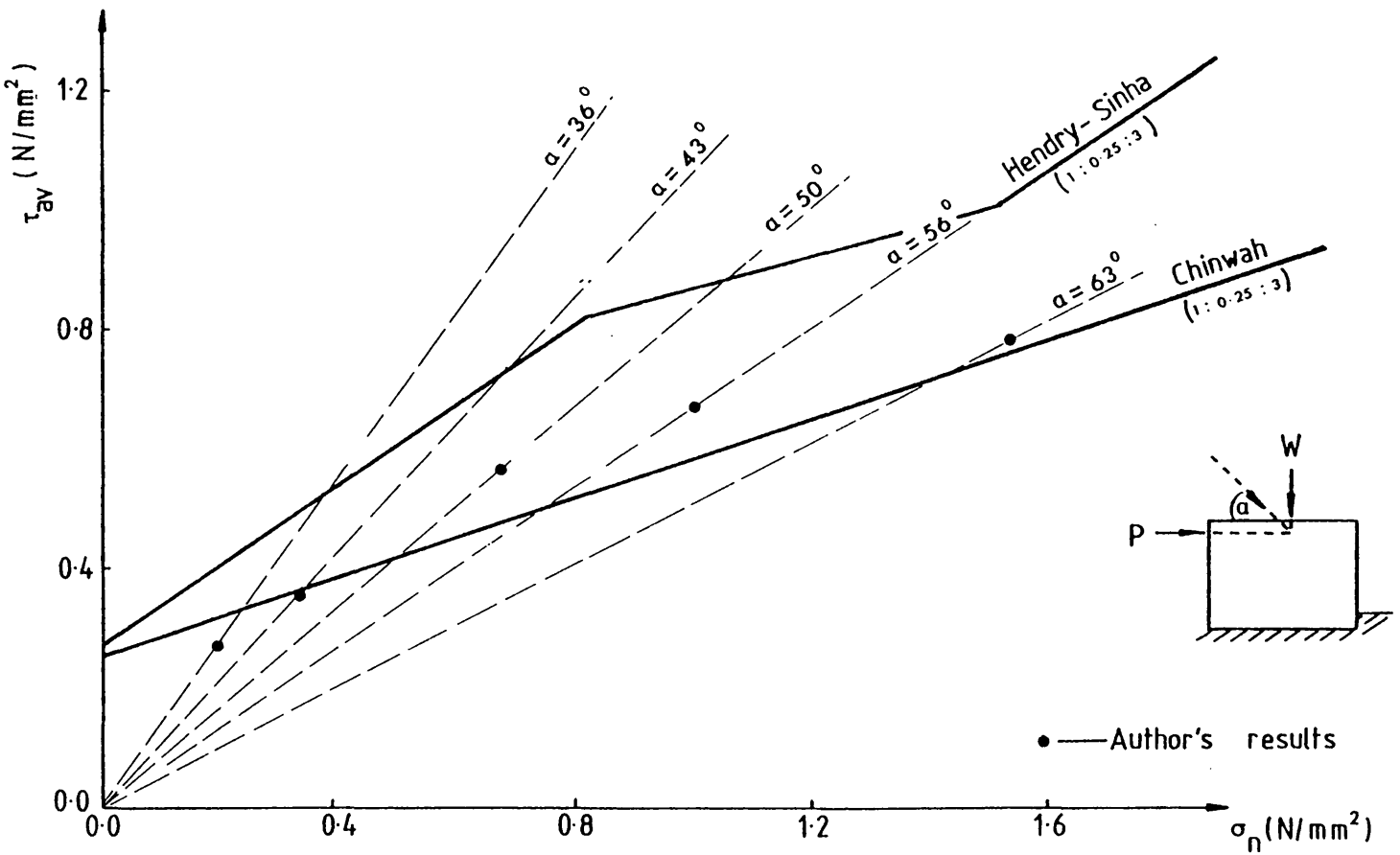

AVERAGE SHEAR STRESS Vs NORMAL STRESS AT FAILURE

FOR SHEAR WALLS

FIGURE 4·21

4.4 CONCLUSIONS

The biaxial strength of brickwork cannot be represented by a two dimensional relationship between σ_1 and σ_2 as for isotropic materials. Since brickwork strength is very much influenced by the presence of bed joints, the failure surface of brickwork in a state of biaxial stress has to be defined by a three dimensional surface in which the axes are the major principal stress, minor principal stress and their orientation relative to the bed joints.

When brickwork is subjected uniform biaxial stresses (tension-compression) failure may be initiated either at perpend or at bed joints depending on the inclination of the bed joints to the major principal stress direction (θ). If $\theta < 45^{o}$, the failure is initiated at perpend joints and the crack propagates either through brick units and perpend joints or in a zig-zag form if the brick units are relatively strong. If $\theta > 45^{o}$, the failure is initiated at a bed joint and the crack follows the bed joint right through. When θ equals 45^{o}, the stress distribution at bed and perpend joints are similar and failure could initiate at any point in the wall and follows the weakest path in the panel.

In the uniaxial compression test when θ changes from 45^{o} to 67.5^{o} the mode of failure changes from joint failure to brick-joint failure which causes a large drop in strength. However, although there is a change of failure mode in uniaxial tension test at 45^{o}, it does not greatly affect the strength.

The strength of brickwork in a state of biaxial stress is greatly affected by the direction of the principal tensile stress to the bed joints. The greater the inclination the lower is the strength of the brickwork. At low principal compressive stress

the shape of the strength envelopes are influenced by the shear bond strength to tensile bond strength ratio. When this ratio increases,the biaxial strength envelopes correspond to different bed joint orientations have a positive gradient whereas when the ratio decreases the gradient is negative, at very low precompression. As the principal compressive stress increases, the principal tensile strength decreases gradually, at high compressive stresses.

No conclusion can be drawn about the shear wall behaviour since only few experiments were carried out for the sake of testing the applicability of the biaxial strength envelope obtained under uniform stress condition in a non uniform stress field. This will be discussed in Chapter 6.

CHAPTER FIVE : A THEORETICAL MODEL FOR THE IN-PLANE BEHAVIOUR OF BRICKWORK

5.1 INTRODUCTION

The main object of this chapter is to describe the development of a computer model using the finite element analysis to predict the initiation of structural failure of brickwork subjected to non uniform stresses. To date, no theoretical model has been developed to explain the complete behaviour of brick masonry, under in-plane loads, due to the non-availability of a sound failure criterion. As has been discussed before, in order to predict the failure of a masonry wall, failure criteria in the stress regions, tension-tension, tension-compression, compression-compression are required. However due to the lack of knowledge in the area of compression-compression and tension-tension stress regions, this theoretical model was developed to use only for the cases where failure is governed by biaxial tensile and compressive stresses.

The following sections explain briefly the different simplifying techniques adopted in the past for the analysis of masonry structures using the finite element method. The basic features of a non-linear elastic model which is developed from a linear elastic model has been discussed. Non linearity in the constitutive laws are ignored whereas non-linearity due to progressive cracking is considered.

The analytical results were compared with experimental results using shear walls. The sensitivity of elastic constants used in the present model are studied.

5.2 REVIEW OF PREVIOUS METHODS OF ANALYSIS

The behaviour of brickwork under in-plane loads has been under investigation for many years and in most of the cases simplified empirical formula have been suggested for design purposes. The majority of work has been carried out in the area of shear walls and walls supported on elastic foundations and beams. The experimental methods are costly and involve a vast array of different geometrical configurations of masonry as well as different boundary conditions. As a result the introduction of finite element method of analysis to brickwork became the most popular and efficient analytical tool during the last decade. It was capable of studying the influence of various parameters on the strength of brickwork at comparatively low cost. However, due to the complication of simulating the behaviour of actual structural components, a number of simplifying assumptions have been made in the analytical methods. The simulation of behaviour of masonry walls and the assumptions that have been made in the past in the finite element method of analysis will be briefly reviewed in this section.

Due to the non-availability of comprehensive information on the fundamental properties of brickwork, most finite element methods of analysis were confined to linear, elastic analysis, in the past. During the early days, it was believed that the strength and the deformation behaviour of walls were influenced by the induced stresses and therefore for a better understanding of the brickwork behaviour, the stress distribution for a given loading condition was studied using elastic analysis.

In 1969, a typical elastic analysis using triangular plane stress element with a linear displacement function was carried out by Male and Arbon [39] as a part of a large programme of research into the problems of house foundations. The stresses at various load levels were calculated with some allowance being made for redistribution due to failure of the joint between the wall and its supporting beam and a reasonable agreement was obtained between experimental and theoretical results. The effect of a typical door opening on stress distribution, the interaction between wall, footing and soil were also studied with relative ease.

A linear elastic finite element method has also been used by Saw [57] in 1974 to study the interaction between walls and their supporting beams. He developed macro elements to achieve a more economical solution rather than using a large number of small elements or higher order displacement functions which lead to a large set of equilibrium equations for the whole structure. The macro elements consisted of large numbers of lower order finite elements, and in the analysis the internal nodes of these subregions were eliminated to achieve a complex element comprising only boundary nodes. Later, mid-side nodes were eliminated to give rise to a new complex element in which only the corner nodes were involved. This type of a finite element can be relatively large and economic in computer time. Although the model adopted was not necessarily representative of the behaviour of brickwork, it was an improvement over the previous analysis.

Linear, elastic finite element analysis was used by Riddington et al.[77] in 1977 to study the stress distribution at various load levels of infilled masonry walls subjected to racking loads. The basic four node rectangular element with linearly varying displacement function along the boundaries was used. In order to simulate the boundary cracks between the frame and the wall, the adjacent node pairs at the interface of the frame and the infill were connected by very short linkage elements. The influence of various parameters were investigated such as separating and non separating and frictional and non frictional boundaries, varying length to height infill ratios, various frame stiffness etc.

In the above mentioned analysis, brickwork was treated as a uniform and isotropic material and the effect of weak mortar joints was completely ignored. In all cases, the elastic continuum was divided into rectangular, square or triangular elements and average elastic properties were assumed for both brick and mortar. However, for the first time Stafford Smith et al.[72 73 74 75 76] treated brickwork as a two phase material with brick and mortar and elastic constants (Youngs Modulus and Poisson's ratio) varied from brick elements to mortar elements, thus allowing mortar elements to be clearly distinguished from those of brick. The influence of various parameters on the strength of brickwork such as brick/mortar modular ratio, joint thickness and types of bonds could be studied with more ease than was previously possible by other methods of analysis. However, the use of narrow and long elements for the simulation of mortar

joints creates the well known aspect ratio problem and does not allow for the possible variation of stress within the thickness of the joints.

Until the recent past, all the analytical methods were used to calculate the stress distribution in masonry assemblages for a given loading condition rather than predicting the ultimate failure. This was simply due to the non-availability of a sufficiently representative failure criterion for masonry. Recent attempts at predicting failure of masonry have been published by Ganju [17], in which brickwork is modelled as a strain hardening, elastic-plastic material. A yield criterion based on the generalized Mohr-Coulomb was used and the failure was defined by a limiting value of strain. Constant strain triangular finite elements were used in conjunction with the initial stress technique, and bricks and mortar were not modelled separately so that the influence of weak mortar joints was not reflected in the model.

A finite element model which was capable of predicting joint failure of a in-plane loaded brick wall was first developed by Page [48 49 50 51]. The model reproduces the non-linearity and progressive joint failure. The masonry was considered as an assemblage of elastic brick continuum elements acting in conjunction with linkage elements simulating the mortar joints. The bricks were modelled using conventional eight parameter rectangular plane stress elements with four internal degrees of freedom and isotropic elastic properties. The joint elements were assumed to have non-linear deformation characteristics with limited shear and tensile capacity. The deformations of

the joints were limited to normal and parallel to the joint direction, so that only normal and shear stresses could be transmitted across the joint. A Coulomb type failure criterion was used in the model and failure at a joint was defined when the shear or tensile bond criterion was exceeded. A shear bond failure was simulated if the failure occurred in combined shear and compression. A tensile bond failure was simulated if the failure occurred under a combination of shear and tensile stress. In the latter case, the stiffness of the joint at failure was assumed as zero. In a shear bond failure, the stiffness of the joint in the normal direction was assumed to remain unchanged and a reduced shear stiffness was allocated to simulate the frictional resistance of the joint after an initial shear bond failure. Although Page's theoretical model was successful in predicting the crack propagation and the ultimate failure load of an in-plane loaded wall, the inability to predict the combined brick-joint failure was a limitation.

A more sophisticated and representative analytical model was recently developed by Arya and Hegmier [2] on non-linear response predictions of concrete masonry assemblies. An incremental finite element method based on tangent stiffness method was adopted. At each end of load increment checks were made for slipping at the interfaces and cracking and crushing of the masonry elements. The material model developed was two dimensional and was limited to plane stress conditions. The concrete masonry was assumed to be elastic and brittle in tension and strain softening to occur in compression. The von-Misses yield criterion was used for failure in compression and the maximum

tensile stress theory was adopted for cracking due to tension. When the material was loaded in compression beyond the yield curve, another failure curve which gradually shrinks to the origin was assumed. The amount of shrinkage was defined as a function of the principal strains. A complete collapse in compression was assumed when the masonry lost all strength and stiffness. When the masonry was cracked in tension, the stresses only parallel to the cracks were allowed to transmit and the compressive strength parallel to the crack was reduced after a certain crack width. The problem of aspect ratio in modelling narrow mortar joints has been overcome by introducing a series of double nodes, one on each side of the interface, but having the same co-ordinates. If the nodal force at a double node pair was tensile and if it exceeded the tensile strength of a pair, a nodal point separation was assumed. Thus they were treated as free nodal points, and no force was transmitted by such a nodal pair. When the normal force at the interface was compressive, shear force between the nodes were allowed to transmit while allowing them to displace independently as long as the shear force between the nodes were less than or equal to the shear strength. The shear strength of a nodal pair was defined by Coulomb friction law. The coefficient of friction and the cohesion were assumed to be functions of relative tangential movement at the interface. The geometric non-linearity was neglected and the nonlinearity due to progressive cracking was considered.

5.3 FINITE ELEMENT METHOD

The finite element method is essentially a generalization of standard analysis procedures which permits the calculation of stresses and deformations in two and three dimensional structures. The basic concept of this method is that a structure may be considered to be an assemblage of individual structural elements. Thus the structure consists of a finite number of such elements, interconnected at a finite number of nodal points. Therefore the approximation which is employed in this case is of a physical nature; a modified structural system is substituted for the actual continuum. There need be no approximation in the mathematical analysis of this substitute system. This feature distinguishes the finite element technique from finite difference methods, in which the exact solutions of the actual physical system are solved by approximate mathematical procedures.

There are two main approaches; the displacement method and the force method. Detailed treatment of these and other approaches have been given in various publications by Zienkiewicz [85], Desai and Abel [12] and others. Of these methods the displacement method appears to be most widely used. In this case, the nodal displacement of the elements are the basic unknowns, while stresses and strains are assumed constant for each finite element. The basic steps of the displacement method can be summarized as follows:

(a) Division of continuum into finite elements.

(b) Representation of its nodal displacements, thus defining the state of stress and strain in the elements.

(c) Formulation of the stiffness matrix of the element hence the complete stiffness matrix of the whole structure.

(d) Setting up and solving the final equilibrium equations for the whole structure to calculate the unknown nodal displacements of the elements.

(e) Evaluation of stresses and strains from the nodal displacements calculated in section (d).

Thus the whole process invariably results in the formation of a large number of simultaneous equations in terms of the properties of the material of the continuum and the displacement or strain at discrete points. However, the availability of large high speed electronic computers with their vast capacity for solving simultaneous equations have now offered the means by which an approach can be made to solve the problems of stresses and displacements of structures using finite element method of analysis.

5.4 NON-LINEAR BEHAVIOUR OF BRICKWORK

Non-linear behaviour in structural systems can be placed in one of three categories.

1. Geometric non-linearity, arising from both non linear strain displacement relations, and from finite changes in geometry.

2. Material non-linearity, arising from non-linearity in the constitutive equations.

3. Combined geometric and material non-linearity.

Non-linearity in brickwork is caused by material non-linearity and progressive cracking either in the bricks and joints or in the joints. However, it has been reported by Page [48 51] that the non-linearity caused by constitutive laws were insignificant compared to the progressive cracking. Phillips and Zienkiewicz [53] in a recent non-linear analysis of reinforced concrete have also found that the tensile crack formation, rather than concrete material properties, was the predominant cause of non-linear behaviour. As a result the material non-linearity was ignored in this analysis and brickwork was considered as a linearly elastic material with average properties.

5.5 THE ADOPTED FINITE ELEMENT MODEL

A linear elastic finite element model developed by Page [48] was used in the present analysis but the model was completely modified to allow for the effect of non-linearity due to progressive cracking. Eight parameter rectangular plane stress elements with four internal degrees of freedom, connected at nodal points were used to represent the brickwork continuum. A portion of typical element subdivision is shown in Figure 5.1.

5.5.1 Displacement Function

The displacement within the element is defined by the following displacement functions:

$$u = \alpha_1 + \alpha_2 x + \alpha_3 y + \alpha_4 xy + \beta_1 (a^2-x^2) + \beta_2 (b^2-y^2)$$

$$v = \alpha_5 + \alpha_6 x + \alpha_7 y + \alpha_8 xy + \beta_3 (a^2-x^2) + \beta_4 (b^2-y^2) \qquad (5.1)$$

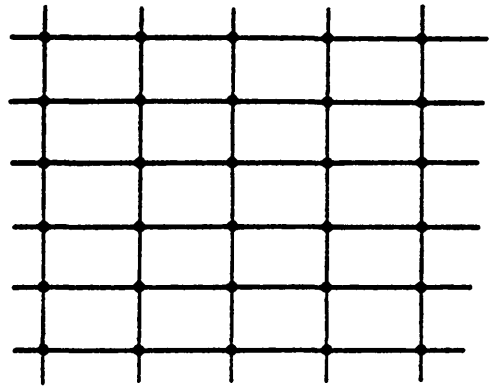

(a) Finite Element Subdivision

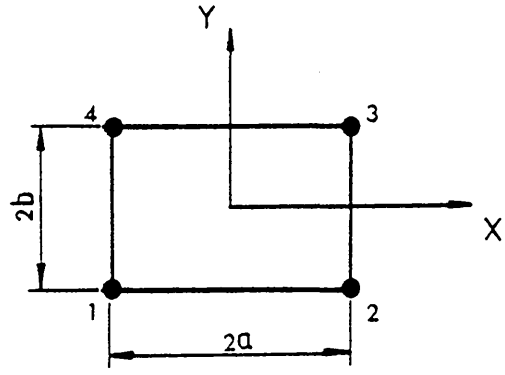

(b) Rectangular Element Details

TYPICAL FINITE ELEMENT SUBDIVISION

FIGURE 5.1

The element properties can be defined from these displacement functions and equation (5.1) can be written in matrix form as;

$$\begin{Bmatrix} u \\ v \end{Bmatrix} = \left[\begin{array}{cccccccc|cccc} 1 & x & y & xy & 0 & 0 & 0 & 0 & (a^2-x^2) & (b^2-y^2) & 0 & 0 \\ 0 & 0 & 0 & 0 & 1 & x & y & xy & 0 & 0 & (a^2-x^2) & (b^2-y^2) \end{array}\right] \begin{Bmatrix} \alpha_1 \\ \alpha_2 \\ \vdots \\ \alpha_8 \\ \hline \beta_1 \\ \vdots \\ \beta_4 \end{Bmatrix}$$

$$\text{i.e.} \quad \{t\} = [Z]\{c\} \qquad (5.2)$$

Using equation (5.1), the nodal displacements of the element can be related to the element displacement {t} as;

$$\{n\} = [Z_n]\{c\}$$

$$\therefore \quad \{c\} = [Z_n]^{-1}\{n\} \qquad (5.3)$$

By substituting equation (5.3) into (5.2)

$$\{t\} = [Z][Z_n]^{-1}\{n\}$$

$$= [P]\{n\} \qquad (5.4)$$

5.5.2 Derivation of Element Stiffness Matrix

The strain in each element can be defined by three components, and those can be expressed by nodal displacements.

$$\{\varepsilon\} = \begin{Bmatrix} \varepsilon_x \\ \varepsilon_y \\ \varepsilon_{xy} \end{Bmatrix} = \begin{bmatrix} \partial/\partial x & 0 \\ 0 & \partial/\partial y \\ \partial/\partial y & \partial/\partial x \end{bmatrix} \begin{Bmatrix} u \\ v \end{Bmatrix}$$

i.e. $\{\varepsilon\} = [s]\{t\}$

$= [s][P]\{n\}$

$$\{\varepsilon\} = [B]\{n\} \qquad (5.5)$$

Similarly the stress in each element can be defined by three components.

$$\{\sigma\} = \begin{Bmatrix} \sigma_x \\ \sigma_y \\ \tau_{xy} \end{Bmatrix} = [D] \begin{Bmatrix} \varepsilon_x \\ \varepsilon_y \\ \gamma_{xy} \end{Bmatrix} = [D]\{\varepsilon\} \qquad (5.6)$$

where $[D]$ is an elasticity matrix for plane stress, isotropic material which is given by;

$$[D] = \frac{E}{1-\nu^2} \begin{bmatrix} 1 & \nu & 0 \\ \nu & 1 & 0 \\ 0 & 0 & \frac{1-\nu}{2} \end{bmatrix}$$

Substituting from equation (5.5), the element stresses can be expressed by nodal displacements.

$$\{\sigma\} = [D][B]\{n\} \qquad (5.7)$$

The total potential energy of an element subjected to body forces can be expressed as;

$$U = \int_{vol} \tfrac{1}{2}\{\varepsilon\}^T\{\sigma\}dv - \int_{vol} \{t\}^T\{F\}dv \qquad (5.8)$$

The last integral represents the work done by body forces {F} over the displacement of the element and the first integral represents the work of internal stresses.

By substituting equations (5.4), (5.5) and (5.7) into (5.8),

$$U = \tfrac{1}{2}\{n\}^T \int_{vol} [B]^T[D][B]\,dv.\{n\} - \{n\}^T \int_{vol} [P]^T\{F\}dv.$$

From the principal of minimum potential energy,

$$\frac{\partial u}{\partial \{n\}} = 0$$

$$\therefore \int_{vol}[B]^T[D][B]\,dv \;\{n\} = \int_{vol}[P]^T[F]\,dv$$

i.e. $[K]\{n\} = \{f\}$

where the element stiffness matrix $[K]$ is defined by;

$$[K] = \int_{vol}[B]^T[D][B]\,dv$$

The stiffness matrix for the whole structure is obtained by the summation of the contribution from each element.

5.5.3 Structure of the Computer Programme and Operation

The computer programme is used to study the behaviour of brickwork under in-plane loads and to predict the initiation of failure under a stress state of biaxial compression-tension. The propagation of cracks and the stress levels at which those cracks take place can be predicted reasonably well. The programme

is capable of handling problems related to walls, with or without openings. It can also be used to analyse walls supported on elastic beams.

As has been stated previously a linear material law was assumed for brickwork and non linearity due to progressive cracking introduced. Thus for each incremental load an iterative procedure was involved to allow for the changing structure stiffness as elements locally failed under biaxial tension-compression stresses.

The Figure 5.2 shows the logic of the programme. The computer programme is listed in Appendix C and it was coded in FORTRAN IV language. It was run at the Edinburgh University computer centre on a ICL 2980 computer. The necessary input data for the programme with their respective format is listed in Appendix C.

5.5.3.1 Explanation of Subroutines

As has been illustrated in the flow diagram, the problem is initially described in subroutine GENNOD and SUPPTS which define the geometry and the boundary conditions of the structure. The subroutine GENNOD reads the nodal co-ordinates along the reference axes (x and y). Element numbers and the member incidences are generated automatically from the number of x and y co-ordinates along the axes. The geometric boundary conditions are identified in the subroutine SUPPTS.

The main function of the subroutine REM4 is to compute the element stiffness matrix of eight parameter rectangular plane stress elements. The material properties are read and printed at the first load increment. Finally subroutine ASSMBL is called to insert the element stiffness matrices into structure stiffness matrix.

FLOW DIAGRAM OF THE COMPUTER MODEL

FIGURE 5.2

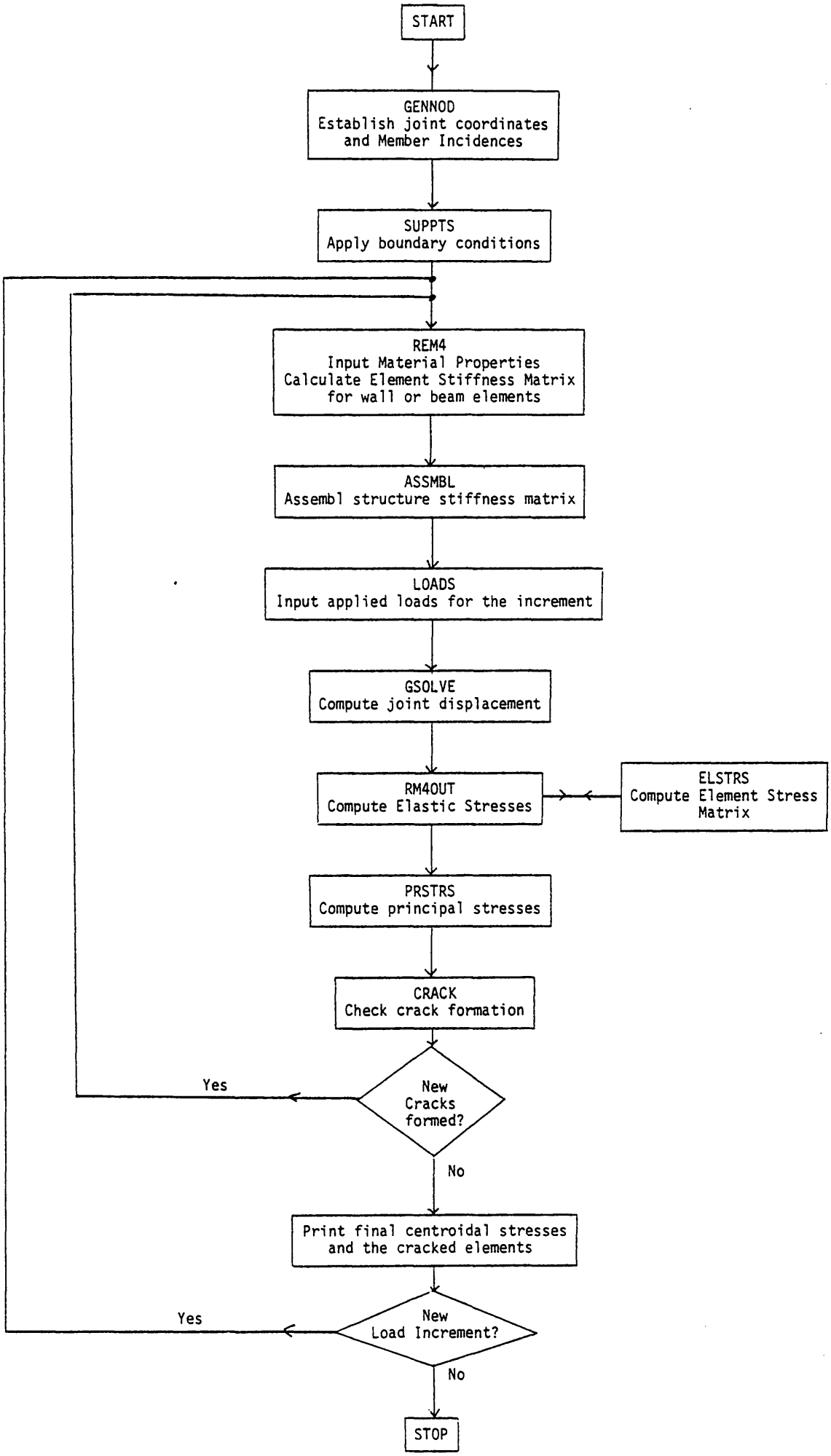

The magnitude, direction and location of the external applied loads are read for the first increment of loading and stored for later use in subroutine LOADS. For each iteration the total load is calculated and printed.

The subroutine GSOLVE determines the nodal displacements {n} from;

$$\{f\} = [k]\{n\}$$

where {f} is the vector of nodal forces and [k] is the structure stiffness matrix. Gaussion elimination technique is used to reduce the structure stiffness matrix into triangular form and then displacements can be calculated for any set of applied loads by the sequential operations of forward elimination and back substitution.

Element stresses due to the incremental load are computed in subroutine RM4OUT from the nodal displacements {n} using the expression;

$$\{\sigma\} = [STR]\{n\} .$$

Subroutine ELSTRS is called within RM4OUT to calculate the stress matrix for each element, where

$$[STR] = [D][B]$$

The total element stresses due to the applied loads are computed by adding the incremental stress to the stress created by previous load increments, and PRSTRS is called to calculate the magnitude and the direction of principal stresses.

Subroutine CRACK is called from RM4OUT and each element is checked for violation of principal stress failure criterion. The failure criterion adopted has been discussed in detail in Chapter 4. When the angle made by the principle tensile stress with the bed joints (θ) is between 67.5^{o} and 90^{o}, a constant value of 0.1 N/mm^2 for the tensile strength of brickwork is assumed irrespective of the value of θ and the magnitude of principal compressive stress. When $0^{o} < \theta < 67.5^{o}$ the tensile strength is computed from;

$$f_t = 0.7e^{-0.14\, f_c} - 1.34\,\frac{\theta}{\pi} - 0.02$$

where f_c is the principal compressive stress in N/mm^2 and θ is the angle in radians.

The elements under biaxial compression are ignored since there is no failure criterion available to predict the failure. Moreover, it is not critically important in predicting the initiation of failure as isotropic materials are generally stronger in biaxial compression than in biaxial tension-compression, unless the whole structure is in a state of biaxial compression.

If any element violates the criterion for failure, the element number is stored to allow for modification of its stiffness properties before the next iteration. Since failure is due to tension, the residual strength capacity is taken as zero, and very low stiffness is assumed for the element. Although the masonry cracked in tension is capable of resisting stresses parallel to the cracks up to a certain crack width, it was ignored in this analysis. After the formation of cracks the structure stiffness is amended accordingly and the problem is

resolved. This iteration continues until no further cracks appear and final convergence has been achieved for the particular load level of applied load. The whole process is repeated for each required loading increment.

5.6 TESTING THE VALIDITY OF FAILURE CRITERION USING THE ANALYTICAL MODEL

Shear walls were solved analytically under the combined action of precompression and racking load. The loads at the initiation of failure and the crack propagation were predicted using the analytical model. The theoretical results were compared with the experimental results obtained from the shear wall tests described in Chapter 4. The shape and size of the walls, the loading and supporting conditions, adopted in the theoretical analysis were the same as in the experiments.

Each test was designed to produce a complex state of biaxial stress within the walls which were different from each other. The stress state could therefore be assumed more general than that present in a specimen under uniform stress condition from which the criterion for failure under biaxial tension-compression was developed. Hence, if agreement was obtained between experimental and analytical model, the idealized failure envelope suggested in Chapter 4 could be considered reasonable, at least to predict the shear wall behaviour.

5.6.1 Idealization of brickwalls

The idealized wall for the analysis is shown in Figure 5.3 and it consisted of 272 elements connected at their nodal points. A thin row of elements was introduced at the base of the wall in

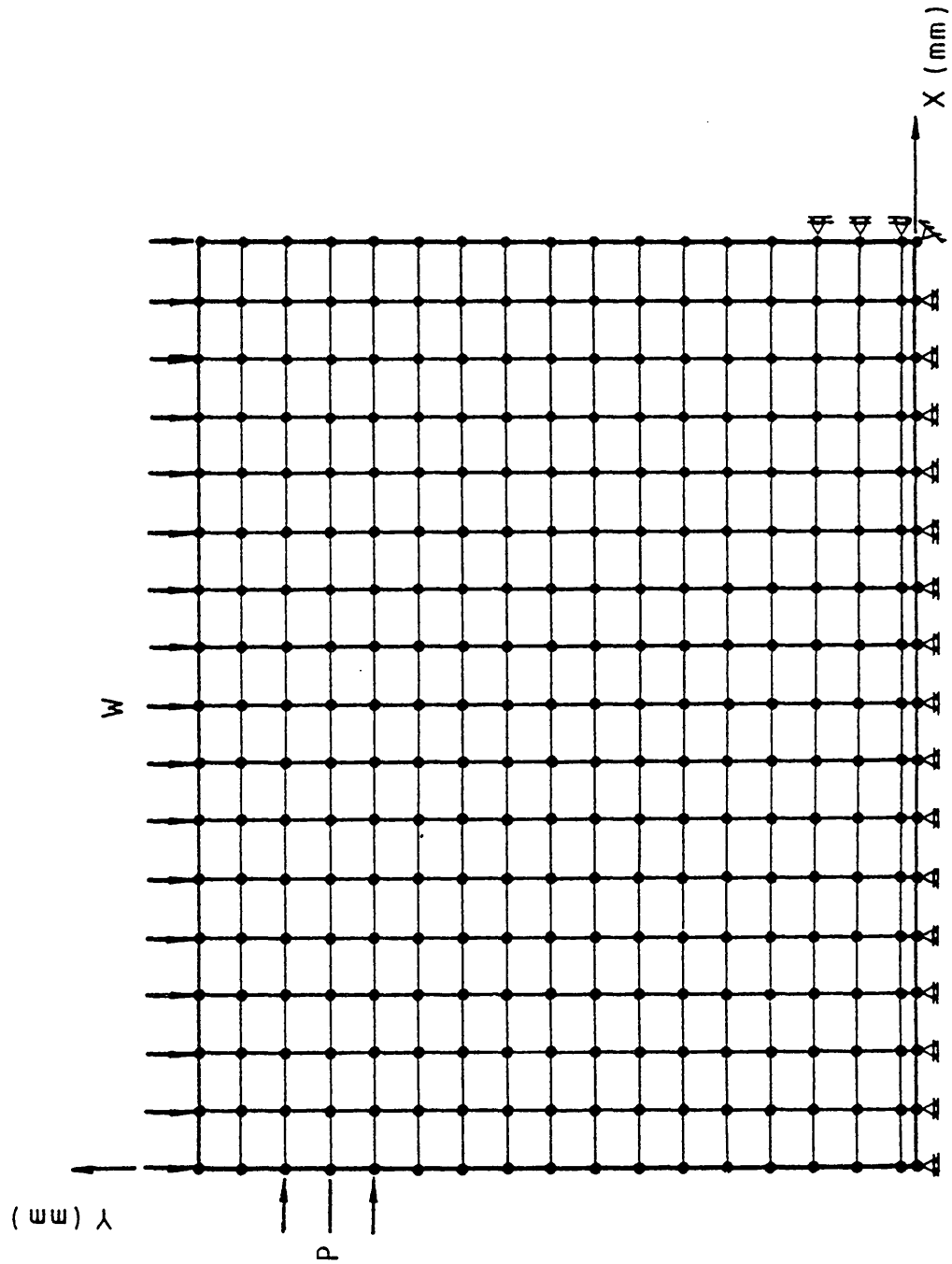

AN IDEALIZED SHEAR WALL FOR ANALYSIS

FIGURE 5.3

order to predict the boundary tensile cracks. The vertical load and the racking load were assumed to be uniformly distributed over the contact area and those were simulated by concentrated loads at the nodal points as shown in Figure 5.3. The nodes at the base of the wall were supported on rollers except at the diagonally loaded bottom corner, allowing for horizontal displacements.

Initially a constant value of 7000.0 N/mm^2 was assumed as the modulus of elasticity of all the brickwork elements. This was an average value obtained from uniaxial compression tests on test panels with different bed joint orientiations to the applied load. As the elements failed locally with the increase of applied loads, a very low stiffness ($E = 0.001\ N/mm^2$) was assumed for the cracked elements. A value of 0.2 has been used for Poisson's Ratio.

Tilting of the wall in this sort of a test commonly occurs due to the presence of racking load, specially if the compression is relatively low. In all cases, a tensile crack formed for some distance along the thin row of boundary elements. To stimulate the tilting of the wall, the restraints in this region were released in subsequent iterations.

5.6.2 Analytical Results

Five shear walls were analysed using the computer model. The magnitudes and the directions of the stresses of the elements were printed for each load increment before the initiation of new cracks. The load increment for each case was different as indicated in Figure 5.4(a) to Figure 5.4(e) which illustrate

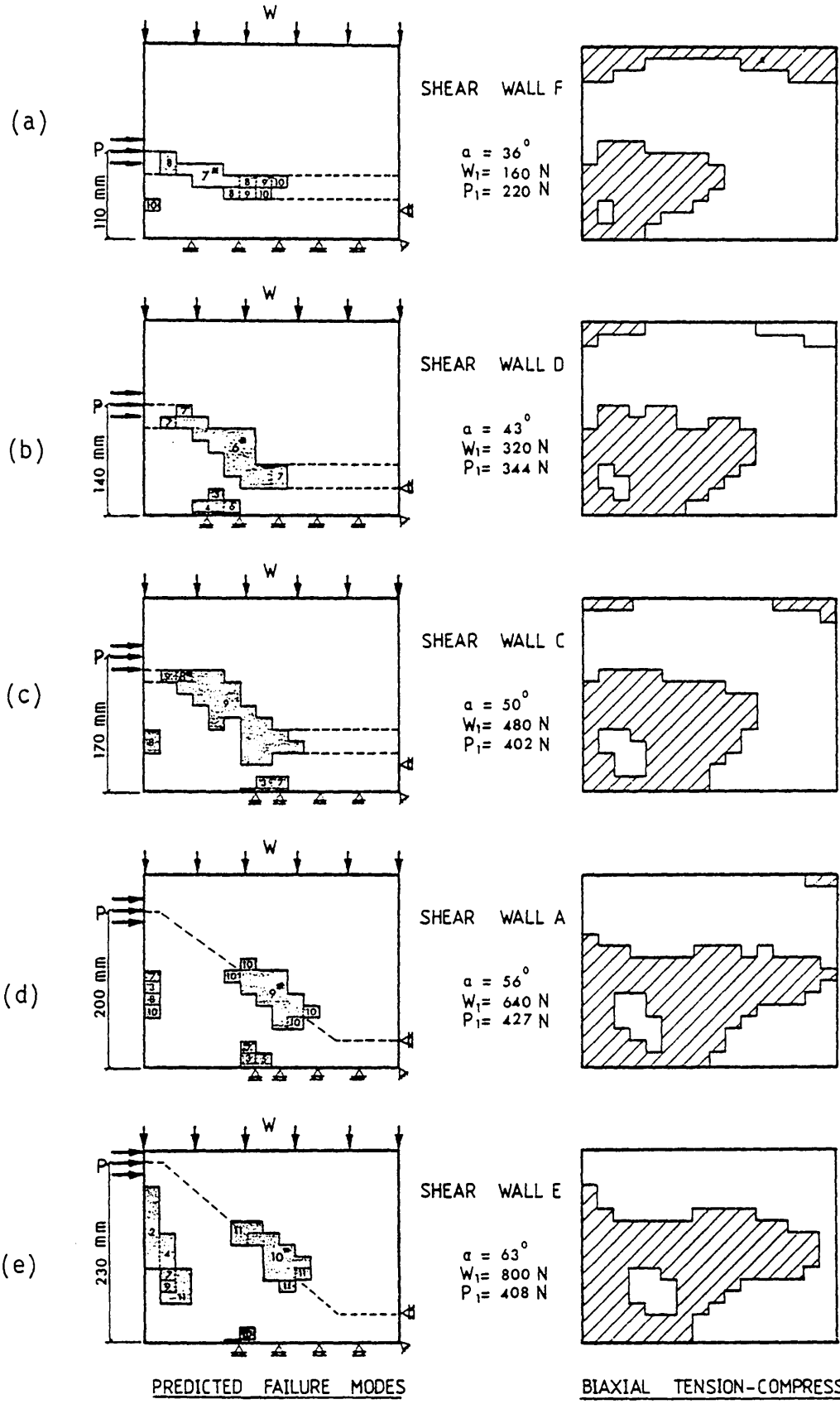

$\alpha = \tan^{-1}(W/P)$
W_1 = The value of W at 1st load increment
P_1 = The value of P at 1st load increment
* : Number of load increments at the initiation of structural failure
▨ : Biaxial tension-compression stress region at the initiation of structural failure
▭ : Biaxial compression-compression stress region at the initiation of structural failure
Panel size : 320 mm wide × 345 mm high × 18 mm thick

CRACK PROPAGATION IN SHEAR WALLS

FIGURE 5.4

the predicted crack pattern. The cracked elements are indicated by the shaded areas and the level of load increment at which the crack took place is indicated within the cracked elements. The probable failure mode has been indicated by a broken line.

It was observed from the cracking sequence, in some walls at the initial stages of load increments, that local cracks tend to appear near to the horizontally loaded edge of the wall. These are caused by the tensile bending stresses generated by the racking load. In brick walls, due to poor tensile bond strength between bricks and mortar, such cracks could very well occur within the joints. However, in this theoretical model it cannot be predicted since bricks and mortar joints have not been modelled separately. In the tests carried out on shear walls such cracks could not have been seen, with the naked eye.

In each wall initiation of major cracks was indicated in the vicinity of the line joining the toe of the wall and the point at which the racking load was applied. Once a crack is initiated, redistribution of stresses takes place in its vicinity and many more cracks appear along the same line to either side of the first crack.

A study of the distribution of stresses at the initiation of failure indicated that most of the area of the walls was in a stress state of biaxial compression, as has been indicated in Figure 5.4(a) to Figure 5.4(e). Thus, ultimate failure load and the complete mode of failure cannot be predicted without a criterion for failure under a biaxial compression stress state. Due to the lack of data a possible failure surface for brickwork under biaxial compression was assumed from the uniaxial

compressive strength values at different bed joint orientations. This has been illustrated in figure 5.5. By comparing the magnitudes of the principal compressive stresses and their directions with this idealized surface, it was found that the element stresses at the toe and the horizontally loaded area of the wall were high enough to crush the elements, at the initiation of the failure. Therefore, after the initiation of structural failure, the ultimate failure may take place very soon in shear walls.

5.6.3 Comparison of Analytical Results with Experimental Results

In order to compare the theoretical results with experimental results, average normal and shear stresses were computed from the analytical results at the initiation of failure. The average shear and normal stresses obtained, at the ultimate failure from experiments and at the initiation of failure from analysis, were plotted and shown in Figure 5.6. The theoretical and experimental results exhibited a reasonable agreement, particularly in view of the inherent variability of the material. A greater deviation of the experimental and predicted failure stresses were observed as the precompression increases. This may be due to the fact that ultimate failure does not take place immediately after the initiation of failure when the wall is subjected to high precompression.

The author's results were compared with some other published results. The average normal and shear stresses obtained from model and full-scale shear walls by Sinha [68], Chinwah [7] and Murthy [46] are shown in the same graph (Figure 5.6) with the

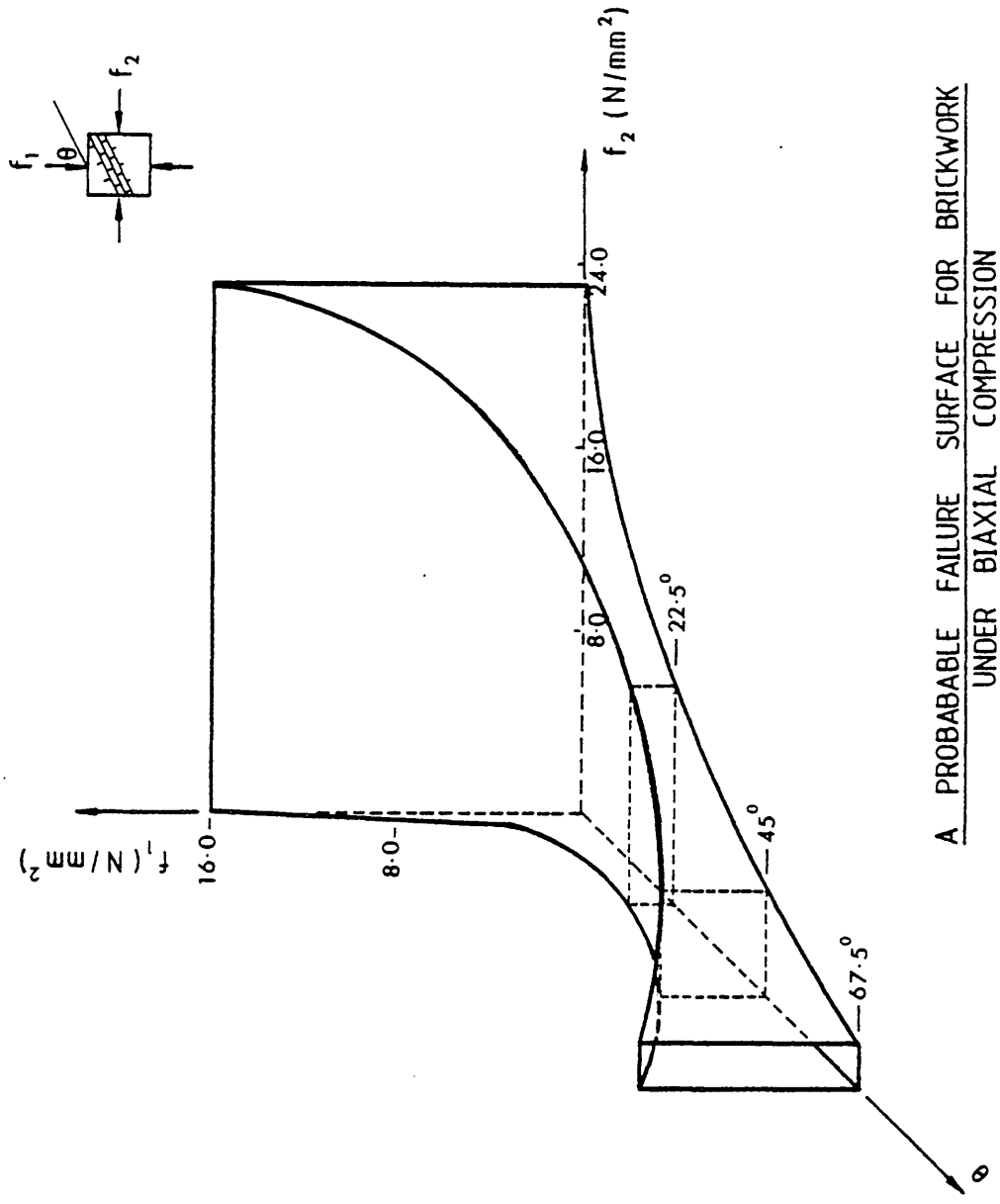

A PROBABABLE FAILURE SURFACE FOR BRICKWORK UNDER BIAXIAL COMPRESSION

FIGURE 5·5

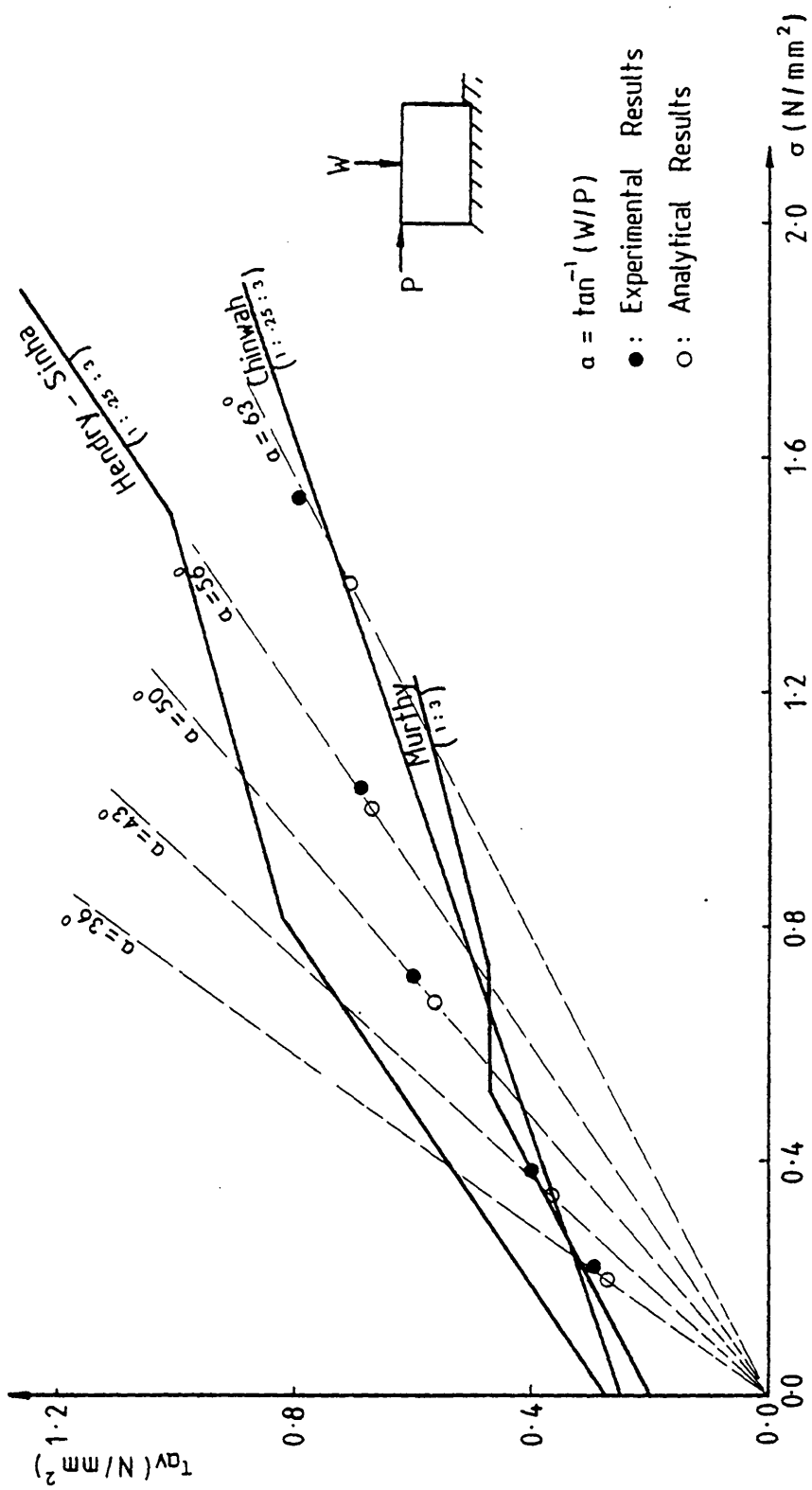

SHEAR STRESS - NORMAL STRESS ENVELOPES FOR SHEAR WALLS

FIGURE 5·6

author's results. A reasonable agreement could be seen within the variability of test arrangement, shape effect, boundary conditions, material properties and workmanship.

The failure modes of the tested walls are shown in the schematic diagrams for comparison with the predicted failure modes in Figure 5.7. Although the theoretical model was not capable of predicting complete failure mode, a close agreement was observed between the experimental and theoretical results, particularly in view of the location of the crack and the direction of crack propagation. However, no exact comparison can be made since the analytical model does not include provision for identifying brick and joint failure separately. Moreover, the cracking sequence, during testing of the walls could not be observed, in order to compare with the predicted cracking sequence. The size of the cracks would have been very small, and those became visible at or near the ultimate failure.

Both the theoretical and experimental results reveal that at low normal stress to shear stress ratios the failure crack tends to propagate mostly in a horizontal direction, as shown typically by shear wall F in Figure 5.7. Obviously, a crack of this nature should take place mostly through bed joints due to low bond strength characteristics, although it cannot be predicted in this model. At high ratios, a diagonal crack connecting the toe and the horizontally loaded point of the wall could be observed as typically shown by shear walls A and E in Figure 5.7. A diagonal failure could be either through joints in a step form or through bricks and joints, depending on the level of precompression applied.

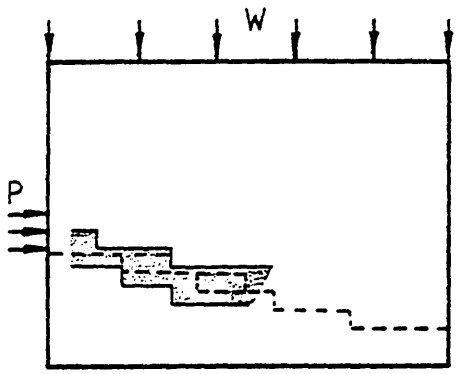

Shear Wall F ($\alpha = 36^{\circ}$)

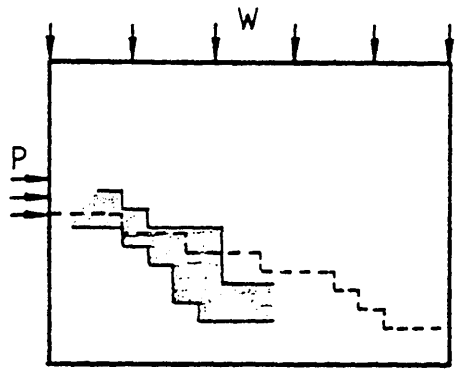

Shear Wall D ($\alpha = 43^{\circ}$)

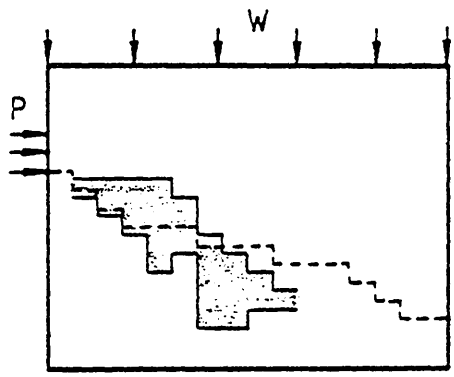

Shear Wall C ($\alpha = 50^{\circ}$)

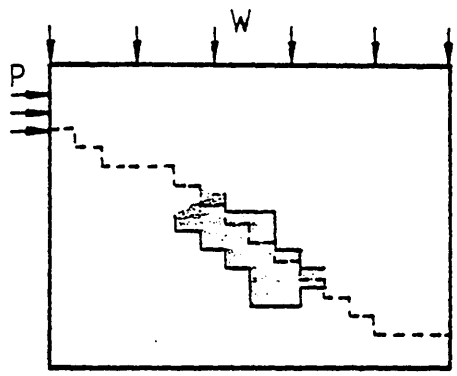

Shear Wall A ($\alpha = 56^{\circ}$)

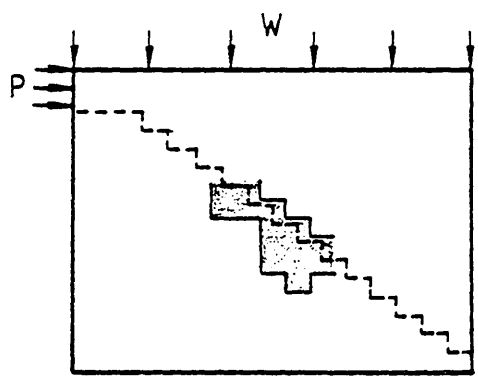

Shear Wall E ($\alpha = 63^{\circ}$)

W/P = tan α

---: Experimental mode of failure

▭ : Predicted zone of failure under biaxial tension-compression

PREDICTED AND EXPERIMENTAL CRACK PATTERNS

FIGURE 5.7

5.7 SENSITIVITY ANALYSIS OF THE ELASTIC CONSTANTS

The previous sections have shown that the initiation of failure and crack propagation of brickwork under in-plane loads can be predicted with reasonable accuracy using the proposed analytical model. In the analysis, a constant value of 7000.0 N/mm^2 for elastic modulus and 0.2 for Poisson's Ratio were assumed although they are dependent on the stress level and the direction of the principal stresses relative to the bed joints. Therefore, a sensitivity analysis is necessary to give some indication of the degree of sophistication required in determining the value of these parameters. If variations in a particular parameter do not exert a great influence, then the experimental evaluation of that property need not be very precise.

The sensitivity of the above mentioned parameters were tested analytically using a shear wall of type A (see Figure 5.4). The finite element sub-division was the same as used in the previous cases. The compressive and racking loads (W and P respectively) were applied in equal increments and at the initial load increment W and P were 460 N and 427 N respectively.

Four values of elastic modulus, 3500.0 N/mm^2, 7000.0 N/mm^2, 14000.0 N/mm^2, 21000.0 N/mm^2 were used whilst holding Poisson's Ratio constant (0.2). Similarly, stresses were computed for three different values of Poisson's ratio, 0.10, 0.2, 0.3 while the elastic modulus was maintained at 7000.0 N/mm^2. The shear stress (τ), vertical stress (σ_y) and horizontal stress (σ_x) distribution along line xx (see Figure 5.8) at the end of 8th load increment were tabulated as shown in Table (5.1) and Table (5.2).

Elastic Modulus (N/mm^2)	stress (σ_y) along xx* (N/mm^2)							
	x = 30.0mm	70.0	110.0	150.0	190.0	230.0	270.0	310.0
3500.0	0.054	-0.298	-0.381	-0.546	-0.901	-1.439	-2.081	-1.910
7000.0	0.056	-0.298	-0.381	-0.546	-0.901	-1.438	-2.081	-1.910
14000.0	0.055	-0.297	-0.374	-0.531	-0.885	-1.437	-2.100	-1.940
21000.0	0.055	-0.297	-0.375	-0.532	-0.886	-1.436	-2.099	-1.938

Elastic Modulus (N/mm^2)	stress (σ_x) along xx* (N/mm^2)							
	x = 30.0mm	70.0	110.0	150.0	190.0	230.0	270.0	310.0
3500.0	-0.014	-0.221	-0.500	-0.706	-0.806	-0.768	-0.423	-0.010
7000.0	-0.011	-0.222	-0.500	-0.706	-0.806	-0.768	-0.423	-0.010
14000.0	-0.011	-0.222	-0.504	-0.715	-0.820	-0.780	-0.429	-0.010
21000.0	-0.011	-0.222	-0.503	-0.715	-0.819	-0.779	-0.428	-0.010

Elastic Modulus (N/mm^2)	stress (τ) along xx* (N/mm^2)							
	x = 30.0mm	70.0	110.0	150.0	190.0	230.0	270.0	310.0
3500.0	0.025	0.230	0.503	0.775	0.997	1.106	0.936	0.149
7000.0	0.027	0.229	0.503	0.775	0.997	1.106	0.936	0.149
14000.0	0.026	0.228	0.501	0.776	1.009	1.127	0.956	0.154
21000.0	0.026	0.228	0.501	0.776	1.007	1.125	0.954	0.153

* Refer to Figure 5.8.

Table 5.1 : Calculated Stresses Along XX* in a Shear Wall for Different Values of Elastic Modulus.

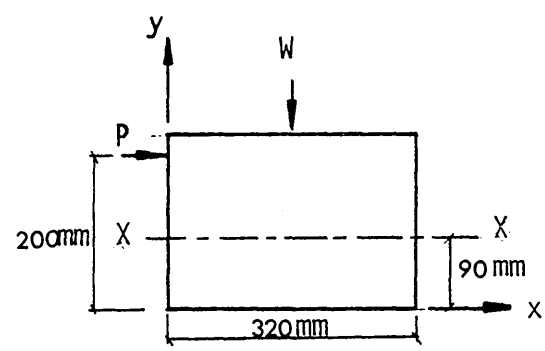

$\alpha = \tan^{-1} W/P = 56^{o}$

A BRICKWALL UNDER RACKING SHEAR AND COMPRESSION

FIGURE 5.8

Poisson's Ratio	stress (σ_y) along xx* (N/mm^2)							
	x = 30.0mm	70.0	110.0	150.0	190.0	230.0	270.0	310.0
0.1	0.056	-0.299	-0.380	-0.543	-0.896	-1.435	-2.087	-1.920
0.2	0.056	-0.298	-0.381	-0.546	-0.901	-1.438	-2.081	-1.910
0.3	0.056	-0.298	-0.380	-0.543	-0.896	-1.437	-2.084	-1.920

Poisson's Ratio	stress (σ_x) along xx* (N/mm^2)							
	x = 30.0mm	70.0	110.0	150.0	190.0	230.0	270.0	310.0
0.1	-0.011	-0.222	-0.501	-0.708	-0.811	-0.733	-0.426	-0.012
0.2	-0.011	-0.222	-0.500	-0.706	-0.806	-0.768	-0.423	-0.010
0.3	-0.010	-0.222	-0.501	-0.708	-0.811	-0.771	-0.423	-0.009

Poisson's Ratio	shear stress (τ) along xx* (N/mm^2)							
	x = 30mm	70.0	110.0	150.0	190.0	230.0	270.0	310.0
0.1	0.026	0.229	0.503	0.774	0.998	1.111	0.944	0.150
0.2	0.027	0.229	0.503	0.775	0.997	1.106	0.936	0.149
0.3	0.027	0.229	0.502	0.774	0.999	1.112	0.940	0.152

* Refer to Figure 5.8

Table 5.2: Calculated Stresses Along XX* in a Shear Wall For Different Values of Poisson's Ratio

It can be seen that the variations in stresses are extremely small compared to the large variations in brickwork elastic modulus and Poisson's Ratio. In all the walls the initiation of the failure was at a point where x = 170.0 mm and y = 90.0 mm, at the 9th load increment. In each case the crack pattern was identical to that shown in Figure 5.4(d).

Therefore, it can be stated that small variations in stiffness of brickwork should not significantly affect the analytical results, and the average values used with regard to elastic modulus and Poisson's ratio can be considered reasonable.

5.8 CONCLUSIONS

This chapter has described a method for the simulation of the in-plane behaviour of masonry using the finite element technique. Non-linearity due to progressive cracking is introduced and masonry is treated as a continuum of isotropic and linearly elastic material.

It has been shown that failure of brickwork subjected to complex stress distribution is generally well predicted by the proposed analytical model together with the biaxial stress failure criterion (tension-compression) suggested in Chapter 4. In particular the loads at which failure is initiated and the location and direction of tensile cracking are determined with sufficient accuracy.

The behaviour of a shear wall has been explained using this theoretical model but, it is recognized that it cannot be fully explained using the present model due to non-availability of a failure criterion for the stress state of biaxial compression.

When the compressive stress/shear stress ratio is below a certain value the failure in a shear wall is initated by biaxial tension-compression but, the overall failure is constituted together with a biaxial compression failure. The difference between initial cracking and final failure depends on the magnitude and direction of biaxial compressive stresses. When the compressive stress/shear stress ratio is higher than the above mentioned value, the whole shear wall is under biaxial compression state and the failure is solely governed by a failure criterion for biaxial compression. At very low normal stress/shear stress ratio (high shear stress), the failure crack propagates more or less along a horizontal bed joint. As this ratio increases the inclination of the crack gradually increases.

From a sensitivity analysis for elastic constants, it appears that small variations in elastic modulus and Poisson's ratio do not significantly affect the computed stresses and hence it is not necessary to know the precise value of these parameters for use in the analytical model.

CHAPTER SIX : BEHAVIOUR OF BRICK MASONRY SHEAR WALLS

6.1 INTRODUCTION

An important requirement of masonry buildings is the ability to withstand lateral loads which can be induced by earthquakes or wind loadings. Most masonry buildings consist of various assemblages of different types of shear walls, and the resistance to the lateral loads is predominantly by their in-plane shear resistance.

In-plane shear resistance of masonry walls has been studied by research workers for many years. The experimental and theoretical behaviour of individual or components of individual, shear walls have been undertaken. As research progressed, investigators tried to determine failure criteria for different assemblages subjected to various combinations of shear and compressive loads. More recently investigators have also considered the behaviour of various assemblages under cycling loading; however, this will not be considered in this investigation.

A criterion for shear failure has been proposed as the summation of initial bond strength between the mortar and the masonry units and the frictional resistance which is said to be proportional to the compressive stress normal to the bed joints. This criterion can be formulated as:

$$\tau_{av} = \tau_o + \mu\sigma_n \qquad (6.1)$$

where τ_{av} = average shear stress at failure,

τ_o = the shear bond strength expressed as the average shear stress when $\sigma_n = 0$,

σ_n = precompression stress, based on the bed joint area,

and μ = a coefficient attributed to friction.

Since this criterion is expressed in terms of the average stress on the bed joint, it is implicitly assumed that the failure load is not sensitive to the stress distribution within the panel. Moreover, the influence of normal stress perpendicular to the bed joints has been completely ignored.

It has been reported[73] that for similar brick and mortar specimens, the value of μ appears to decrease substantially with increasing normal compressive stress σ_n, and in order to support the friction theory, it has been necessary to adopt an average value. However, the equation (6.1) has been used, as an empirical expression, to predict the shear strength of brick masonry for the range of precompression up to 20% of the masonry compressive strength. Above this level, equation (6.1) no longer applies since the failure mode changes from joint failure to failure through bricks and joints.

An aim of this part of the investigation is to find out the influence of non-uniformity of stress distribution existing in shear walls on the shear strength. The effect of direct stress (σ_x) perpendicular to the normal stress (σ_y) on the shear resistance has been considered. A family of τ - σ_y (shear stress and normal stress

at local points) curves has been suggested for different values of σ_x, for local failure in shear walls under biaxial tension and compression. The influence of the method of load application, boundary conditions and the panel geometry has also been discussed.

6.2 LOCAL STRESS DISTRIBUTION IN A SHEAR WALL

Many investigators have adopted different techniques to simulate the behaviour of shear walls. One popular method is to subject a wall panel to a combination of vertical load applied along the top of the wall, and horizontal racking load to an upper corner. Some investigators tested square wall panels under a diagonal load with combined precompression normal to the bed joints. Whatever the test technique adopted, the test results were typically presented as a relationship between the average shear stress and average vertical stress at failure, calculated in each case by dividing the applied normal force to the bed joints and shear force parallel to the bed joints by the bed joint area.

As has been discussed in the previous chapter, the failure of shear walls may take place progressively rather than at one load level. Initially, local failure may occur at some location and gradually spread over the other regions of the structure until global failure takes place. Therefore walls having the same average stresses at failure but, different boundary conditions and/or loading conditions would initiate failure at different locations, and therefore the collapse mechanism and failure mode

may be different. Hence a study of the local stress distribution in shear walls is worthwhile for a better understanding of their behaviour.

6.2.1 Local Stress Distribution for Different Geometrical Shapes of Shear Walls

Three different rectangular shapes were analysed under the combined action of precompression and racking shear. The Figure 6.1 illustrates the typical arrangement for a shear wall test and the corresponding distribution of stress near the centre of the panel for three different height/length ratios. In each case the average shear and average vertical stresses were the same. The stress distributions were obtained from the elastic finite element analysis described in Chapter 5.

Stress distribution is affected by the length (or shape) of the wall. Non-uniform distribution of shear (τ) and normal stress (σ_y) along section B-B is evident from Figure 6.1. The horizontal stress (σ_x) is increased with increasing panel length in shear walls. The σ_x down the centre line is substantial and of the same order of magnitude as the vertical applied stress.

6.2.2 The Influence of Method of Load Application and Boundary Conditions

Various testing techniques have been adopted in the past to study the behaviour of masonry under shearing loads. Test methods

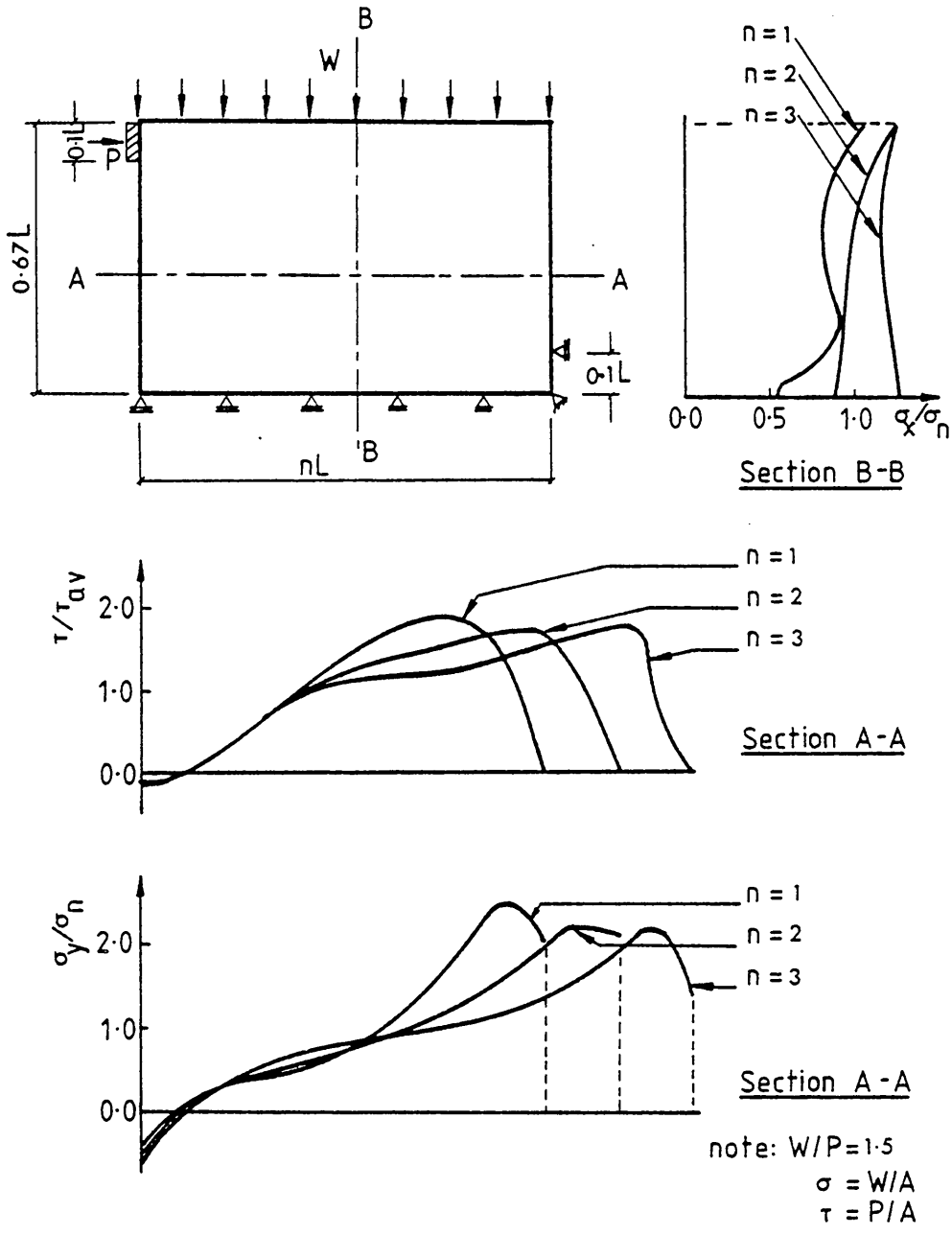

INFLUENCE OF PANEL GEOMETRY ON THE STRESS DISTRIBUTION IN SHEAR WALLS

FIGURE 6·1

were developed either to simulate the conditions in an actual shear wall and to measure "whole wall" shear strength or to determine the "masonry" shear strength as a characteristic property of the material. However, in both cases results have been interpreted in terms of average stress.

In order to examine the influence of the method of load application and boundary conditions, three testing techniques(as shown in Figure 6.2) which can be used to investigate the "masonry" shear strength may be considered:

(a) a wall panel subjected to combined racking shear and compression normal to the bed joints ("racking test"),

(b) a wall panel subjected to diagonal compression and a compressive load normal to the bed joints ("diagonal test"),

(c) a wall panel subjected to uniform shear stress along the boundaries together with a compressive load normal to the bed joints ("open frame test").

In the 'racking test' the horizontal racking load is applied at a distance of 200 mm from the base, instead of at the upper corner as is typical for shear wall tests, in order to maintain the equilibrium of the specimen. The average normal and shear stresses for each case have been calculated using the equations shown in Figure 6.2.

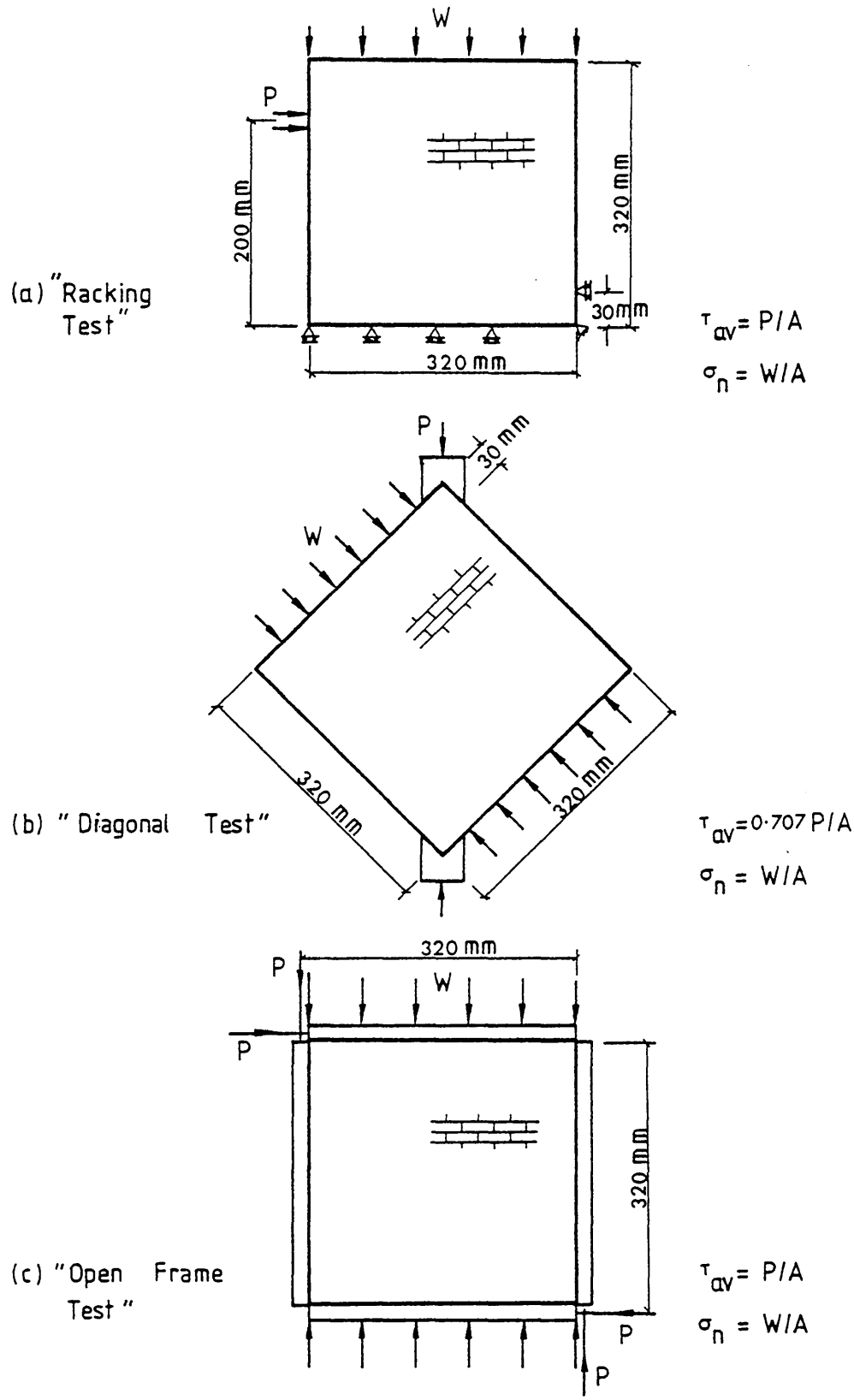

SHEAR TEST SPECIMENS UNDER DIFFERENT LOAD CONDITIONS

FIGURE 6·2

Each of these panels was analysed using an elastic analysis. The computed stresses were compared, for the same average shear and normal stresses at the bed joints, but for different loading and boundary conditions.

The σ_y and τlocal stress distributions along a section parallel to the bed joints and σ_x local stress distribution down a section parallel to the perpend joints are shown in Figure 6.3. Non-uniform stress distributions in the "racking test" and in the "diagonal test" are evident. Although in the "diagonal test" the σ_y stress distribution appears to be uniform at the centre line of the panel (section a_1 - a_1 in Figure 6.3), non-uniform stress distribution is quite evident at a section away from the centre line as shown by section a_2 - a_2 in Figure 6.3 . In both cases the magnitude of σ_x stress is substantial.

In the "diagonal test" the stress perpendicular to the bed joints (σ_y) is influenced by the diagonal load and diminishes rapidly near the edges of the panel. The average value of σ_y over the bed joint area is 65% higher than the average value calculated using the standard equation;

$$\sigma_n = W/A$$

where W = applied compressive load normal to the bed joints,

and A = bed joint area.

Hence, the "diagonal test" would give rise to misleading results if no account is taken of the influence of the diagonal load on the σ_y stress distribution.

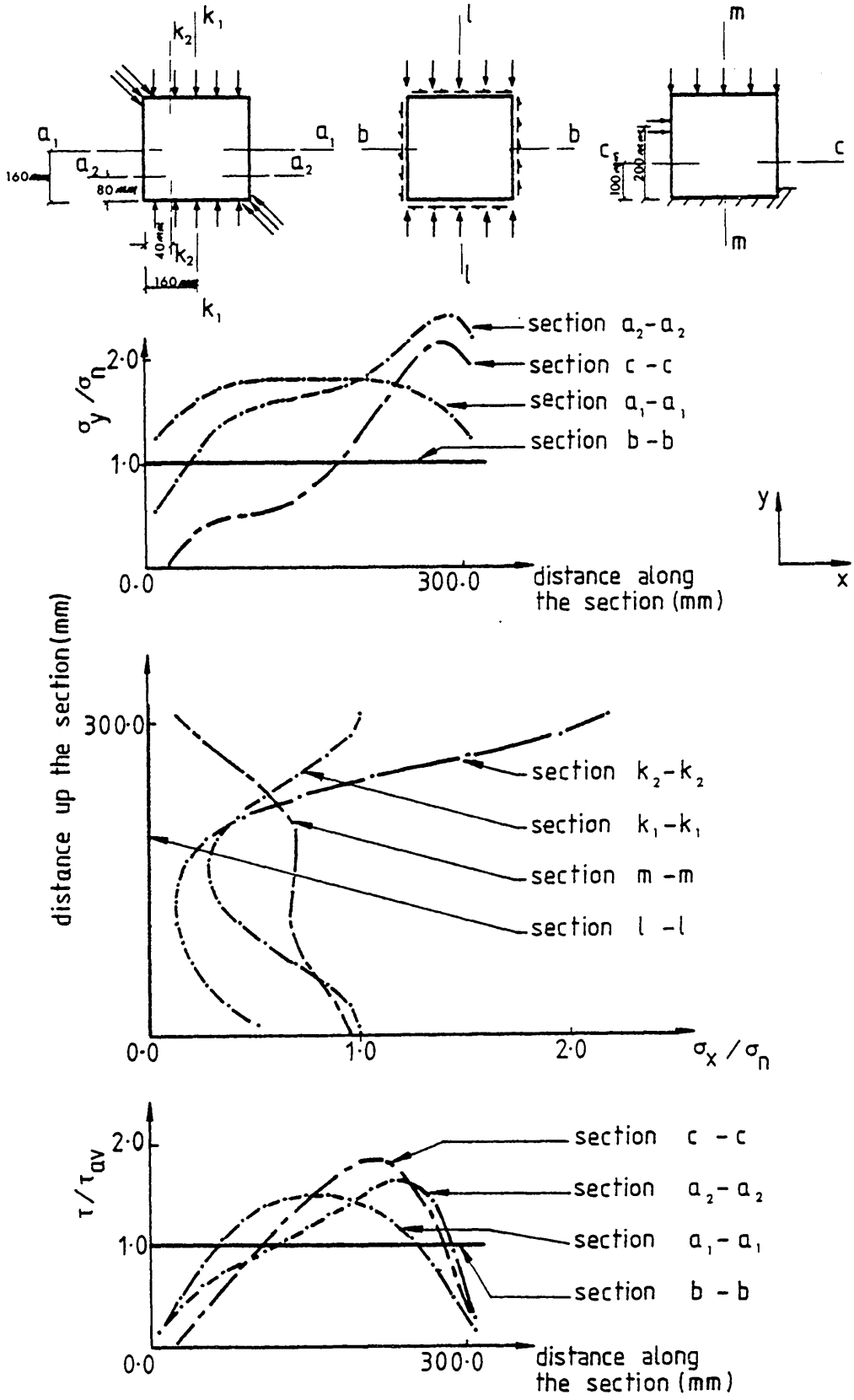

INFLUENCE OF THE TEST TECHNIQUE ON THE STRESS DISTRIBUTION OF SHEAR WALLS

FIGURE 6·3

A uniform distribution of σ_y and τ is observed in the panel subjected to the "open frame test", with zero horizontal stress. This will be true provided the testing frame is capable of applying a uniform shear stress along the boundaries of the wall.

From the foregoing results, it appears therefore that a test of the "open frame" type will produce the most uniform state of stress within the wall. Provided the difficulties of applying a uniform shear force along the panel boundaries can be overcome, it is apparent that this would be the most effective test for the determination of characteristic shear strength of masonry. The influence of local variations in stress on panel failure are minimized, thus allowing more effective study of the other parameters governing shear strength of masonry.

6.3 REVIEW OF SHEAR WALL TESTS

Investigators over the last few decades have used many different test techniques in their experimental programmes on the shear strength of masonry assemblages. The diversity of methods has arisen due to the difficulty of simulating the conditions in an actual shear wall or due to the difficulty of creating a uniform stress field within the test specimen and/or due to the type of test equipment available. In this section most of these basic test methods will be briefly reviewed. Some of the results have been plotted for the purpose of comparison.

6.3.1 Test Techniques

The Figure 6.4(a) to Figure 6.4(j) illustrate the schematic diagrams of typical test methods adopted by investigators in order to determine the shear strength of masonry assemblages. Full and model scale structures, brick-mortar couplets and brick-mortar triplets are the usual test specimens used in these test programmes.

Schneider[42], Scrivener[61] and Structural Clay Products Research Foundation[10] adopted a test set up as shown in Figure 6.4(a) which was later modified by Schneider[42] by introducing an internal hold down in order to eliminate the large compressive stress at the edge of the panel. However, to what extent the state of stress is influenced by the boundary conditions and tie downs is a matter of speculation.

Some investigators[6,18] adopted the diagonal test method with added compressive load to determine the shear strength of square wall panels, as shown in Figure 6.4(c). Brochlet[6] produced an analytical solution for the shear strength of such specimens assuming a uniform stress distribution with zero σ_x stress condition. However, σ_x is substantial and stress distribution is non uniform as was shown before.

The test techniques adopted by Haller[20] and Pieper et al.[54] are shown in Figure 6.4(d) and in Figure 6.4(e), respectively. Both configurations are not capable of producing a uniform stress state, although the results are presented in average stresses. Moreover, the author considers that the σ_x stress within the

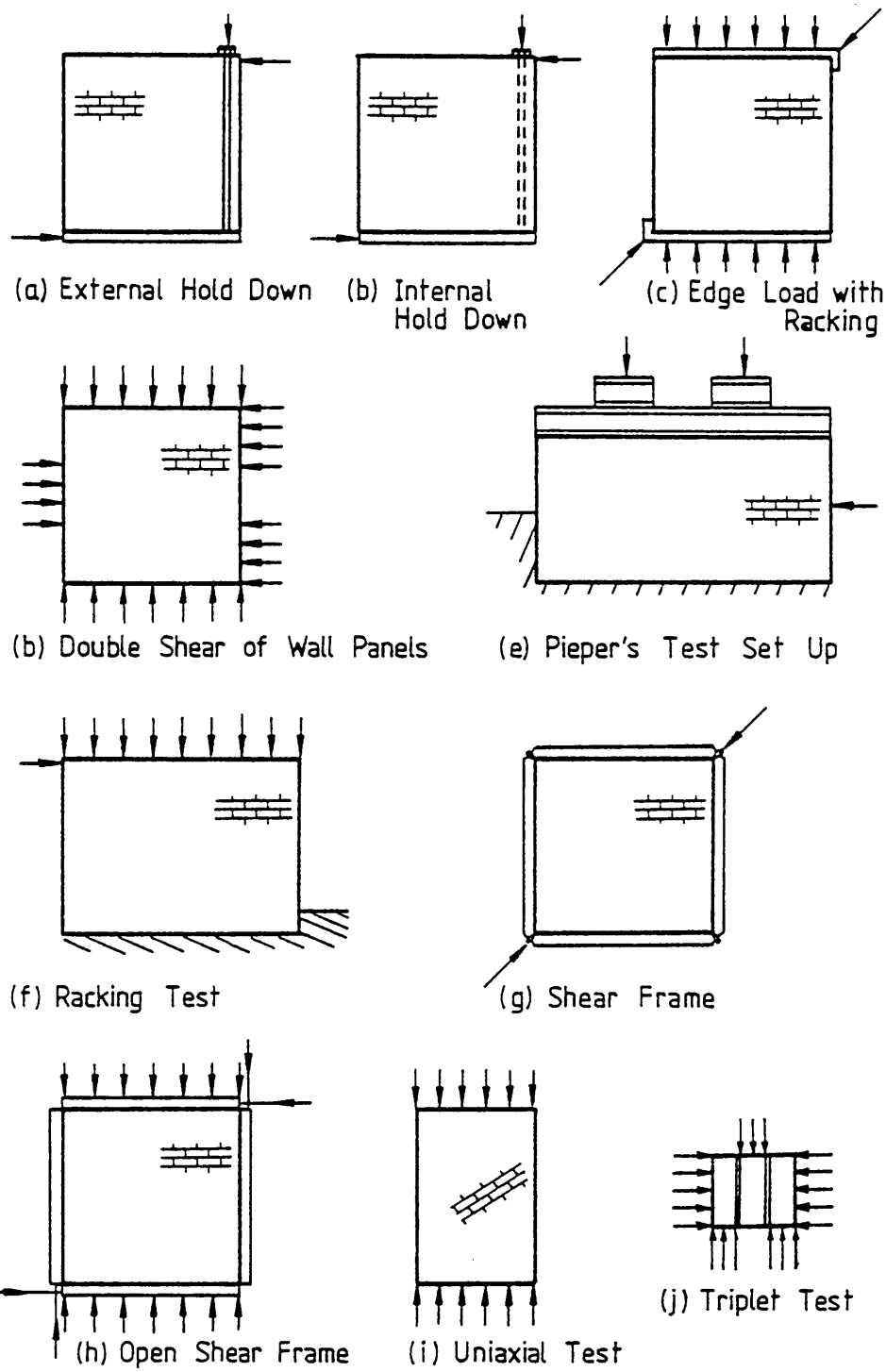

TEST TECHNIQUES FOR THE DETERMINATION OF "MASONRY" SHEAR STRENGTH

FIGURE 6.4

panel is substantially high. Pieper et al. carried out a parameter study, and their results should only be regarded as indicative of the effects of various parameters due to the unusual method of application of the shearing force.

A large number of investigators[7,26,28,42,46,62,64,68,80,83] carried out a "racking test" as shown in Figure 6.4(f). Hendry et al.[26,28,66,68] performed "racking tests" on full and model scale structures, and the attempt has been made to represent typical parts of a building with some surrounding structural components and to interpret the results in terms of average stresses. Non-uniform stresses in such specimens are quite evident and hence the results presented in this manner can be misleading if due regard is not paid to factors which can significantly change the stress distribution.

In order to produce a uniform shear stress state in the test panel, a shear frame was suggested by Monk[59] as typically shown by Figure 6.4(g). However, the application of a normal force to the bed joints to obtain the shear strength under different normal stress was not possible with this arrangement. An improvement of Monk's method was adopted by Schneider et al.[59], as shown in Figure 6.4(h) by introducing a shear frame with open joints. As shown in the section 6.2.2, calculations have indicated a uniform stress state in the wall panel with magnitude of σ_x being zero. This arrangement has the advantage over Monk's method in that the vertical compressive forces can be introduced independently of the shear forces. However, both cannot be treated as representative of conditions in an actual shear wall but they are useful to determine the characteristic shear strength of the

masonry and for parameter studies.

Polyakov[55], Benjamin[4] and Hendry et al.[45,63] performed tests on brick-mortar couplets to determine a failure criterion under combined compression and shear. Benjamin achieved different normal stress to shear stress ratio by shearing pairs of brick, joined under different angles in relation to the force direction. In both cases a non-uniform stress state at the brick-mortar interface is inevitable. An analytical study carried out by Stafford Smith et al.[73] on brick mortar triplets under combined compression and double shear [Figure 6.4(j)] has clearly shown the existance of non-uniform stresses at the mortar joints. It has also been shown that very high tensile stresses usually tend to occur in the mortar joints close to the loaded ends of the bricks.

Some investigators[47,48] loaded panels in uniaxial compression with load applied at differing angles to the bed joint [Figure 6.4(i)], producing varying ratios of shear and compression. Under a uniform compressive load, τ and σ_y distributions can be assumed as uniform but, as the inclination of the bed joint to the direction of loading decreases the influence of σ_x increases.

6.3.2 Shear Wall Test Results

Some of the results of previous investigations have been plotted and shown in Figure 6.5. The broad scatter of results is evident and this can be caused due to three reasons.

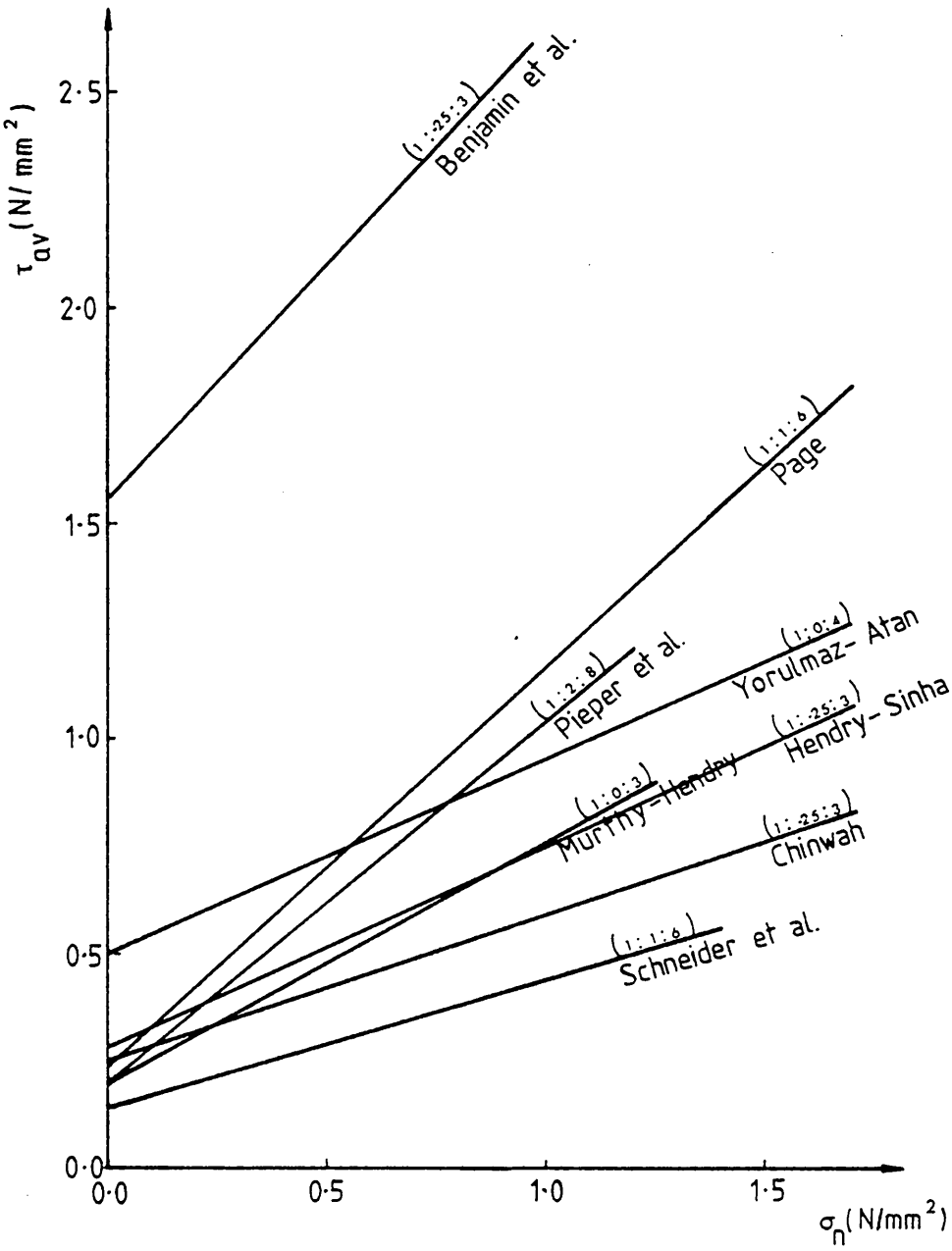

SHEAR WALL TEST RESULTS PRESENTED BY DIFFERENT INVESTIGATORS

FIGURE 6·5

(a) The results have been presented in average shear and normal stresses at the bed joints at failure and it has been assumed that the stress distribution is completely insensitive to the failure load. However, each of these test results presented by different authors correspond to different stress fields caused by the variability in boundary conditions and load application technique and the shape effect of the specimen.

(b) The results have been presented in terms of τ_{av} and σ_n without any regard to the σ_x stress distribution. In fact, most of the test methods adopted in the past produce substantially high σ_x which can influence the criterion for failure.

(c) Variability in workmanship and material properties.

However, each of these tests would represent a point on a general failure surface for that type of masonry and hence, the disparate test results can be unified if the failure is defined in terms of principal stresses and their orientation to the bed joint direction.

6.4 INFLUENCE OF σ_x ON τ - σ_y CURVE AT FAILURE

The typical stress state of an element at the centre of a shear wall panel is shown in Figure 6.6. The elements are usually subjected to direct horizontal and vertical stresses and pure shear stress. For a particular combination of τ, σ_x and σ_y, the principal stresses σ_1 and σ_2 and their orientation (θ) can be calculated. Different combinations of principal stresses and θ at failure can be obtained from the biaxial failure envelope described in Chapter 4. Therefore, this envelope can be used to investigate the significance of σ_x on the failure of masonry walls under the combined action of normal stress and shear stress.

In this analysis, the stresses determined from the biaxial failure envelope will correspond to the local failure of shear walls. Nevertheless, the τ_{av} - σ_n curves presented by many investigators correspond to global failure of structural components. Therefore direct comparison, between experimental results and τ - σ_y curves which can be obtained from the biaxial envelope, cannot be made. However, the influence of σ_x on τ-σ_y curves should still reflect the effect of σ_x on the τ_{av} - σ_n curves.

6.4.1 τ - σ_y Curve at Failure for Zero Value of σ_x

Initially an element subjected to σ_x, σ_y direct stresses and shear stress, τ, is considered. From the Mohr circle of stress diagram it can be shown that,

$$\sigma_x = (f_t + f_c)\sin^2\theta - f_t \qquad (6.2)$$

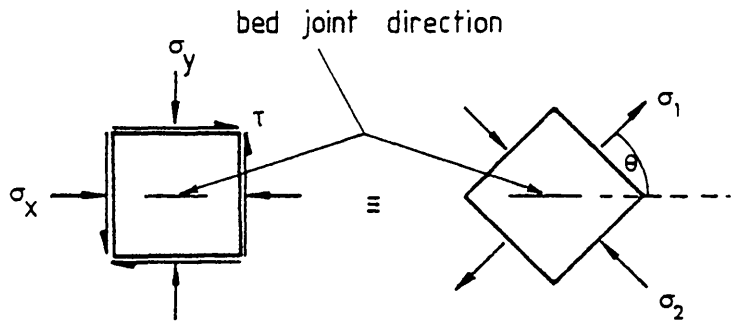

THE STRESSES ON A SMALL ELEMENT IN A SHEAR WALL

FIGURE 6.6

where f_c = principal compressive stress,

and f_t = principal tensile stress.

When $\sigma_x = 0$,

$$f_t = (f_t + f_c)\sin^2\theta$$

$$\frac{f_c}{f_t} = \frac{1}{\sin^2\theta} - 1 \qquad (6.3)$$

Therefore, for a zero σ_x and for a particular value of θ, there will be only one possible f_c/f_t ratio and hence one relevant point on the biaxial stress failure envelope. The equation of the biaxial failure surface is given by,

$$f_t = 0.7e^{-0.14 f_c} - 1.34 \frac{\theta}{\pi} - 0.02 \qquad (6.4)$$

Hence, in order to find out the stresses at failure under zero σ_x condition, the intersection line of the two surfaces defined by equations (6.3) and (6.4) should be obtained. Therefore for different values of θ, principal stresses at failure can be calculated from which τ and σ_y can be derived from the following equations,

$$\tau = \frac{(f_t + f_c)}{2} \sin^2\theta \qquad (6.5)$$

$$\sigma_y = (f_c \cos^2\theta - f_t \sin^2\theta) \qquad (6.6)$$

However due to the complex nature of equations(6.3) and (6.4), a graphical method was adopted. The steps involved are outlined below.

(a) Determine f_c/f_t ratio for a particular value of θ(say α) using equation (6.3), (say $f_c/f_t = k$).

(b) Plot the failure envelope extracted from biaxial failure surface corresponding to α.

(c) Obtain the intersection point between the failure envelope corresponding to α and the line $f_c/f_t = k$.

(d) Read the values of f_c and f_t at the intersection point.

(e) Compute τ and σ_y using equations (6.5) and (6.6)

(f) Repeat the steps (a) to (e) for different values of θ.

Therefore, if a range of values of θ is taken, a complete failure criterion for masonry in terms of τ and σ_y can be derived for zero σ_x condition. This is shown in Figure 6.7. Since shear wall test results usually lie in the range where $\sigma_n < 2.0$ N/mm^2, a part of the curve in Figure 6.7 relevant to this range is shown to a larger scale in Figure 6.8.

From Figure 6.7 it is clear that the shear strength of masonry increases with increase of precompression to a certain limit and

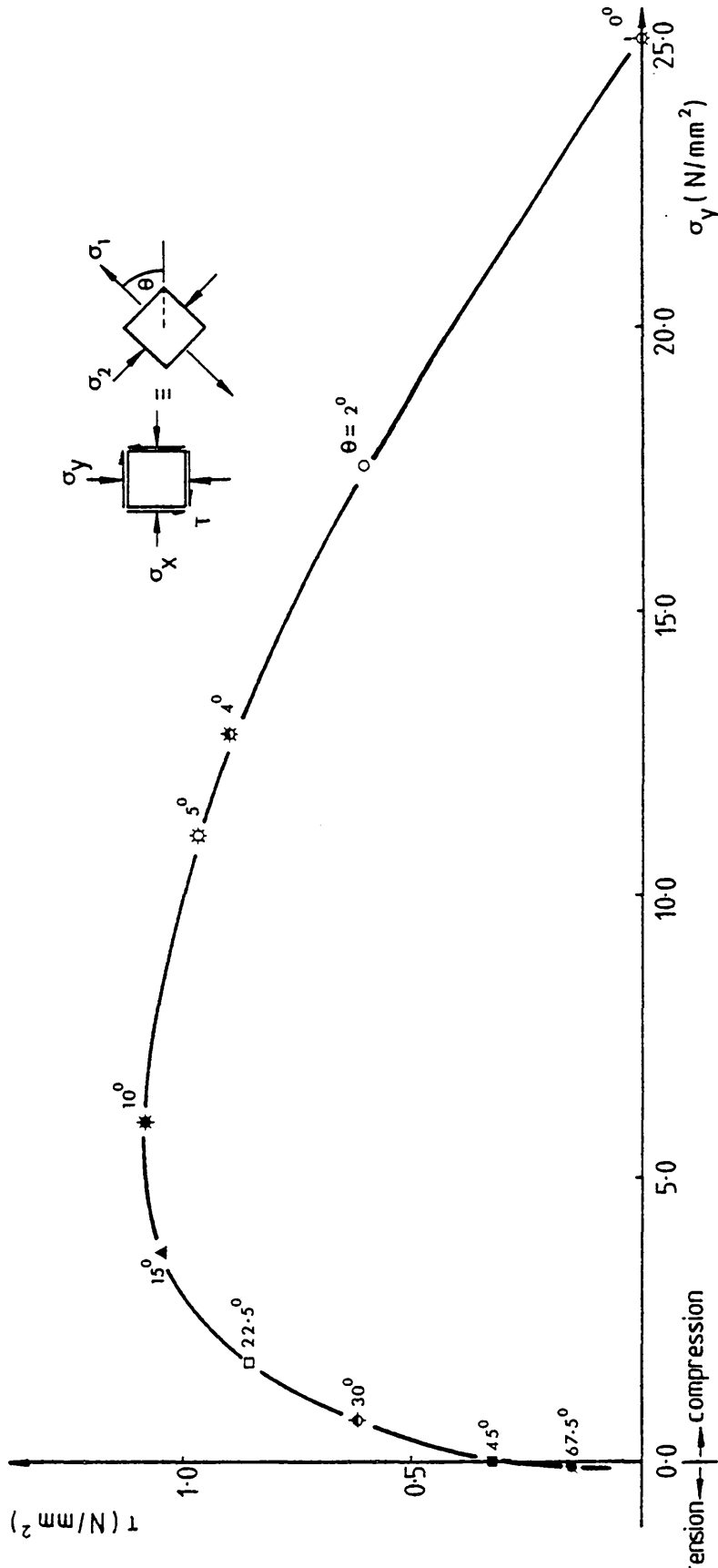

FAILURE CRITERION FOR BRICK MASONRY IN TERMS OF τ AND σ_y ($\sigma_x = 0{\cdot}0$)

FIGURE 6·7

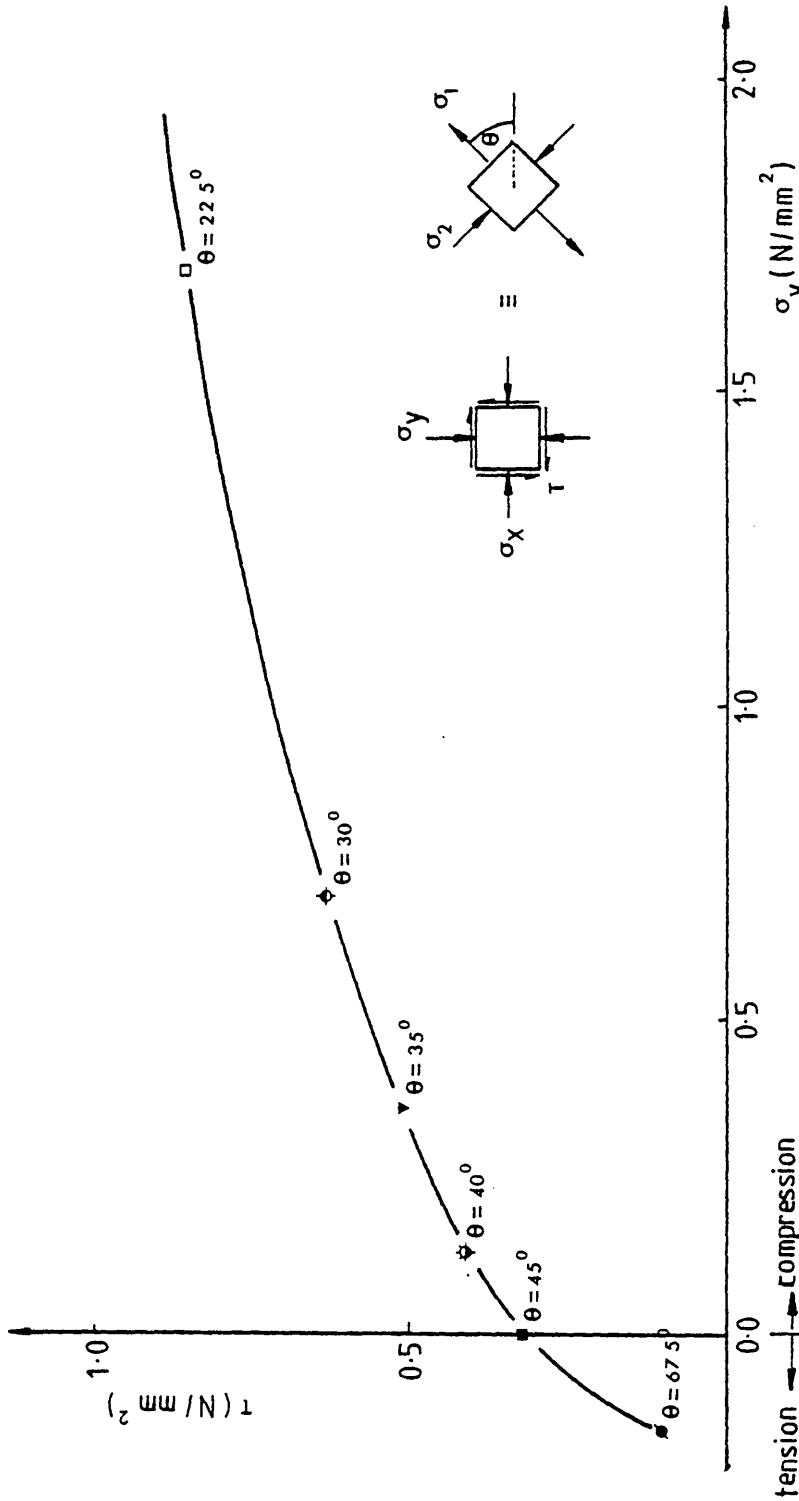

FAILURE CRITERION FOR BRICK MASONRY IN TERMS OF τ AND σ_y ($\sigma_x = 0$)

(Enlarged Scale)

FIGURE 6·8

thereafter it gradually decreases. As was explained in Chapter 4, values of θ in excess of 45^{o} definitely fail in the joints. Although a precise angle at which failure changes from joint failure to brick-joint failure cannot be given in this investigation, the author considers that values of θ in excess of approximately 30^{o} correspond to failure in the joints alone. As θ becomes smaller, the compressive stress plays a more dominant role and a combined brick-mortar failure results. As θ approaches zero, a brick compression failure is exhibited. Therefore, from Figure 6.7 the mode of failure can be predicted for any combination of τ and σ_y.

6.4.2 τ - σ_y Curves for Different Values of σ_x

A graphical method was developed to derive the τ - σ_y curves which define masonry failure for different values of σ_x. This method can be used to determine the τ - σ_y curve for zero σ_x condition as well. It consisted of the following steps.

(a) Different combinations of the principal stresses at failure corresponding to a particular value of θ were extracted from the biaxial failure envelope and tabulated.

(b) The values of σ_x, σ_y and τ at failure were calculated using equations 6.2, 6.6 and 6.5 respectively.

(c) The shear stress (τ) against normal stress (σ_y) was plotted for different values of σ_x.

As shown in Figure 6.9, it can be seen that for a particular value of θ, there can be different combinations of σ_x, σ_y and τ at failure. σ_y and τ exhibited a linear relationship for a particular value of θ and for different values of σ_x. The magnitudes of σ_x were marked on this straight line.

(d) This procedure was repeated for a range of values θ, such as 22.5^0, 30^0, 35^0, 40^0, 45^0 and 67.5^0 as shown in Figure 6.9.

(e) τ - σ_y failure envelopes for brick-masonry corresponding to different values of σ_x, such as 0.5 N/mm^2, 1.0 N/mm^2 and 1.5 N/mm^2 were interpolated from the τ - σ_y curves for different values of θ, and shown in Figure 6.10.

From Figure 6.10 it can be seen that variations of σ_x do not play a significant role for very low values of vertical compression and shear. All the curves converge and meet very near to each other on the shear stress axis (τ) at zero normal stress (σ_y). However, as the normal stress increases, the influence of σ_x on the τ - σ_y curves becomes quite significant.

As the magnitude of σ_x increases, the shear strength of wall panels increases. The lowest shear strength of brick masonry is attained at zero σ_x or in other words when the wall is subjected to pure shear and vertical stress perpendicular to the bed joints. This has been reflected in Schneider's[60] test results. As was

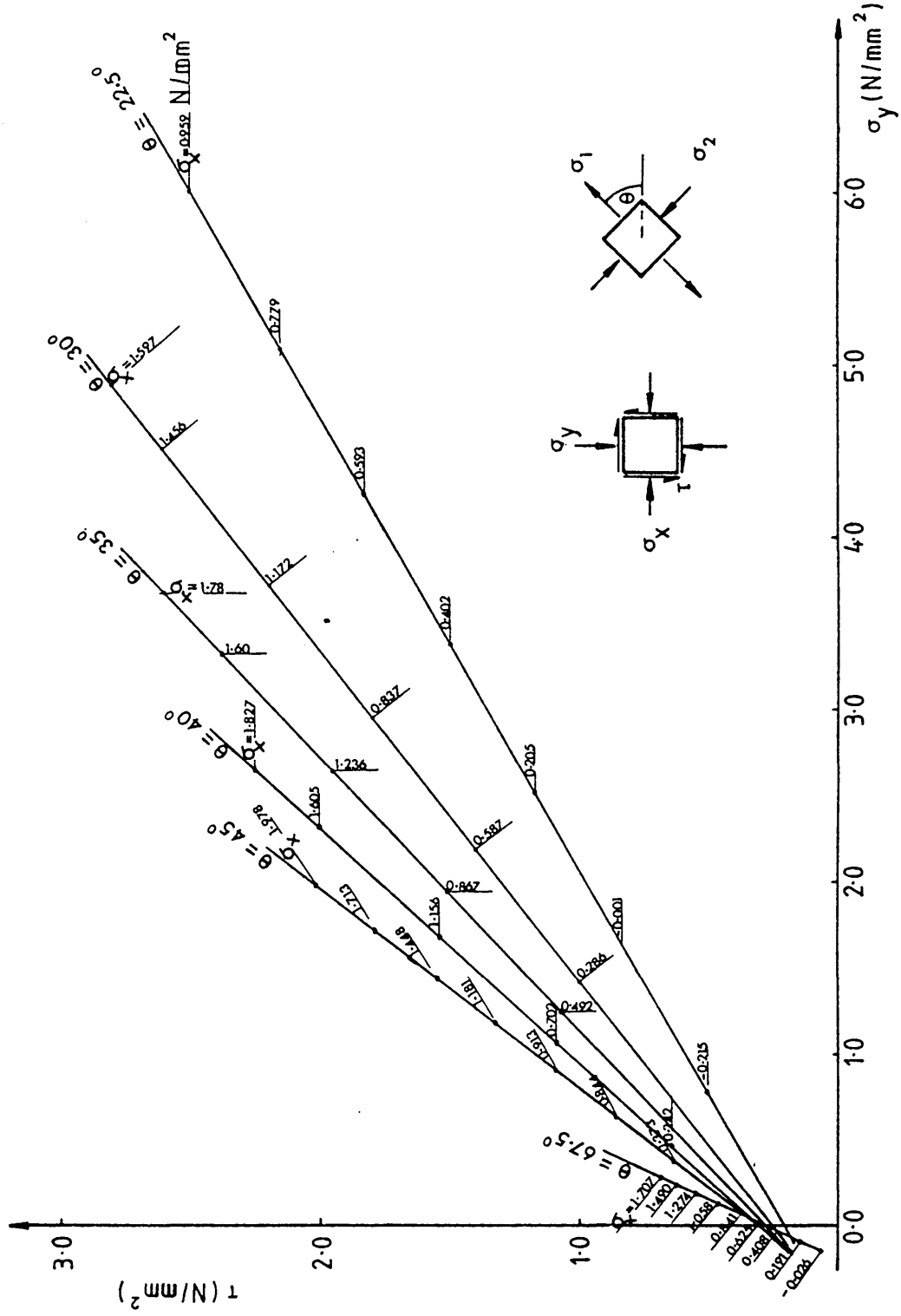

τ-σy INTERACTION FOR DIFFERENT VALUES OF θ

FIGURE 6.9

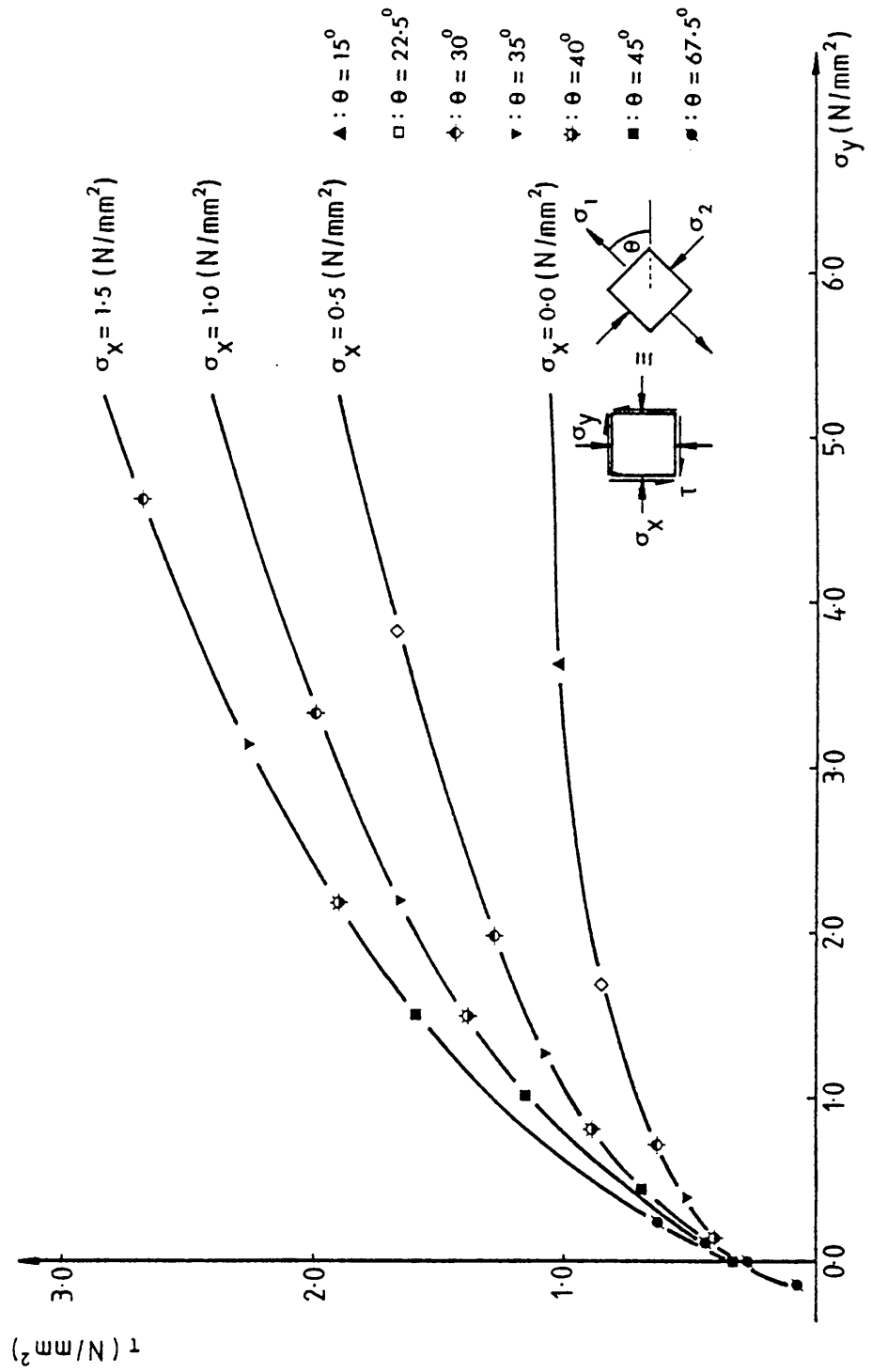

τ – σy FAILURE CRITERION FOR VARYING VALUES OF σx

FIGURE 6·10

explained previously Schneider was successful in producing a uniform stress state within the panel with zero σ_x condition in his shear wall tests. With reference to Figure 6.5 it can be seen his results are much lower than the results obtained by others. In particular the envelope obtained by Page[48] in which brickwork has been built with the same 1:1:6 (cement: lime:sand) mortar is relatively much higher than Schneider's envelope. However direct comparison of Schneider's results with others in Figure 6.5 may not be reasonable since those walls were built with 1:¼:3 (cement:lime:sand) mortar mix. From Figure 6.10, however, it appears that as σ_x increases the rate of increase of shear strength decreases for a fixed value of normal stress.

6.5 INFLUENCE OF SOME PARAMETERS WHICH AFFECT THE SHEAR STRENGTH

Shear wall tests have usually been concerned with the overall behaviour of masonry panels. Failure has been defined as collapse of the panel which takes place after substantial cracking has occurred. As previously noted, results are usually presented in the form of a failure criterion in terms of average normal (σ_n) and shear (τ_{av}) stresses although some aspect of the test specimen or test procedure has the potential of producing non uniform stresses.

A comprehensive investigation was carried out by Nuss et al[47] on the parameters influencing shear strength between clay masonry

units and mortar. The influence of properties of materials such as mortar cube strength, clay unit initial rate of absorption (IRA) and the water/cement ratio of mortar, were considered. An increase in strength was reported with increasing water/cement ratio and mortar cube strength, whereas a decrease in strength with increasing IRA. Sinha[64] reported an increase of shear bond strength between brick-mortar couplets with an increase of brick moisture content up to about 10% and thereafter a decrease in strength. However, in the present investigation the effect of material properties on the shear strength of brickwork has not been studied.

Pieper et al.[54] have indicated that the thickness and length of walls affect the shear strength. He stated that the shear strength of the wall panel gradually increases with the thickness of the wall whereas it decreases with the increase of length of the wall panel.

Generally, variations in panel geometry for the same ratios of σ_n/τ_{av}, non uniform application of the shearing load or racking load along the length of the panel, and inconsistent boundary conditions, cause variation in local stresses in critical regions of the panel with consequent differences in the failure load. The biaxial failure envelope has been used to study the influence of those parameters on the shear strength of brick masonry panels. As discussed in Chapter 5, the biaxial failure criterion defines local failure in masonry and cannot therefore be directly compared to the strength of the panels unless final

failure takes place immediately after the first crack. It does however, highlight some important factors that should be considered in the design of shear wall tests and in the comparison of results from different tests.

6.5.1 The Influence of Panel Geometry on the Shear Strength

In order to study the influence of panel geometry on the shear strength of masonry walls, nine wall panels of different wall lengths were analysed by the non-linear finite element analysis described in Chapter 5. In all the cases, the average normal stress at the bed joints was kept constant at 1.0 N/mm^2 and the initiation of structural failure was observed.

The expected crack pattern and the location of initiation of failure are shown in Figure 6.11 for each case. The influence of the panel geometry on the mode of failure is evident.

The variation of average shear stress at the initiation of failure for constant normal stress at the bed joints with varying panel geometry has been illustrated in Figure 6.12. An increase in strength with increase in panel length/shear arm ratio (L/H) has been observed up to L/H = 1.77. When L/H > 1.86, the shear strength gradually decreases. Hence, it can be stated that the shape of the specimen has a marked influence on the shear strength.

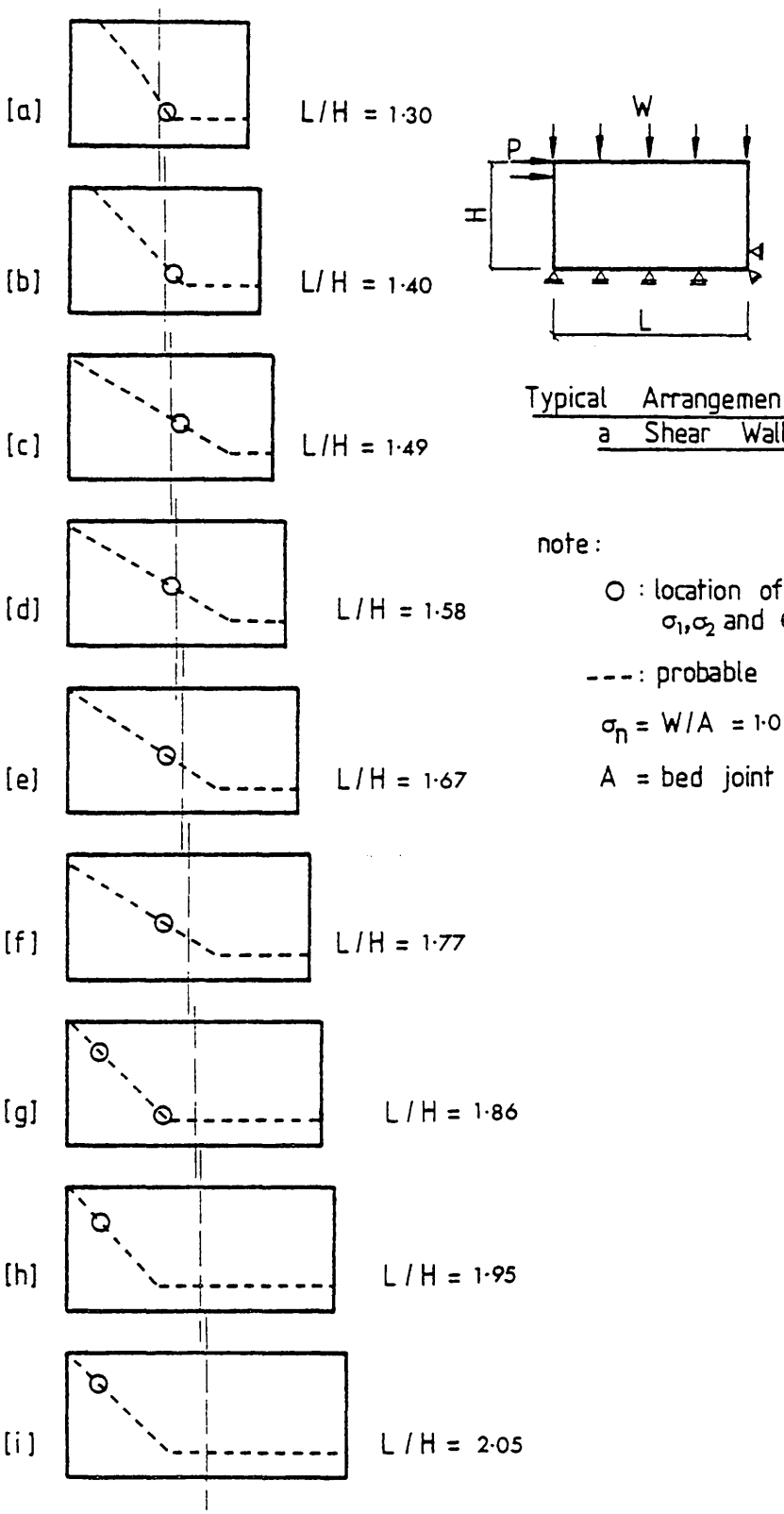

PREDICTED FAILURE MODES FOR SHEAR WALLS HAVING DIFFERENT WALL LENGTHS

FIGURE 6·11

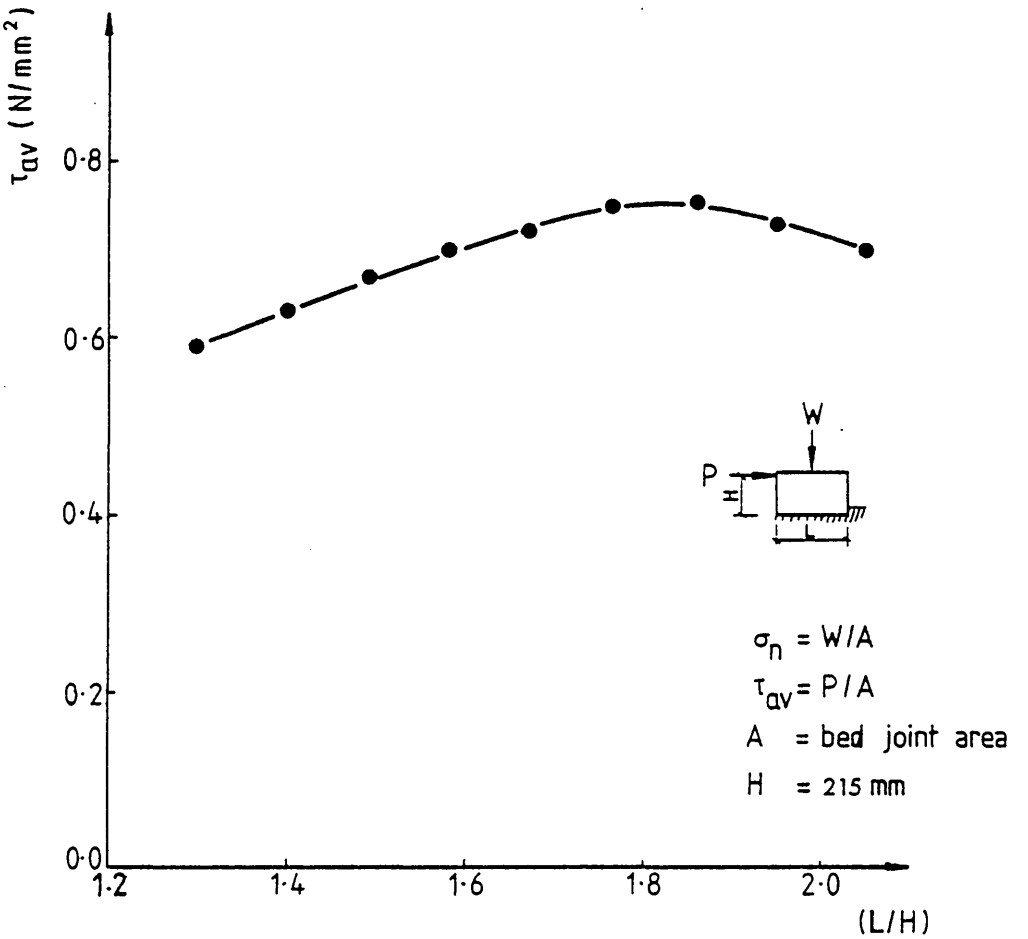

VARIATION OF SHEAR STRENGTH WITH PANEL GEOMETRY [σ_n = 1·0 N/mm^2]

FIGURE 6·12

As has been stated before, previous investigators have calculated the shear strength of wall panels without any regard to the panel geometry using the equation (6.1). It assumes that for any value of σ_n there is only one relevant value of τ_{av}. This may not be strictly true since the panel geometry affects the shear stress at initial failure for constant σ_n, as illustrated by Figure 6.12. However, due to its simplicity, the equation (6.1) can still be used within reasonable limits of L/H, so that the deviation of results can be minimized. The maximum deviation of about $\pm$10% of τ_{av} is observed when L/H varies from 1.2 to 2.0 and hence these limits may be treated as the limit of accuracy of the $\tau_{av} = \tau_o + \mu\sigma_n$ relationship in terms of panel geometry.

6.5.2 The Influence of Method of Load Application and Boundary Conditions on the Shear Strength

The method of load application and boundary conditions play an important role in determining the shear strength. The author considers that the large variation in test results (see Figure 6.5) produced by different investigators is caused mainly by variation in test methods. The different test techniques produce different stress states within the panels which subsequently give rise to different failure loads and failure modes.

In this study three types of test, similar to the tests described in Section 6.2.2 were considered. The typical arrangement

of the test specimens are shown in Figure 6.2. The 320 mm square specimens were analysed using the elastic finite element analysis described in Chapter 5. The loads were applied in increments so that at the end of each load increment the average shear and normal stresses at the bed joints were the same.

The predicted failure modes are illustrated in Figure 6.13. The specimen subjected to 'open-frame test' (see Figure 6.2c) was under a uniform stress state and as a result the whole panel collapsed at one load level. The diagonally loaded test panel failed along the loaded diagonal as was expected, and at the initial cracking load level the crack propagated over a length of 40% of the diagonal. The observation of the magnitudes of stresses near the diagonally loaded corners revealed that those stresses were high enough to cause biaxial compression failure at the corners, at the initiation of biaxial tension-compression failure at the centre. Therefore global failure could be expected immediately after the first crack. The specimen subjected to racking test failed typically along a diagonal connecting the toe and the horizontally loaded point.

The prinicipal stresses at the locations where the initiation of failure took place as the applied load was increased, are shown in Table (6.1). A significant difference in magnitude of critical stresses is evident, despite the fact that the values of τ_{av} and σ_n are the same. The average stresses at the initiation of failure are tabulated in Table (6.2) and it confirms the fact that the test and boundary conditions influence the shear strength of the panel.

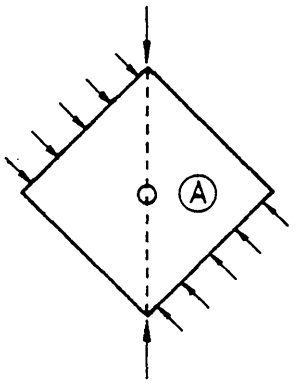

"Diagonal Test"

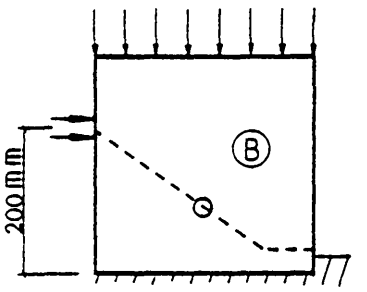

"Racking Test"

note:

---: predicted crack pattern

O : critical location of σ_1, σ_2, and θ

Ⓐ, Ⓑ: 320 mm square specimens

PREDICTED FAILURE MODES FOR SHEAR WALL SPECIMENS

FIGURE 6-13

Test Method	σ_x (N/mm^2)	σ_y (N/mm^2)	τ (N/mm^2)	σ_1 (N/mm^2)	σ_2 (N/mm^2)	θ^o
'Racking Test'	-0.169	-0.122	0.188	0.044	-0.335	48.5
'Open Frame Test'	0.00	-0.222	0.144	0.071	-0.293	26.2
'Diagonal Test'	-0.067	-0.401	0.213	0.037	-0.505	25.9

(i) $\sigma_n = 0.22\ N/mm^2$; $\tau_{av} = 0.072\ N/mm^2$

(ii) compressive stresses are negative

Table 6.1: Critical Stresses for Different Test Techniques

Test Method	σ_n (N/mm^2)	τ_{av} (N/mm^2)
'Racking Test'	1.10	0.722
'Open Frame Test'	1.10	0.722
'Diagonal Test'	1.44	0.936

Table 6.2: Average Stresses at Initiation of Failure Under Different Loading Techniques

6.6 THE VARIATION OF PRINCIPAL TENSILE STRESS AT FAILURE WITH NORMAL STRESS (σ_y) IN SHEAR WALLS

A few investigators[6,68,82] have attempted to find a theoretical solution for shear wall behaviour, in the past. It was hypothesized that the failure of masonry assemblages subjected to combined action of compression and shear occurs when the principal tensile stress reaches a constant value. The tensile strength of brickwork was assumed as a constant and it was obtained either by diameteral testing of a circular disc [Figure 6.14(a)] or by diagonal loading of a square panel [Figure 6.14(b)]. Recently Hamid[23] has shown analytically that instead of a circular disc a hexagonal disc [Figure 6.14(c)] could be used to determine the diagonal tensile strength of brickwork.

Both Chinwah[7] and Schneider[60] have found a relationship between the principal tensile stress at failure and the normal stress from shear wall tests as given by equation (6.7).

$$\sigma_t = \sigma_{to} + 0.05\ \sigma_n \qquad (6.7)$$

σ_{to} is the value of principal tensile stress at failure when the normal stress (σ_n) is zero. The results of both Chinwah and Schneider lie in the range of $\sigma_n < 1.5$ N/mm^2. Therefore the validity of this relationship at high normal stress is a matter of speculation.

[a]

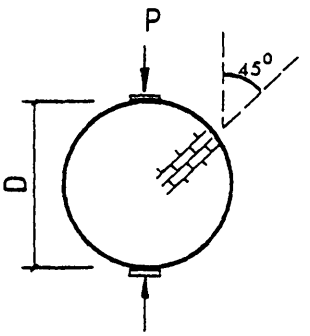

$$f_t = \frac{2P}{\pi D t}$$

[b]

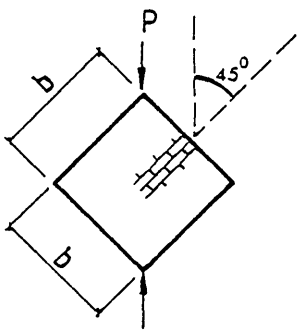

$$f_t = \frac{0.707P}{b\,t}$$

[c]

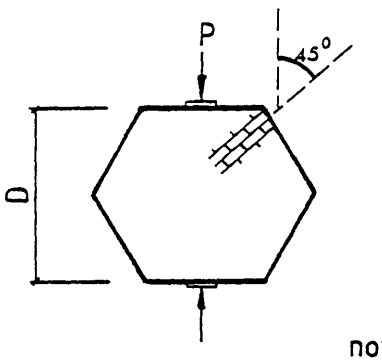

$$f_t = \frac{2P}{\pi D t}$$

note : f_t = diagonal tensile strength of brickwork

t = thickness of wall

DETERMINATION OF DIAGONAL TENSILE STRENGTH OF BRICKWORK

FIGURE 6·14

The variation of the principal tensile stress at failure for brickwork with the increase of normal stress was studied using the biaxial failure envelope. As explained before the failure of shear walls can be defined as a family of $\tau - \sigma_y$ curves corresponding to different magnitudes of lateral stress (σ_x). From each of these curves principal stresses at failure for different combinations of normal and shear stresses can be computed using equation (6.8).

$$\sigma_t = -\frac{(\sigma_x - \sigma_y)}{2} + \tfrac{1}{2}\sqrt{(\sigma_x - \sigma_y)^2 + 4\tau^2} \qquad (6.8)$$

Figure 6.15 illustrates the variation of principal tensile stress at failure with increasing normal stress for different values of σ_x. According to Figure 6.15 for a particular value of σ_x, the principal tensile stress at failure increases to a certain limit with σ_n and thereafter it decreases.

Since most of the shear wall results lie in the range of $\sigma_n < 2.0$ N/mm^2, Figure 6.15 was redrawn to a larger scale and shown (Figure 6.16) for the range of $\sigma_y < 2.0$ N/mm^2. When σ_x is zero, the principal tensile stress at failure seems to be more or less uniform within this range of σ_y. However, this condition does not hold with any other value of σ_x.

Therefore formulation of a general relationship between the principal tensile stress at failure and the normal stress at the bed joints is rather difficult. Nevertheless, as shown above

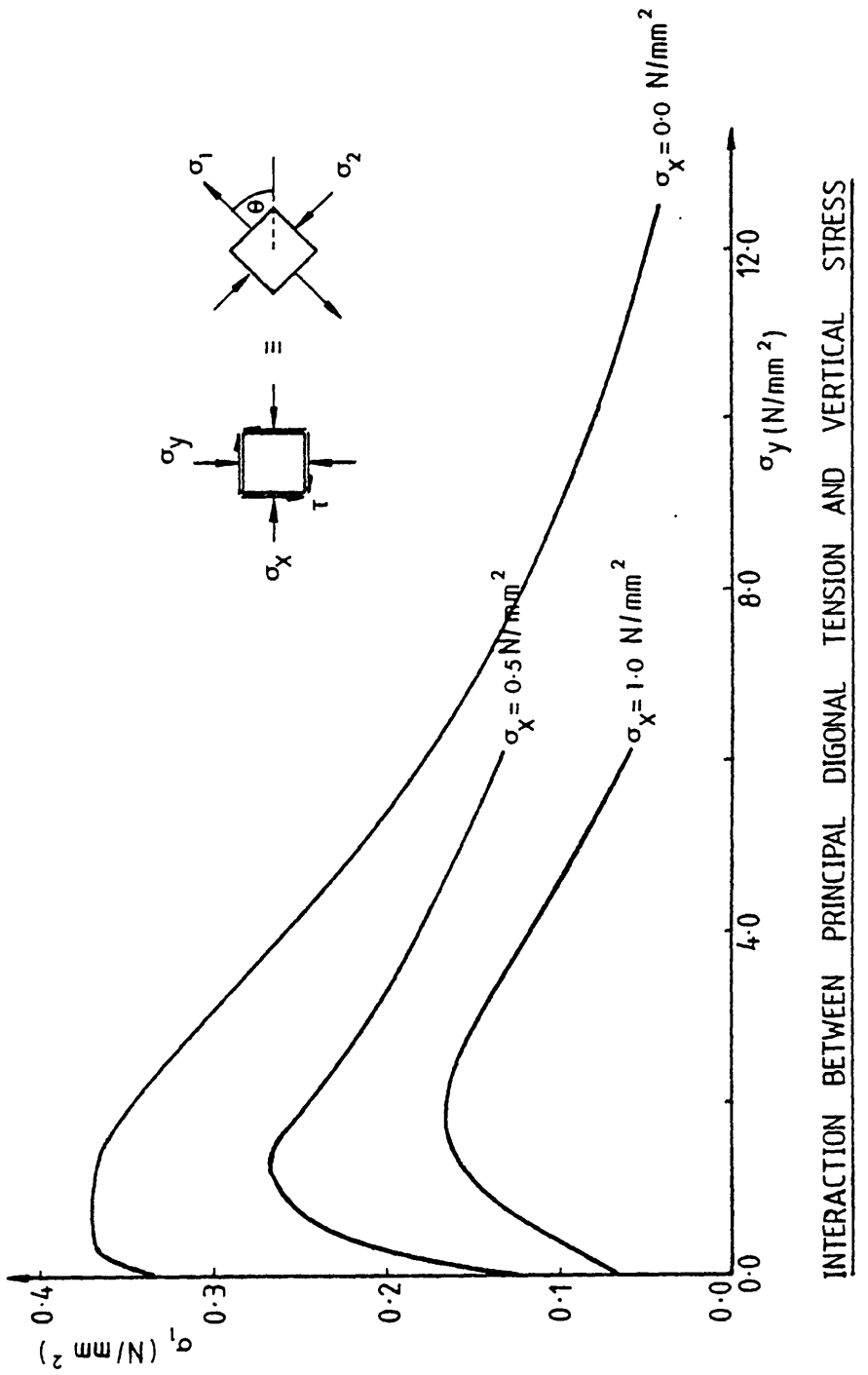

INTERACTION BETWEEN PRINCIPAL DIGONAL TENSION AND VERTICAL STRESS

FIGURE 6·15

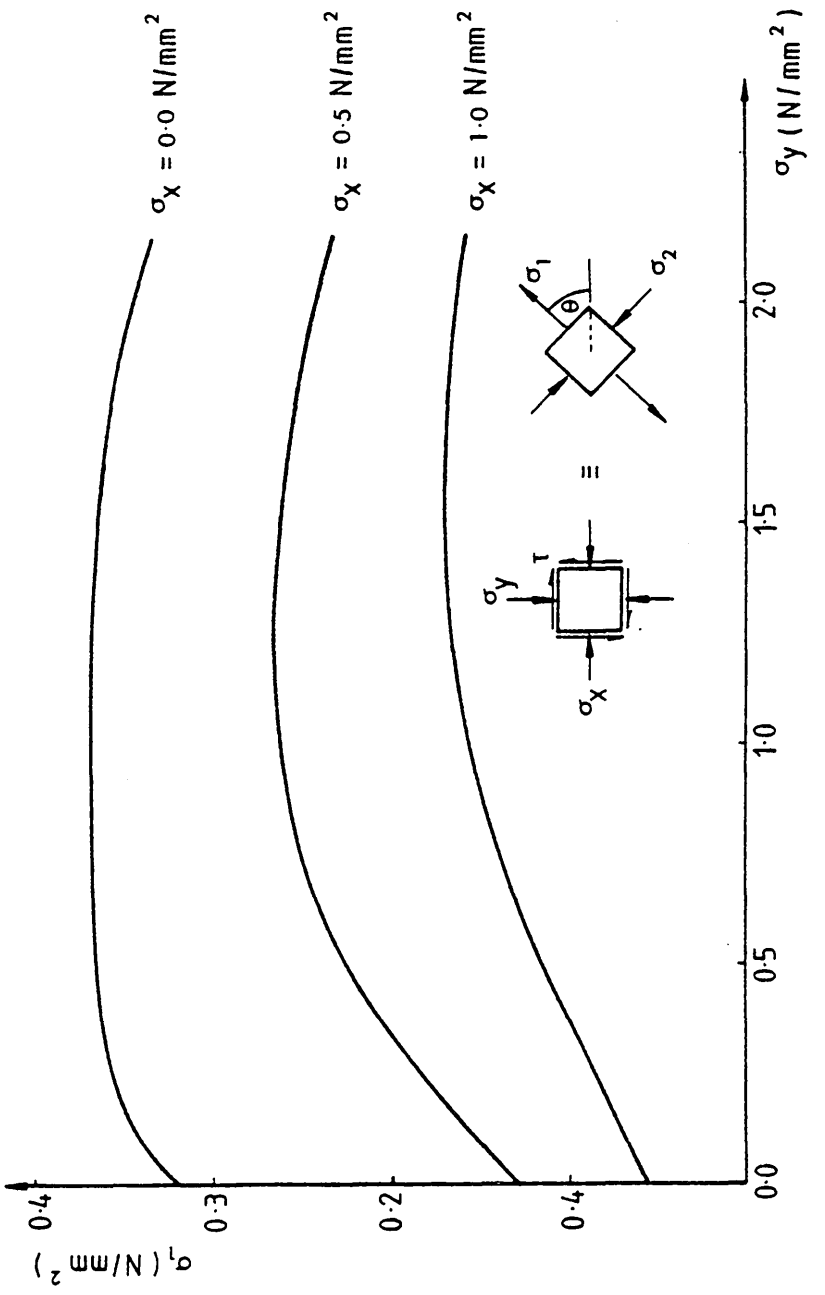

INTERACTION BETWEEN PRINCIPAL DIAGONAL TENSION AND VERTICAL STRESS

FIGURE 6·16 (Enlarged Scale)

where a pure shear condition exists with $\sigma_x = 0$, then the principal stress at failure can be treated as constant for normal stresses up to 2.0 N/mm^2.

6.7 CONCLUSIONS

The derivation of a failure criterion for local failure in brick masonry shear walls have been described. This criterion, in terms of the vertical stress and shear stress at a point, has been derived for particular values of horizontal stress from a three dimensional failure surface which is a function of the principal tensile and compressive stresses at a point and their inclination to the bed joint direction.

It has been shown that, particularly for higher values of vertical compressive stress, variation in the horizontal stress (σ_x) at any point can cause significant changes in the $\sigma_y - \tau$ combination at failure. Substantial differences in the horizontal stress distribution can be produced in shear wall tests which at first glance may appear to be similar. These variations can be caused by the method of application of the shearing load, differences in wall geometry for constant values of σ_n/τ_{av}, and in support conditions at the boundaries of the panel.

The shear strength of the wall panels varies with panel geometry for constant value of precompression. Finite element

calculations indicate that it gradually increases to a certain value and then decreases. Hence the relationship between τ_{av} and σ_n presented by equation (6.1) is not independent of panel geometry. However, it appears that deviation of results due to panel geometry is relatively small if the L/H (panel length/ shear arm) ratio lies between 1.2 and 2.0.

Most of the test techniques adopted for shear wall behaviour have produced non-uniform stresses in the specimen together with a substantial amount of horizontal stress. This is caused by some aspect of the specimen or test procedure. However, the 'open frame test' described in this Chapter appears to be a reasonable technique to determine 'masonry' shear strength from which a τ_{av} - σ_n failure criterion could be developed.

The magnitude of the principal tensile stress at failure of a brickwall subjected to uniform stresses varies with the degree of precompression applied. However, if the wall panel can be subjected to $\sigma_x = 0$ condition then, the principal tensile stress at failure can be treated as constant for normal stresses up to 2.0 N/mm^2.

Although this study is concerned with local failure in shear walls, the effects will be reflected to some extent in the results of tests on complete shear wall panels. These effects will certainly be one of the contributing factors in the differences between results that become evident when comparing tests by different investigators.

CHAPTER SEVEN : SUMMARY AND CONCLUSIONS

7.1 SUMMARY

The behaviour of brick masonry subjected to in-plane loads is described in this thesis. The strength characteristics of brickwork subjected to uniform biaxial stress field have been investigated, and a failure criterion is proposed for the failure of brick masonry under a stress state of biaxial tension-compression. An iterative plane stress finite element computer programme incorporating this information is used to simulate the in-plane behaviour. The results of shear wall tests have been used to test the validity of the analytical model.

An experimental investigation was initiated to study the strength properties under different loading conditions. One-sixth scale model brickwork panels (150 mm wide x 150 mm high x 18 mm thick) built with 1:¼:3 (cement:lime:sand) mortar have been tested in uniaxial tension, uniaxial compression, and in biaxial tension and compression, with different ratios of compression to tension. For each of these cases, a series of tests has been carried out for different bed joint orientations (θ) to the applied loading directions. An idealized surface in terms of principal stresses σ_1 and σ_2 ($\sigma_1 \geq 0$, $\sigma_2 \leq 0$) is suggested based on the experimental results, and the effect of shear bond strength and tensile bond strength on the results is discussed.

In the theoretical model brickwork is treated as a linearly elastic, isotropic material with limited capacity when stressed in a state of biaxial tension-compression. The computer model reproduces the non-linear behaviour of masonry produced by progressive cracking.

The effectiveness of the theoretical model to predict the in-plane failure of brick masonry is checked using shear walls subjected to the combined action of racking load and pre-compression. Sensitivity analysis in respect of the elastic constants used in the analytical model have been performed to illustrate their influence on the calculated stresses.

The derivation of a failure criterion for local failure in masonry shear walls has been described. This criterion, in terms of the vertical stress and shear stress at a point, has been derived for particular values of horizontal stress from the biaxial failure surface:

$$f(\sigma_1 , \sigma_2 \quad \theta) = 0$$

The influence of the local stress distribution on the shear wall behaviour has been investigated. Their failure is usually defined in terms of the average shear and normal stresses on the bed joints, regardless of the shape of the specimen, testing technique and boundary conditions. This study shows that results presented in this way can be misleading if account is not taken of the influence of local stresses on initial failure in critical regions of the panel.

7.2 CONCLUSIONS

Conclusions concerning this study are presented at the end of each chapter. However, general conclusions are also presented below to help gain an overall understanding.

1. Masonry exhibits distinct directional properties due to the influence of mortar joints acting as planes of weakness. To completely define its in-plane failure, a surface in terms of the principal stresses and bed joint orientation is required. Local failure of masonry under uniaxial loading or a combination of shear and compressive load represents particular points on this general failure surface.

2. The strength of brickwork in a state of biaxial stress is greatly affected by the direction of the principal tensile stress relative to the bed joints. In general, the greater the inclination, the lower is the strength of brickwork.

3. The mode of failure of a specimen under a uniform biaxial stress field (σ_1 and σ_2) is governed by the inclination of the bed joints to the major principal stress direction and the ratio of σ_1/σ_2.

4. At low principal compressive stress, the shape of the experimentaly obtained biaxial strength curves are influenced by the shear bond strength to tensile bond strength ratio. When this ratio increases (low tensile

bond strength) the biaxial strength envelopes corresponding to different bed joint orientations have a positive gradient whereas when the ratio decreases (high tensile bond strength) the gradient is negative, at very low compression. At high compression the tensile strength decreases with the increase of compression as for a typical brittle material.

5. The biaxial strength envelope obtained under uniform biaxial stress field can be successfully used to predict the failure of brick masonry subjected to non-uniform biaxial stress.

Satisfactory agreement was obtained between the experimental and theoretical results of shear walls which were used as a basis for comparison between predicted theory and experimental evidence.

The theoretical model is capable of predicting shear wall failure when failure is initiated in the centre of the panel and cracking propagates rapidly in the tension-compression region. For cases where failure is more progressive due to the strengthening effect of the compression-compression stress region, the programme is still capable of predicting "initial" failure. In order to predict the complete behaviour of a shear wall, a criterion in the compression-compression region is therefore also required.

6. Variations in elastic modulus and Poisson's Ratio required for the analytical model do not appreciably influence the calculated stresses. Therefore, isotropic elastic properties can be assumed for brickwork in the application of finite element analysis.

7. Non-uniform stress distribution existing in the specimens is quite evident in the general shear wall tests. Hence the results present in average terms (τ_{av} and σ_n) can be misleading if due regard is not paid to the stress distribution in the test panel.

Local direct stress parallel to the bed joints (σ_x) is quite substantial, and it causes significant changes in a failure criterion for local failure in terms of σ_y (local stress perpendicular to the bed joints) and τ (local shear stress). Particularly for high values of vertical stress, the influence of σ_x is quite substantial. The variation in σ_x distribution from test to test can be caused by the method of application of the loads, differences in wall geometry, and by the support conditions at the boundaries of the panel. This will explain the large differences in results produced by different investigators in terms of the average shear and normal stress on the bed joint.

8. The 'open frame test' described in Chapter 6, section 6.2.2 (Figure 6.2), produce the most uniform state of stress within the wall in comparison to the existing shear wall tests. Provided that the difficulties of applying a uniform shear force along the panel boundaries can be overcome, it is apparent that this would be the most effective test for research purposes. The influence of local variations in stress on panel failure are minimized, thus allowing the more effective study of the other parameters governing shear wall behaviour.

REFERENCES

1. ALLEN, H., "Effect of Direction of Loading on Compressive Strength of Brick Masonry", Proc. of Third International Brick Masonry Conference, Essen, 1973, pp 98-105.

2. AYRA, S.K. & Hegmier, G.A., "On Non-Linear Response Predictions of Concrete Masonry Assemblies, Proc. of North American Masonry Conference, Boulder, Colorado, August 1978, Paper No. 19.

3. BARONI, E., Tozzini, B & Vasarri, V., "Masonry Structures: Masonry as a Continuum Medium with Generalized Planes of Weakness", Paper presented to Fifth International Brick Masonry Conference, Washington D.C., October 1979.

4. BENJAMIN, J.R. & Williams, H.A., "The Behaviour of One-Storey Brick Shear Walls", Journal of Structural Div., A.S.C.E., Vol 84, No 4, July 1958, Paper 1723, pp 1-30.

5. BRADSHAW, R.E. & Hendry, A.W. "Crushing Tests on Storey-Height Walls, 4½ in. Thick: Further Results", The British Ceramic Research Association, Technical Note, No. 105, June 1967.

6. Brochelt, J.G., "Analysis of Brick Walls Subject to Axial Compression and In-Plane Shear", SIBMAC Proc., British Ceramic Research Association, Stoke-on-Trent, England, 1971, pp 263-265.

7. Chinwah, J.C.G., "Shear Resistance of Brick Walls', Ph.D. Thesis, University of London, 1972.

8. "Compressive, Flexural and Diagonal Tensile Testing of Small Scale Four Inch Brick Masonry Specimens", Structural Clay Products Research Foundation, Geneva, Illinois, Research Report No 1, October 1964.

9. "Compressive and Transverse Tests of Five-Inch Brick Walls", Structural Clay Products Research Foundation, Geneva, Illinois, Research Report No. 8, May 1965.

10. "Compressive, Transverse and Racking Strength Tests of Four Inch Brick Walls", Structural Clay Products Research Foundation, Geneva, Illinois, Research Report No. 9, August, 1965.

11. "Compressive and Transverse Strength Tests of Eight-Inch Brick Walls", Structural Clay Products Research Foundation, Geneva, Illinois, Research Report No. 10, October 1966.

12. DESAI, C.S. & Abel, J.F., "Introduction to the Finite Element Method", (Van Nostrand Reinhold, 1972).

13. DRYSDALE, R.G. & Hamid, A.A. "Behaviour of Concrete Block Masonry Under Axial Compression", A.C.I. Proc., Vol. 76, No. 6, June 1979, pp 707-721.

14. DRYSDALE, R.G., Hamid, A.A. & Heidebrecht, A.C., "Tensile Strength of Concrete Masonry", Journal of the Structural Division, A.S.C.E., Vol. 105, No 517, July 1979, pp 1261-1276.

15. DRYSDALE, R., Vanderkeyl, R. & Hamid, A., "Shear Strength of Brick Masonry Joints", Paper presented to Fifth International Brick Masonry Conference, Washington D.C., October 1979.

16. FRANCIS, A.J., Horman, C.B. & Jerrems, L.B., "Effect of Joint Thickness and Other Factors on the Compressive Strength of Brickwork", SIBMAC Proc., British Ceramic Research Association, Stoke-on-Trent, England, 1971, pp 31-37.

17. GANJU, T.N., "Non-Linear Finite Element Analysis of Clay Brick Masonry", Proc. of Sixth Australian Conference on the Mechanics of Structures and Materials, August 1977, pp 59-65.

18. GREENLEY, D.G. & Cattaneo, L.E., "The Effects of Edge Load on the Racking Strength of Clay Masonry", SIBMAC Proc., British Ceramic Research Association, Stoke-on-Trent, England, 1971, pp 157-160.

19. GRIMM, C.T., "Strength and Related Properties of Brick Masonry", Journal of Structural Div., A.S.C.E., Vol. 101, No. ST1, January 1975, pp 217-232.

20. HALLER, P., "Load Capacity of Brick Masonry", Designing, Engineering and Constructing with Masonry Products, Gulf Publishing Co., Houston, Texas, 1969, pp 129-149.

21. HAMID, A.A., Drysdale, R.G. & Heidebrecht, A.C., "Shear Strength of Concrete Masonry Joints", Journal of the Structural Div., A.S.C.E., Vol. 105, No ST7, July 1979, pp 1227-1240.

22. HAMID, A.A. & Drysdale, R.G., "Suggested Failure Criteria for Grouted Concrete Masonry Under Axial Compression", A.C.I. Proc., Vol. 76, No. 10, October 1979, pp 1047-1061.

23. HAMID, A.A., "Behaviour Characteristics of Concrete Masonry", Ph.D. Thesis, McMaster University, Canada, Sept. 1978.

24. HERMIER, G.A., Nunn, R.O. & Arya, S.K., "Behaviour of Concrete Masonry Under Biaxial Stresses", Proc. of the North American Masonry Conference, Boulder, Colorado, August 1978, Paper No. 1.

25. HENDRY, A.W. & Murthy, C.K., "Comparative Tests on 1/3 and 1/6 Scale Model Brickwork Piers and Wall", Proc. British Ceramic Society, No. 4, July 1965, pp 45-66.

26. HENDRY, A.W. & Sinha, B.P., "Shear Tests on Full-Scale Single Storey Brickwork Structures Subjected to Pre-compression", The British Ceramic Research Association, Technical Note, No 134, May 1969.

27. HENDRY, A.W., "A Note on the Strength of Brickwork in Combined Racking Shear and Compression", Proc. of British Ceramic Society, No. 27, December 1978, Load-Bearing Brickwork (6), pp 47-52.

28. HENDRY, A.W. & Sinha, B.P., "Shear Tests on Full-Scale Single Storey Brickwork Structures Subjected to Precompression", Civil Eng. and Public Works Review, 66, No 785, 1971.

29. HILSDORF, H.K., "An Investigation into the Failure Mechanism of Brick Masonry Loaded in Axial Compression", Designing, Engineering and Constructing with Masonry Products, Gulf Publishing Co., Houston, Texas, 1969, pp 34-41.

30. HUGHES, B.P. & Bahramian, B., "Cube Tests and the Uniaxial Compressive Strength of Concrete", Magazine of Concrete Research, Vol. 17, No 53, Dec. 1965, pp 177-182.

31. JOHNSON, F.B. & Thompson, J.N., "Development of Diametral Testing Procedures to Provide a Measure of Strength Characteristics of Masonry Assemblages", Designing, Engineering and Constructing with Masonry Products, Gulf Publishing Co., Houston, Texas, 1969, pp 51-57.

32. KALITA, U.C. & Hendry, A.W., "An Experimental and Theoretical Investigation of the Stresses and Deflections in Model Cross-Wall Structures", The British Ceramic Research Association, Technical Note, No. 148, October 1969.

33. KHOO, C.L. & Hendry, A.W, "Triaxial Compression of Brickwork Mortar", The British Ceramic Research Association, Technical Note, No. 172, July 1971.

34. KHOO, C.L. & Hendry, A.W., "A Failure Criterion for Brickwork in Axial Compression", British Ceramic Research Association, Heavy Clay Division, Technical Note No. 179, February 1972.

35. KHOO, C.L. & Hendry, A.W., "Strength Tests on Brick and Mortar under Complex Stresses for the Development of a Failure Criterion for Brickwork in Compression", Proc. of British Ceramic Society, No. 21, April 1973, Load-Bearing Brickwork (4), pp 51-66.

36. KUPFER, H., Hilsdorf, K. & Rusch, H., "Behaviour of Concrete under Biaxial Stresses", A.C.I. Proceedings, Vol. 66, 1969, pp 656-666.

37. LENCZNER, D., "Elements of Load-Bearing Brickwork", Pergamon Press, 1972.

38. LOSBERG, A. & Johansson, S., "Sideways Pressure on Masonry Walls of Brickwork", Paper presented at the International Symposium on Bearing Walls in Warsaw, June 1969.

39. MALE, D.J. & Arbon, P.F., "A Finite Element Study of Composite Action in Walls", Proc. of the 2nd Australian Conference on the Mechanics of Structures and Materials, Adelaide, South Australia, August 1969, paper No. 14.

40. MANN, W. & Muller, H., "Theoretical and Experimental Behaviour of Tangentially Stressed Masonry", paper presented to Fifth International Brick Masonry Conference (VIBMAC), Washington D.C., October 1979.

41. McKEAUGE, M.J., "Lateral Strength of Brickwork Panels", A Project Report for B.Sc. (Eng), University of Edinburgh, 1978.

42. MAYES, R.L. & Clough, R.W., "A Literatuve Survey - Compressive, Tensile Bond and Shear Strength of Masonry", Report No. EERC 75-15, University of California, Berkeley, 1975.

43. MURTHY, C.K., "Model Studies Related to Load-Bearing Brickwork", Ph.D. Thesis, University of Liverpool, October 1964.

44. MURTHY, C.K. & Hendry, A.W., "Investigation of the Behaviour of a Three-Storey Model Brickwork Structure", Technical Note, No. 66, February 1965.

45. MURTHY, C.K. & Hendry, A.W., "Preliminary Investigation of the Shear Strength of One-Sixth Scale Model Brickwork", Technical Note, No. 65, February 1965.

46. MURTHY, C.K. & Hendry, A.W., "Model Experiments in Load-Bearing Brickwork", Building Science, Vol. 1, 1966, pp 289-298.

47. NUSS, L.K., Noland, J.L. & Chinn, J., "The Parameters Influencing Shear Strength Between Clay Masonry Units and Mortar", Proc. of North American Masonry Conference Boulder, Colorado, August 1978, Paper No. 13.

48. PAGE, A.W., "The In-Plane Deformation and Failure of Brickwork", Ph.D. Thesis, University of Newcastle, Australia, 1977.

49. PAGE, A.W., "A Model for the In-Plane Deformation and Failure of Brickwork", Engineering Bulletin CE8, March, 1978, University of Newcastle, N.S.W. Australia.

50. PAGE, A.W., "Finite Element Model for Masonry", Journal of Structural Div., A.S.C.E. Vol. 104, No. ST8, August 1978, pp 1267-1285.

51. PAGE, A.W., "A Model for the In-Plane Behaviour of Masonry and a Sensitivity Analysis of its Critical Parameters", paper presented to Fifth International Brick Masonry Conference (VIBMAC), Washington D.C., October 1979.

52. PAGE, A.W., "A Biaxial Failure Criterion for Masonry in the Tension-Tension Range", International Journal of Masonry Construction, March 1980.

53. PHILLIPS, D.V. & Zienkiewicz, D.C., "Finite Element Non-Linear Analysis of Concrete Structures", Proc. Institution of Civil Engineers, Part 2, 1976, Vol. 61, March, pp 59-88.

54. PIEPER, K. & Trautsch, W., "Shear Tests on Walls", SIBMAC Proc., British Ceramic Research Association, Stoke-on-Trent England, 1971, pp 140-143.

55. POLYAKOV, S.V., "Masonry in Framed Buildings", G.L. Cairns, Trans., National Lending Library for Science and Technology, Boston Spa., England, 1963.

56. SAHLIN, S., "Structural Masonry", 1st ed., Prentice Hall, N.J. 1971.

57. SAW, C.B., "Linear Elastic Finite Element Analysis of Masonry Walls on Beams", Building Science, Vol. 9, 1974, pp 299-307.

58. SAW, C.B., "Composite Action of Masonry Walls on Beams", Proc. of British Ceramic Society, No. 24, Sept. 1975, Load-Bearing Brickwork (5), pp 139-146.

59. SCHNEIDER, H., "Tests on Shear Resistance of Masonry", Proc. of Fourth International Brick Masonry Conference, Bruges, 1976, paper 4.b.12.

60. SCHNEIDER, H. & Schnell, W., "Tests on the Shear Strength of Brickwork", Betonwork and Fertigteil-Technik, 44 (1978) Heft 6, S. 303-309, Heft. 7., S.369-375.

61. SCRIVENER, J.C., "Static Racking Tests on Masonry Walls", Designing, Engineering and Constructing with Masonry Products, Gulf Publishing Co., Houston, Texas, 1969, pp 185-191.

62. SIMMS, L.G., "The Shear Strength of Some Storey-Height Brickwork and Blockwork Walls", CPTB Technical Note, Vol. 1. No 5, April 1964.

63. SINHA, B.P. & Hendry, A.W., "The Effect of Brickwork Bond on the Load-Bearing Capacity of Model Brick Walls", The British Ceramic Research Association, Technical Note, No. 81, March 1966.

64. SINHA, B.P., "Model Studies Related to Load-Bearing Brickwork", Ph.D. Thesis, 1967, University of Edinburgh, U.K.

65. SINHA, B.P., "Further Crushing Tests on Model Storey Height Brick Walls", The British Ceramic Research Association, Technical Note, No. 130, August 1968.

66. SINHA, B.P. & Hendry, A.W., "Investigation of the Behaviour of a Five-Storey Cross-Wall Structure in Brickwork", The British Ceramic Research Association, Technical Note, No. 127, June 1968.

67. SINHA, B.P., "The Influence of Numbers of Courses and the Effect of Brick Strength on Brickwork Strength", The British Ceramic Research Association, Technical Note, No. 131, August 1968.

68. SINHA, B.P. & Hendry, A.W., "Racking Tests on Storey-Height Shear Wall Structures with Openings, Subjected to Precompression", Designing, Engineering and Constructing with Masonry Products, Gulf Publishing Co., Houston, Texas, 1969, pp 192-199.

69. SINHA, B.P. & Hendry, A.W., "Further Tests on Model Brick Walls and Piers", Proc. of British Ceramic Society, No. 17., February 1970.

70. SINHA, B.P. & Hendry, A.W., "Tensile Strength of Brickwork Specimens", The British Ceramic Research Association, Technical Note, No. 219, March 1974.

71. SINHA, B.P., "A Simplified Ultimate Load Analysis of Laterally Loaded Model Orthotropic Brickwork Panels of Low Tensile Strength", The Structural Engineer, Vol. 56B, No. 4., December 1978, pp 81-84.

72. STAFFORD-SMITH, B., Carter, C. & Choudhury, J.R., "The Diagonal Tensile Strength of Brickwork", The Structural Engineer, Vol. 48, No. 6, June 1970, pp 219-225.

73. STAFFORD-SMITH, B. & Carter, C., "Hypothesis for Shear Failure of Brickwork", Journal of Structural Division, A.S.C.E., Vol. 97, No. ST4, pp 1055-1062, April 1971.

74. STAFFORD-SMITH, B. & Carter, C., "Distribution of Stresses in Masonry Walls Subjected to Vertical Loading", SIBMAC Proc., British Ceramic Research Assocation, Stoke-on-Trent, England 1971, pp 119-124.

75. STAFFORD-SMITH, B. & Rahman, K.M.K., "The Variations of Stress in Vertically Loaded Brickwork Walls", Proc. of the Institution of Civil Engineers, Vol. 51, 1972, pp 689-700.

76. STAFFORD-SMITH, B. & Rahman, K.M.K., "The Variation of Stresses in Brickwork Walls Subject to Shear Forces", Proc. of Third International Brick Masonry Conference, Essen, 1973, pp 167-173.

77. RIDDINGTON, J.R. & Stafford-Smith, B., "Analysis of Infilled Frames Subject to Racking with Design Recommendations", The Structural Engineer, Vol. 55, No. 6, June 1977, pp 263-268.

78. THOMAS, K. & O'Leary, D.C., "Tensile Strength Tests on Two Types of Brick", SIBMAC, Proc., Stoke-on-Trent, England, 1970, pp 69-74.

79. THOMAS, K., "Structural Brickwork-Materials and Performance", The Structural Engineer, October 1971, Vol. 49, No. 10, pp 441-450.

80. TURNSEK, V. & Cacovic, F., "Some Experimental Results on the Strength of Brick Masonry Walls", SIBMAC Proc., British Ceramic Research Association, Stoke-on-Trent, England, 1971, pp 149-156.

81. YOKEL, F.Y., Mathey, R.G. & Dikkers, R.D., "Strength of Masonry Walls Under Compressive and Transverse Loads", U.S. National Bureau Standards of Building Science, Series 34, 1971.

82. YOKEL, F.Y. & Fattal, S.G., "Failure Hypothesis for Masonry Shear Walls", Journal of Structural Division, A.S.C.E., Vol. 102, No. ST3, March 1976, pp 515-532.

83. YORULMAZ, M. & Atan, Y., "Behaviour of Model Masonry (brick) Walls under Biaxial Loading", Proc. of Seventh C.I.B. Congress, Edinburgh, 1977, Vol. B, pp 279-288.

84. ZELGER, C., "Shear Design of Brick Lintels", SIBMAC Proc., British Ceramic Research Association, Stoke-on-Trent, England, 1971, pp 161-164.

85. ZIENKIEWICZ, O.C. & Cheung, Y.K., "The Finite Element Method in Structural and Continuum Mechanics", (McGraw-Hill).

86. B.S. 5628: Part 1: 1978, Code of Practice for Structural Use of Masonry, Part 1, Unreinforced Masonry, British Standards Institution.

87. B.S. 3921. Bricks and Blocks of Fired Brickearth, Clay or Shale.

APPENDIX A : Material Properties

APPENDIX A

B.S. Seives	% by wt. passing
14	100
25	85.2
52	7.9
100	0.8

Table A1: Grading of Sand

Stress (N/mm^2)	Vertical Strain		Lateral Strain	
	Panel No		Panel No	
	1	2	1	2
1.45	6	8	0	1.5
2.90	14	16	1	2
4.36	27	29	3	6
6.00	34	38	4	7
7.25	48	52	5	9
9.00	63	69	9	13
10.80	96	104	17	23
14.40	122	138	24	32
19.00	147	169		

Table A2: Brickwork Panels $\theta = 0^{o}$

Strain Readings on 50 mm Gauge Length $(x \frac{10^{-4}}{4.08})$

Stress (N/mm^2)	Vertical Strain		Lateral Strain	
	Panel No		Panel No	
	1	2	1	2
1.45	8	9	2	2
2.90	21	20	4	5
4.36	36	30	7	9
6.0	54	50	11	14
7.32	73	63	14	19
9.00	94	82	18	25
10.06	118	98	22	29
10.91	137	119	-	-
12.06	160	140	-	-

Table A.3: Brickwork Panels $\theta = 22.5^{o}$

Strain Readings on 50 mm gauge length ($\times 10^{-4}/4.08$)

Stress (N/mm^2)	Vertical Strain		Lateral Strain	
	Panel No		Panel No	
	1	2	1	2
0.72	4.0	2.0	1	1
2.05	13.0	21.0	7	3
2.80	21.0	31.0	11	5
3.45	37.0	53.0	21	15

Table A.4: Brickwork Panels $\theta = 45^{o}$

Strain Readings on 50 mm gauge length ($\times 10^{-4}/4.08$)

Stress (N/mm^2)	Vertical Strain Panel No 1	Vertical Strain Panel No 2	Lateral Strain Panel No 1	Lateral Strain Panel No 2
0.36	4	2	1	0.5
0.95	5	7	2	1
1.45	7	13	4	2
1.80	10	16	7	4

Table A.5: Brickwork Panel $\theta = 67.5^{o}$

Strain Readings on 50 mm Gauge Length ($\times 10^{-4}/4.08$)

Stress (N/mm^2)	Vertical Strain Panel No 1	Vertical Strain Panel No 2	Lateral Strain Panel No 1	Lateral Strain Panel No 2
1.45	2	4	0	1
2.90	8	10	1	2
4.36	15	19	2	3
6.00	23	27	2	5
7.45	40	42	5.5	7.5
8.89	52	56	9	13
10.34	65	71	13	19
12.00	79	89	-	-

Table A.6: Brickwork Panel $\theta = 90^{o}$

Strain Readings on 50 mm Gauge Length ($\times 10^{-4}/4.08$)

APPENDIX B : Biaxial Test Results and Failure Modes

θ^o	Cube Strength of Mortar N/mm²			Tensile Bond Strength N/mm²		f_c N/mm²	f_t N/mm²
	Test 1	Test 2	Test 3	Test a	Test b		
0.0	10.6	8.54	9.86	0.05	0.06	0.00	0.301
0.0	9.2	9.7	9.9	0.04	0.07	0.00	0.310
0.0	10.1	9.2	8.8	0.06	0.06	0.220	0.550
0.0	9.3	9.8	9.6	0.07	-	0.810	0.441
0.0	10.1	9.1	8.8	0.07	-	0.810	0.676
0.0	8.7	8.8	9.1	0.05	0.06	3.00	0.556
0.0	9.9	9.7	9.6	0.08	0.07	3.00	0.525
0.0	9.5	9.4	10.0	0.06	0.06	6.01	0.280
0.0	8.9	9.7	9.3	0.07	0.06	6.00	0.200
0.0	9.5	9.4	9.6	-	-	12.01	0.085
0.0	10.1	9.8	9.5	0.06	0.07	19.44	0.00
0.0	9.1	9.8	9.6	0.08	0.07	20.15	0.00
0.0	9.4	9.5	9.5	0.09	0.07	16.41	0.00
22.5	9.7	9.0	9.5	0.05	0.07	0.00	0.301
22.5	8.8	9.3	9.6	0.08	0.06	0.00	0.285
22.5	9.4	9.6	9.5	0.03	0.05	1.02	0.365
22.5	8.1	8.3	8.7	0.03	0.05	0.99	0.391
22.5	7.2	9.3	9.0	0.08	0.09	3.00	0.408
22.5	9.5	9.6	9.6	0.08	0.09	3.03	0.315
22.5	8.3	8.6	8.5	0.07	0.06	6.00	0.150
22.5	8.9	9.5	9.4	-	0.08	6.20	0.135
22.5	9.2	10.1	9.8	0.07	0.06	13.44	0.00
22.5	9.5	9.6	9.6	0.09	0.08	16.01	0.00
45.0	7.9	8.2	8.3	0.07	0.05	0.00	0.131
45.0	9.6	9.4	9.3	0.08	0.07	0.00	0.180
45.0	9.5	9.2	9.4	0.05	0.07	0.83	0.196
45.0	7.5	9.4	9.1	0.07	0.09	0.80	0.207
45.0	8.0	9.1	9.2	0.06	0.05	1.94	0.182
45.0	9.5	9.4	9.3	0.07	0.06	1.85	0.233
45.0	9.6	9.6	9.1	0.05	0.09	3.01	0.164
45.0	8.9	9.9	9.8	0.05	0.06	2.98	0.121
45.0	9.4	9.3	9.2	0.07	0.05	5.97	0.00
45.0	9.6	9.5	9.2	-	0.04	3.75	0.00
45.0	10.2	9.8	8.8	0.05	0.08	4.01	0.00
67.5	9.1	9.3	9.4	0.09	0.04	0.00	0.073
67.5	8.5	8.6	8.7	0.06	0.08	0.00	0.065
67.5	9.7	9.4	9.5	0.07	0.08	0.46	0.085
67.5	9.8	9.9	9.1	0.07	0.06	0.43	0.092
67.5	9.3	9.7	9.1	0.09	0.07	0.93	0.065
67.5	8.0	7.5	8.6	0.06	0.08	1.01	0.083
67.5	9.2	9.1	9.7	0.05	0.08	1.51	0.046
67.5	9.8	9.9	9.8	0.07	0.09	2.25	0.00
67.5	10.0	9.2	9.3	0.05	0.07	1.66	0.00
67.5	9.5	9.6	9.4	-	-	1.89	0.00
90.0	8.6	8.7	7.0	0.07	0.06	0.00	0.03
90.0	8.0	7.6	8.9	0.03	0.05	0.00	0.02
90.0	9.2	9.1	9.6	0.05	0.09	0.00	0.07
90.0	8.8	9.1	9.6	0.05	0.07	15.71	0.00
90.0	9.5	9.3	9.8	0.08	0.09	16.65	0.00

Table B1: Biaxial Strength of Brickwork

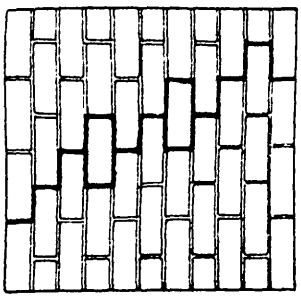

$f_t:f_c$ = 1:0

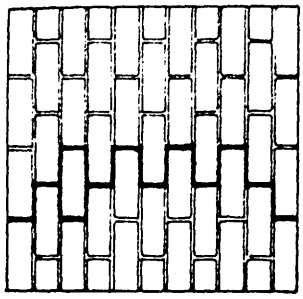

$f_t:f_c$ = 1:0

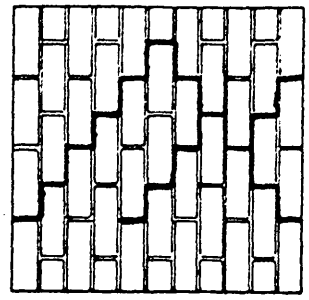

$f_t:f_c$ = 1:0.4

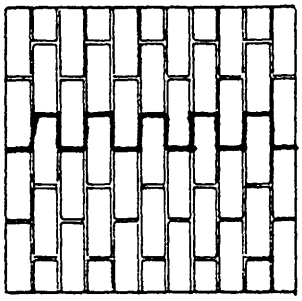

$f_t:f_c$ = 1:1.8

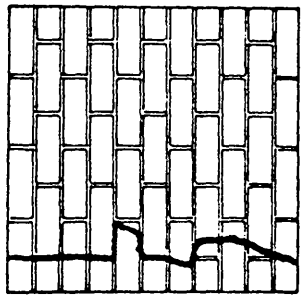

$f_t:f_c$ = 1:1.2

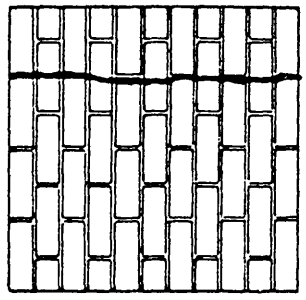

$f_t:f_c$ = 1:5.4

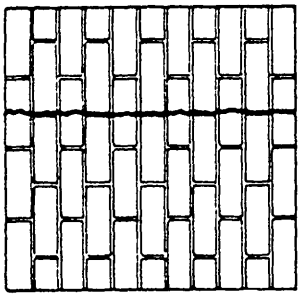

$f_t:f_c$ = 1:5.7

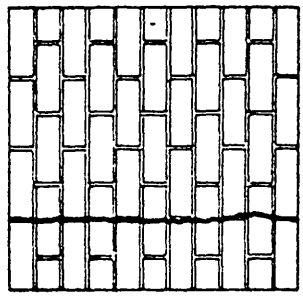

$f_t:f_c$ = 1:21.4

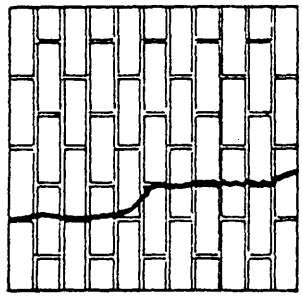

$f_t:f_c$ = 1:30

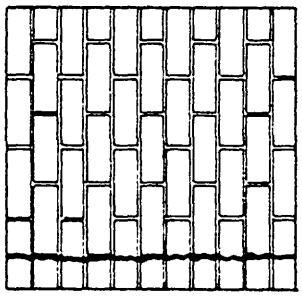

$f_t:f_c$ = 1:140

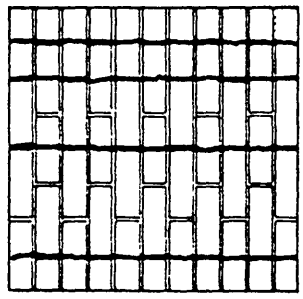

$f_t:f_c$ = 0:1

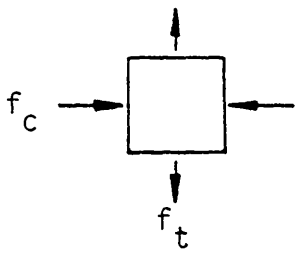

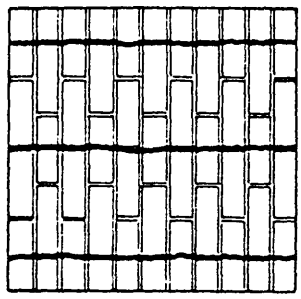

$f_t:f_c$ = 0:1

FIGURE B1 : Failure Modes for $\theta = 0^o$

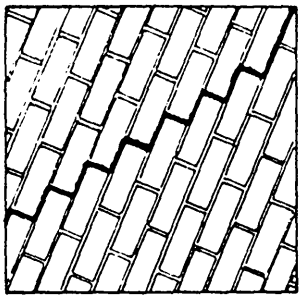

$f_t:f_c$ = 1:0

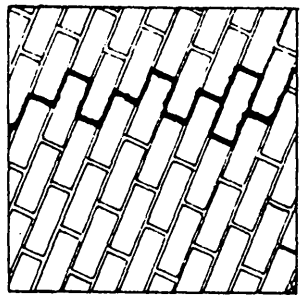

$f_t:f_c$ = 1:0

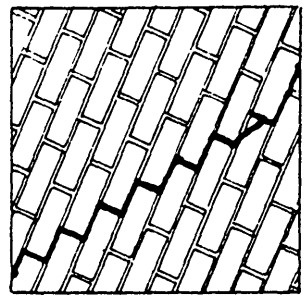

$f_t:f_c$ = 1:2.8

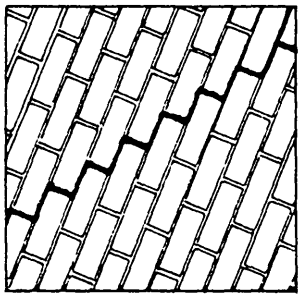

$f_t:f_c$ = 1:2.5

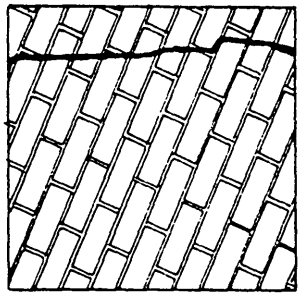

$f_t:f_c$ = 1:7.4

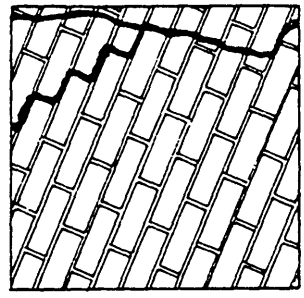

$f_t:f_c$ = 1:33

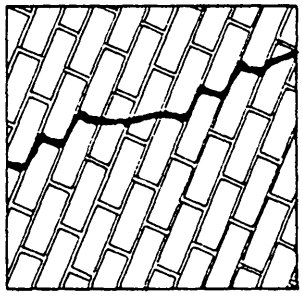

$f_t:f_c$ = 1:40

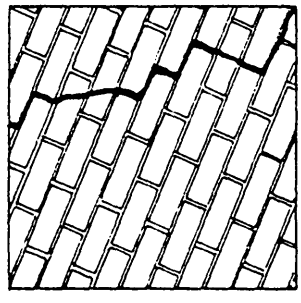

$f_t:f_c$ = 1:46

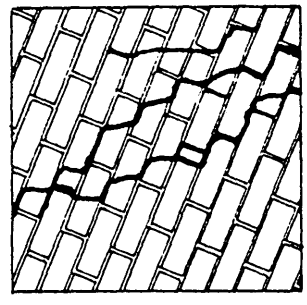

$f_t:f_c$ = 0:1

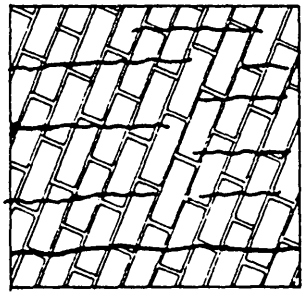

$f_t:f_c$ = 0:1

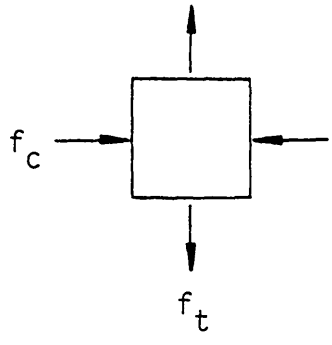

FIGURE B2 : Failure Modes for $\theta = 22.5^{o}$

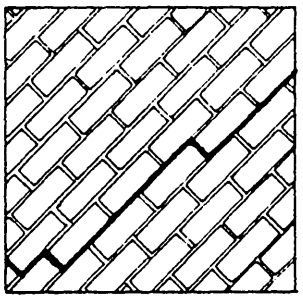

$f_t:f_c$ = 1:0

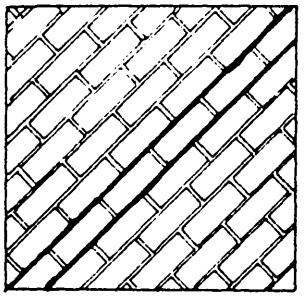

$f_t:f_c$ = 1:0

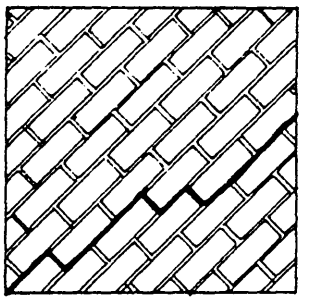

$f_t:f_c$ = 1:4.2

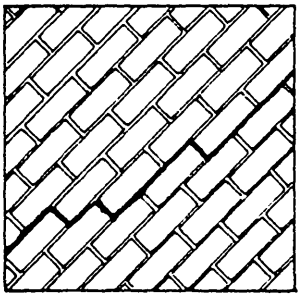

$f_t:f_c$ = 1:3.9

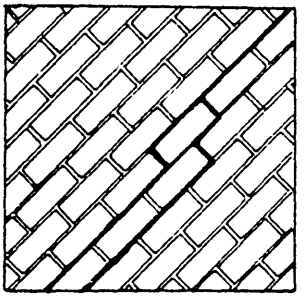

$f_t:f_c$ = 1:7.9

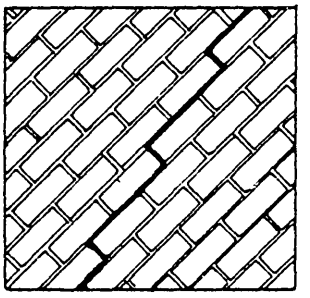

$f_t:f_c$ = 1:10.7

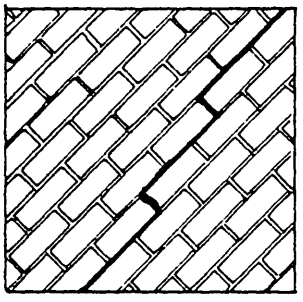

$f_t:f_c$ = 1:18.4

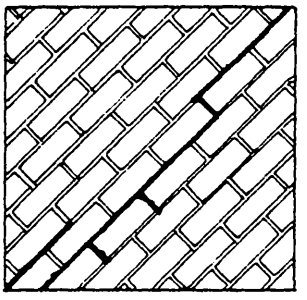

$f_t:f_c$ = 1:24.6

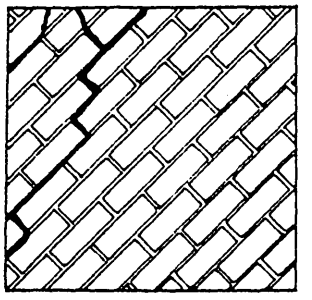

$f_t:f_c$ = 0:1

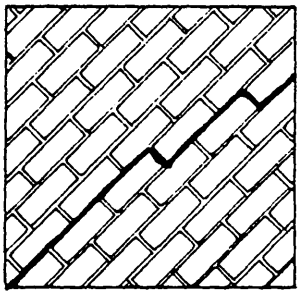

$f_t:f_c$ = 0:1

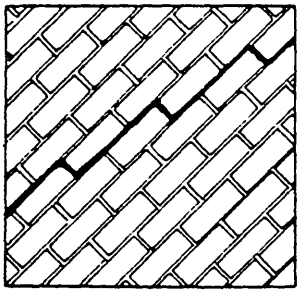

$f_t:f_c$ = 0:1

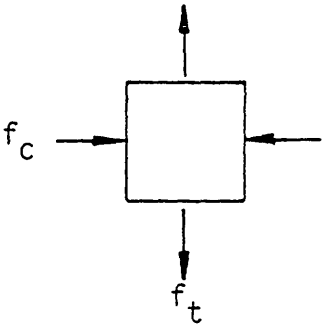

FIGURE B3 : Failure Modes for $\theta = 45^o$

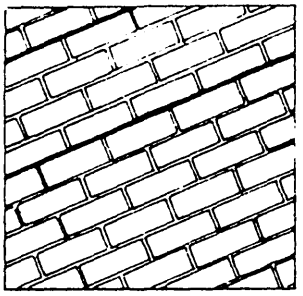

$f_t:f_c$ = 1:0

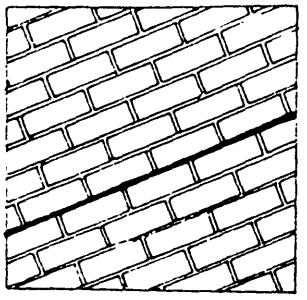

$f_t:f_c$ = 1:0

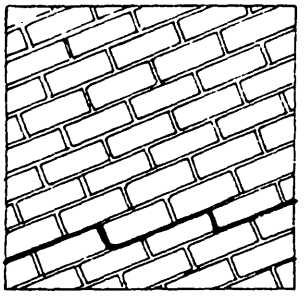

$f_t:f_c$ = 1:0

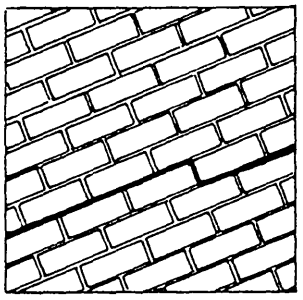

$f_t:f_c$ = 1:4.7

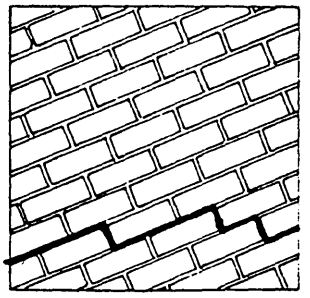

$f_t:f_c$ = 1:12.2

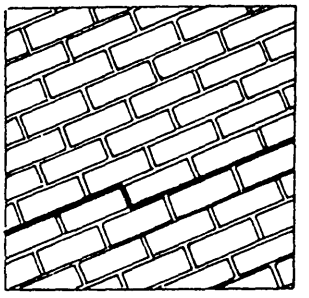

$f_t:f_c$ = 0:14.3

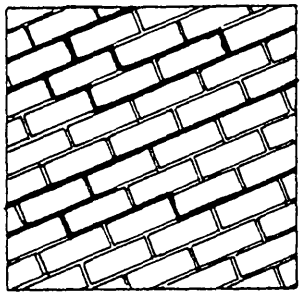

$f_t:f_c$ = 1:12.2

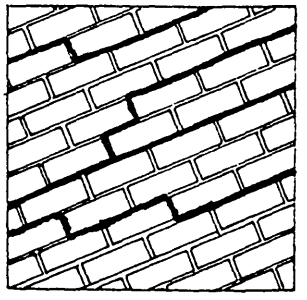

$f_t:f_c$ = 1:32.8

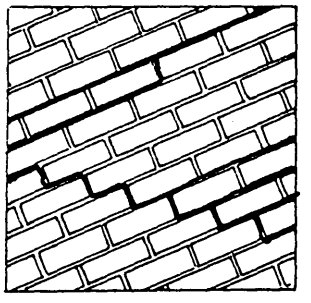

$f_t:f_c$ = 0:1

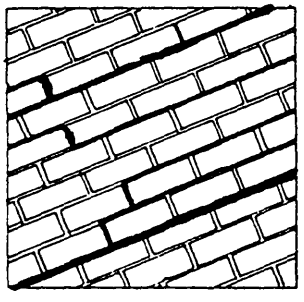

$f_t:f_c$ = 0:1

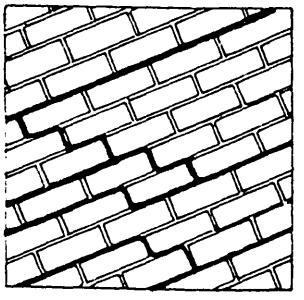

$f_t:f_c$ = 0:1

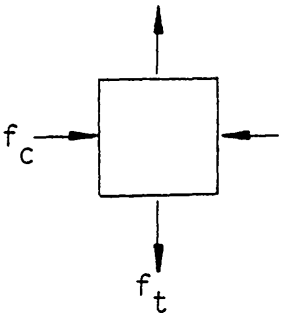

FIGURE B4 : Failure Modes for $\theta = 67.5^{o}$

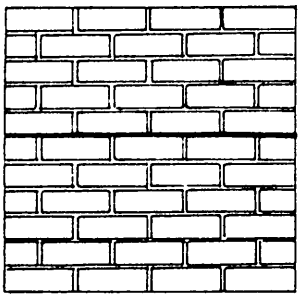

$f_t:f_c$ = 1:0

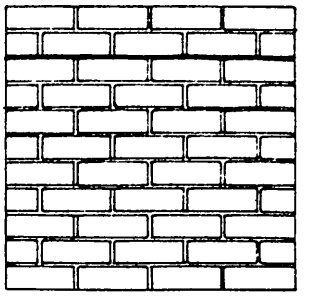

$f_t:f_c$ = 1:0

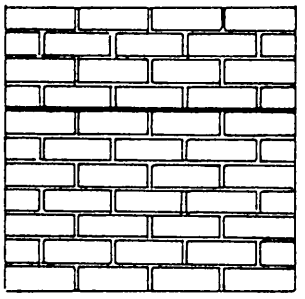

$f_t:f_c$ = 1:0

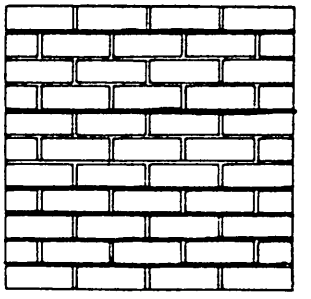

$f_t:f_c$ = 0:1

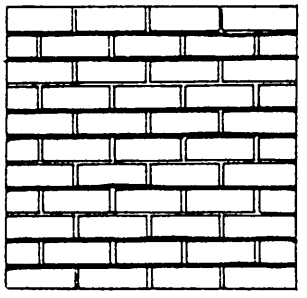

$f_t:f_c$ = 0:1

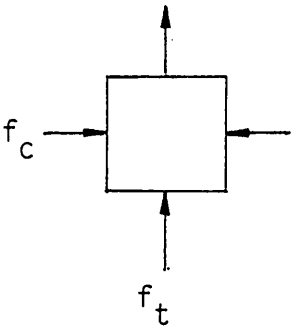

FIGURE B5 : Failure Modes for $\theta = 90^o$

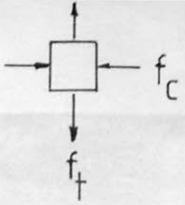

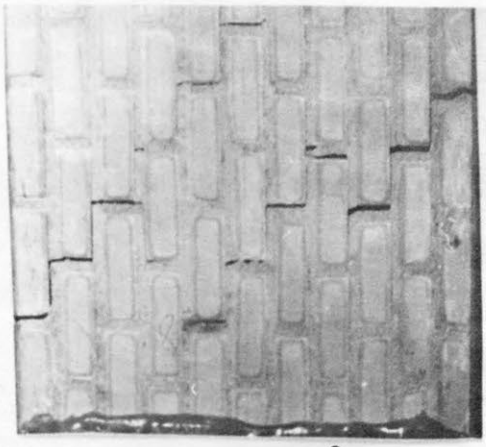

$f_t:f_c$ = 1:0 (θ = 0°)

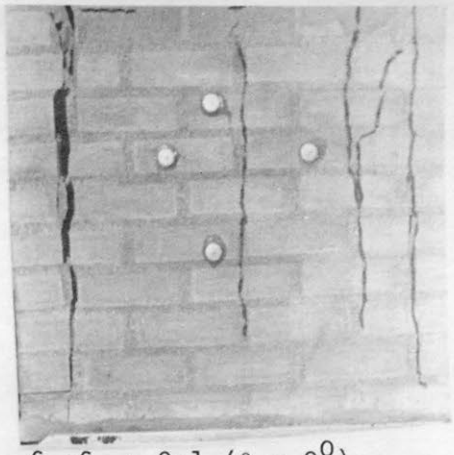

$f_t:f_c$ = 0:1 (θ = 0°)

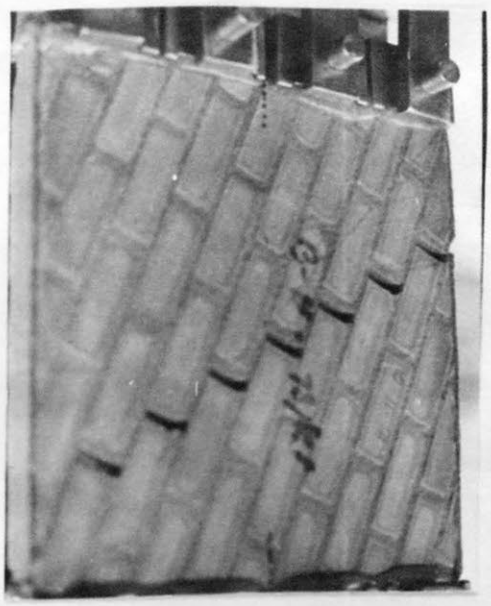

$f_t:f_c$ = 1:2.5 (θ = 22.5°)

$f_t:f_c$ = 1:33 (θ = 22.5°)

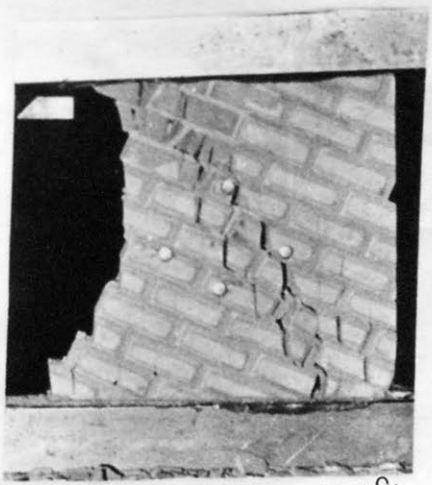

$f_t:f_c$ = 0:1 (θ = 22.5°)

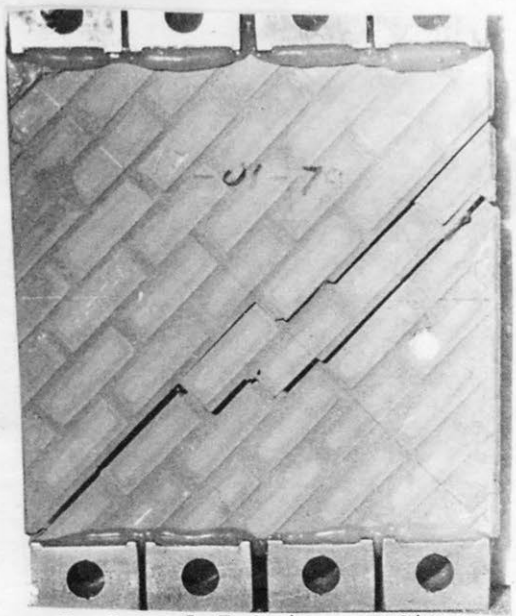

$f_t:f_c$ = 1:7.9 (θ = 45°)

FIGURE B6 : Typical Failure Modes Under Biaxial Stress
(Photographic Illustration)

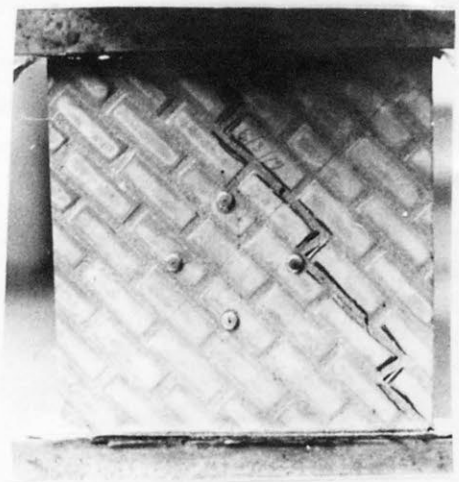

$f_t:f_c$ = 0:1 (θ = 45°)

$f_t:f_c$ = 1:3.9 (θ = 45°)

$f_t:f_c$ = 0:1 (θ = 67.5°)

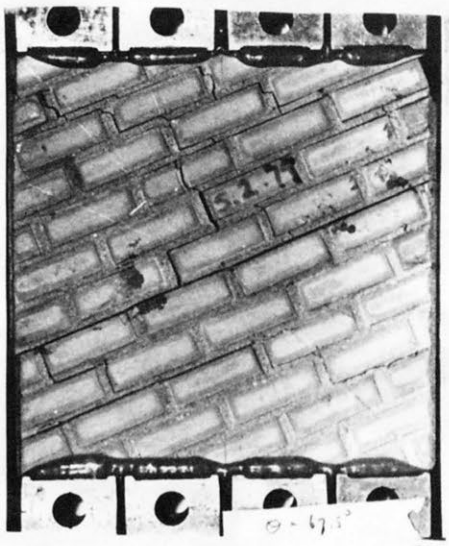

$f_t:f_c$ = 1:12.2 (θ = 67.5°)

$f_t:f_c$ = 0.1 (θ = 90°)

FIGURE B6 cont.

FIGURE B7 : SHEAR WALL F ($\alpha = 36^{o}$)

FIGURE B8 : SHEAR WALL D ($\alpha = 43^{o}$)

FIGURE B9 : SHEAR WALL C ($\alpha = 50^{o}$)

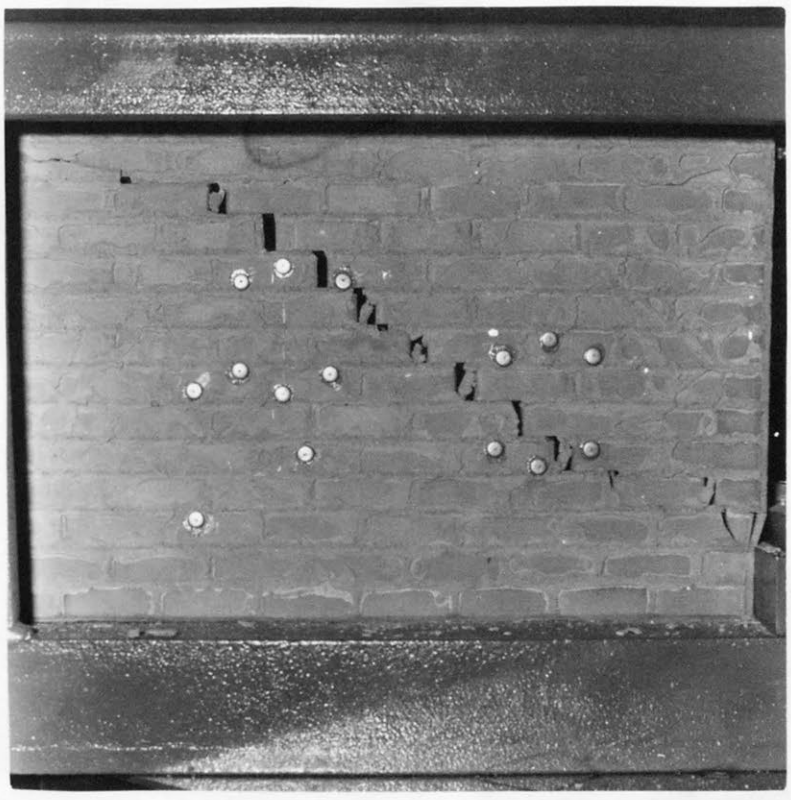

FIGURE B10 : SHEAR WALL A ($\alpha = 56^{o}$)

FIGURE B11 : SHEAR WALL E ($\alpha = 63^{o}$)

APPENDIX C

NOTATION FOR COMPUTER PROGRAMME

The following is the summary of the notation used in the computer programme. All important variables and arrays are listed.

SYMBOL	MEANING
NJ	Number of joints (nodes)
NM	Number of elements
NS	Number of supported joints
NCD	Number of constrained displacements
NPD	Number of prescribed displacements
NL	Number of loaded joints
NLC	Number of loading cases
KS	Order of stiffness matrix (2 x NJ)
NB	Bandwidth
KSMAX	Maximum size of stiffness matrix
NBMAX	Maximum bandwidth
NEQCOR	Number of equations in core during solution of equations
TW	Total width (mm)
TH	Total height (mm)
NX	Number of X co-ordinates
NY	Number of Y co-ordinates
E1	Modulus of elasticity of supporting beam (if any)
E2	Modulus of elasticity of brickwork
E3	Modulus of elasticity of opening (if any)
POIS1	Poisson's Ratio of beam (if any)
POIS2	Poisson's Ratio of brickwork
POIS3	Poisson's Ratio of opening (if any)
NZE	Number of zero elements
NBE	Number of beam elements
JNL	Number of load increments
LCL	Counter for the number of load increments
AF	Area of flange
NODE	Nodal number
XF	Force in X direction

SYMBOL	MEANING
YF	Force in Y direction
IX, IY	Indicators for boundary conditions. IX or IY = 0 if node is restrained in the X or Y direction, respectively. If node is unrestrained in the respective direction, IX or IY = 1.
JCJ	Counter to indicate new crack formation
APLOD(2.NJ)	Vector of nodal loads
AJ(NJ,2)	Joint co-ordinates
JNUM(NM,4)	Member incidences
NODCON(2.NJ)	Vector describing nodal boundary conditions (0 for constrained displacement, 1 for unconstrained displacement and 2 for prescribed displacement)
SK (8,8)	Element stiffness matrix
NOD1(40)	Flange nodes for I beam (if any)
MOD1(40)	Beam elements (if any)
MOD2(40)	Elements in the opening (if any)
MC(200)	Elements cracked under biaxial tension-compression
EE(NM)	Elastic moduli of elements
ANG(NM)	Angle between the principal tensile stress and the bed joint direction
XCRD(NX)	Vector for X co-ordinates
YCRD(NY)	Vector for Y co-ordinates
ND(65)	Nodes at which loads are applied
SLD(NL,2)	Applied loads for increment (X and Y directions)
AK(NEQCOR,NB)	Portion of stiffness matrix in core
SOL(2.NJ,NLC)	Nodal displacements
DISP(8)	Element displacements
STR(3,8)	Stress matrix for rectangular element
STRES(3,NM)	Incremental stress for each element
STREC(3,NM)	Current stress for each element
STRSF(3,NM)	Final stress for each element
PSTR(2,NM)	Principal stress for each element

THE COMPUTER PROGRAMME

```
C     ELASTIC PLANE STRESS(BRICKWORK) PROGRAM-RECTANGULAR ELEMENTS

          COMMON NJ,NM,NS,NCD,NPD,NL,NLC,KS,NB,KSMAX,NBMAX,NEQCOR,TW,TH
      COMMON/ONE/NX,NY,APLOD(1000) ,AJ(500,2),JNUM(450,4),NODCON(1000)
      COMMON/TWO/E1,E2,POIS1,POIS2,SKE(8,8),NOD1(50)
      COMMON/FOUR/MOD1(40),MOD2(40),E3,POIS3,NZE,NBE
      COMMON/FILE/MSTIF,LOSOL
      COMMON/SIX/JNL,LCL,STRSF(3,450),MC(200),EE(450),STRES(3,450),
     1STREC(3,450),PSTR(2,450),ANG(450),JCJ
      DEFINE FILE 1(1000,60,U,MSTIF),6(1,1000,U,LOSOL)
      KSMAX=1000
         NBMAX= 60
         NEQCOR=60
         NLC   = 1
      CALL GENNOD
      CALL SUPPTS
    1 CALL REM4
      CALL LOADS
      CALL GSOLVE(NODCON)
      CALL RM4OUT
      IF(JCJ.EQ.1)GO TO 1
      IF(LCL.EQ.JNL)GO TO 3
      GO TO 1
    3 CONTINUE
      STOP
      END



      SUBROUTINE GENNOD
      DIMENSION XCRD(27),YCRD(25)
      COMMON NJ,NM,NS,NCD,NPD,NL,NLC,KS,NB,KSMAX,NBMAX,NEQCOR,TW,TH
      COMMON/ONE/NX,NY,APLOD(1000) ,AJ(500,2),JNUM(450,4),NODCON(1000)
      COMMON/TWO/E1,E2,POIS1,POIS2,SKE(8,8),NOD1(50)
      COMMON/FILE/MSTIF,LOSOL
      COMMON/SIX/JNL,LCL,STRSF(3,450),MC(200),EE(450),STRES(3,450),
     1STREC(3,450),PSTR(2,450),ANG(450),JCJ
      READ(2,80)NX,NY,NL,NLC,NS,NCD,NPD,TW,TH
   80 FORMAT(7I3,2F7.1)
      WRITE(3,90)
   90 FORMAT(1H1,15X,'ELASTIC ANALYSIS FOR BRICKWORK')
      WRITE(3,82)NX,NY,NL,NLC,NS,NCD,NPD,TW,TH
   82 FORMAT(////,10X,'NX=',I10,7X,'NY=',I10,/,10X,'NL=',I10,7X,'NLC=',
     1I10,/,10X,'NS=',I10,7X,'NCD=',I10,7X,'NPD=',I10,/,10X,'TW=',F10.1,
     27X,'TH=',F10.1)
      LCL=0
      JCJ=0
      READ(2,84)(XCRD(I),I=1,NX)
      READ(2,84)(YCRD(I),I=1,NY)
   84 FORMAT(10F8.1)
      NB=(NX+2)*2
  802 IF(NB.GT.NBMAX)GO TO 200
      NM=(NX-1)*(NY-1)
      NJ=NX*NY
      NZ=1
      NE=NX-1
C           CALCULATION OF MEMBER INCIDENCES
      WRITE(3,81)
   81 FORMAT(///10X,'MEMBER INCIDENCES',/)
      NY1=NY-1
      DO 100 K=1,NY1
      DO 105 NNN=NZ,NE
      JNUM(NNN,1)=NNN+K-1
      JNUM(NNN,2)=NNN+K
      JNUM(NNN,3)=NNN+NX+K-1
      JNUM(NNN,4)=NNN+NX+K
  105 CONTINUE
      WRITE(3,110)(JNUM(N,1),JNUM(N,2),N=NZ,NE)
      WRITE(3,110)(JNUM(N,3),JNUM(N,4),N=NZ,NE)
  110 FORMAT(5X,22I5)
      NZ=NE+1
      NE=NZ+NX-2
  100 CONTINUE
C        CALCULATION OF JOINT COORDINATES
      WRITE(3,120)
  120 FORMAT(///10X,'JOINT COORDINATES IN MM')
      DO 140 J=1,NY
      DO 140 I=1,NX
      K=I+(J-1)*NX
         AJ(K,1)=XCRD(I)
  140    AJ(K,2)=YCRD(J)
      DO 150 J=1,NY
      KK=NJ-J*NX
      KL=KK+1
      WRITE(3,145)KL,(AJ(KK+I,1),I=1,NX)
  145 FORMAT(/,1X,I3,12(F9.1))
      WRITE(3,146)(AJ(KK+I,2),I=1,NX)
```

```
  146 FORMAT(4X,12(F9.1))
  150 CONTINUE
      READ(2,86)JNL
   86 FORMAT(I3)
      WRITE(3,87)JNL
   87 FORMAT(//10X,'NUMBER OF LOAD INCREMENTS =',I3)
      DO 850 I=1,3
      DO 850 J=1,NM
  850 STRSF(I,J)=0.0
      DO 855 I=1,200
  855 MC(I)=0.0
      DO 856 I=1,NM
  856 EE(I)=0.0
      GO TO 130
  200 WRITE(3,160)
  160 FORMAT(33X,'MAXIMUM BANDWIDTH EXCEEDS NBMAX')
  130 RETURN
      END



      SUBROUTINE SUPPTS
      COMMON NJ,NM,NS,NCD,NPD,NL,NLC,KS,NB,KSMAX,NBMAX,NEQCOR,TW,TH
      COMMON/ONE/NX,NY,APLOD(1000) ,AJ(500,2),JNUM(450,4),NODCON(1000)
      COMMON/FILE/MSTIF,LOSOL
         KS=NJ*2
      DO 480 I=1,KS
      NODCON(I)=0
  480 APLOD(I)=0.0
      WRITE(3,450)
  450 FORMAT(///20X,'SUPPORT INFORMATION',/,12X,'JOINT NUMBER',11X,'X',
     113X,'Y')
      DO 10 J=1,NS
      READ(2,5)NODE,IX,IY
    5 FORMAT(I5,3X,2I2)
      WRITE(3,451)NODE,IX,IY
  451 FORMAT(16X,I4,I16,I14)
         KR=2*NODE-1
      IF(IX.EQ.0)NODCON(KR)=1
      IF(IY.EQ.0)NODCON(KR+1)=1
   10 CONTINUE
      IF(NCD.EQ.0)GO TO 21
C NODES WITH SLAVE DISPLACEMENTS
      WRITE(3,460)
  460 FORMAT(///20X,'SLAVE DISPLACEMENTS',/,12X,'JOINT NUMBER',5X,'DISP
     1NO',5X,'CONTROL NODE')
      DO 20 J=1,NCD
      READ(2,15)NODE,IDISP,NODEC
      WRITE(3,461)NODE,IDISP,NODEC
  461 FORMAT(16X,I4,I16,I14)
         KR=2*(NODE-1)+IDISP
         KRC=2*(NODEC-1)+IDISP
         NODCON(KR)=-KRC
   15 FORMAT(I3,I2,I3)
   20 CONTINUE
   21 IF(NPD.EQ.0)GO TO 31
C NODES WITH PRESCRIBED DISPLACEMENTS
      WRITE(3,470)
  470 FORMAT(///20X,'PRESCRIBED DISPLACEMENTS',/,12X,'JOINT NUMBER',5X,'
     1DISP NO',5X,'DISPLACEMENT VALUE')
      DO 30 J=1,NPD
      READ(2,25)NODE,IDISP,DISP
      WRITE(3,471)NODE,IDISP,DISP
  471 FORMAT(16X,I4,I16,F14.3)
         KR=2*(NODE-1)+IDISP
         NODCON(KR)=2
         APLOD(KR)=DISP
   25 FORMAT(I3,I2,F10.0)
   30 CONTINUE
      WRITE(3,1000)(NODCON(I),I=1,60)
 1000 FORMAT(//,6(5X,10I10,/))
   31 RETURN
      END



      SUBROUTINE REM4
      DIMENSION V(60),SK(8,8),ZN1(8,8),ZN1T(8,8),BDB(8,8),ZB(8,8)
      COMMON NJ,NM,NS,NCD,NPD,NL,NLC,KS,NB,KSMAX,NBMAX,NEQCOR,TW,TH
      COMMON/ONE/NX,NY,APLOD(1000) ,AJ(500,2),JNUM(450,4),NODCON(1000)
      COMMON/TWO/E1,E2,POIS1,POIS2,SKE(8,8),NOD1(50)
      COMMON/FOUR/MOD1(40),MOD2(40),E3,POIS3,NZE,NBE
      COMMON/FILE/MSTIF,LOSOL
      COMMON/SIX/JNL,LCL,STRSF(3,450),MC(200),EE(450),STRES(3,450),
     1STREC(3,450),PSTR(2,450),ANG(450),JCJ
C         MATERIAL PROPERTIES INPUT
      IF(LCL.NE.0)GO TO 220
      READ(2,715)E1,E2,POIS1,POIS2,T1,T2,E3,POIS3,NZE,NBE
  715 FORMAT(8(F8.0),2I4)
      WRITE(3,716)E1,E2,E3,POIS1,POIS2,POIS3,T1,T2,NZE,NBE
  716 FORMAT(//10X,'E1=',F10.1,5X,'E2=',F10.1,5X,'E3=',F10.4,//,10X,'POI
     CS1=',F10.1,2X,'POIS2=',F10.1,2X,'POIS3=',F10.1,//,10X,
     C//,10X,'T1=',F10.1,5X,'T2=',F10.1,//,10X,'ZERO ELEMENTS='
     C,I4,/,10X,'BEAM ELEMENTS=',I4)
      NX1=2*(NX-1)
      READ(2,717)(NOD1(I),I=1,NX1)
      READ(2,717)(MOD1(I),I=1,NBE)
      READ(2,717)(MOD2(I),I=1,NZE)
  717 FORMAT(20I4)
      READ(2,718)AF
  718 FORMAT(F8.1)
      WRITE(3,719)AF
```

```
  719 FORMAT(//10X,'FLANGE AREA=',F8.1)
      WRITE(3,720)(NOD1(I),I=1,NX1)
  720 FORMAT(//10X,'FLANGE NODES',/,10X,10(I4,2X))
      WRITE(3,721)(MOD1(I),I=1,NBE)
  721 FORMAT(//10X,'E1 ELEMENTS',/,10X,10(I4,2X))
      WRITE(3,724)(MOD2(I),I=1,NZE)
  724 FORMAT(//10X,'ELEMENTS IN THE OPENING',/,10X,10(I4,2X))
  220 CONTINUE
      DO 300 I=1,NBMAX
  300 V(I)=0.0
      DO 86 I=1,KS
   86 WRITE(1'I)(V(J),J=1,NB)
         R=0.0
      DO 110 NNN=1,NM
         J1=JNUM(NNN,1)
         J2=JNUM(NNN,2)
         J3=JNUM(NNN,3)
         TXINT=AJ(J2,1)-AJ(J1,1)
         TYINT=AJ(J3,2)-AJ(J1,2)
         TR=TYINT/TXINT
      DO 726 I=1,NBE
      IF(NNN.NE.(MOD1(I))) GO TO 726
C     BEAM ELEMENT
      E=E1
      T=T1
      POIS=POIS1
      GO TO 203
  726 CONTINUE
      DO 725 I=1,NZE
      IF(NNN.NE.(MOD2(I))) GO TO 725
C     ELEMENT IN THE OPENING
      E=E3
      T=T2
      POIS=POIS3
      GO TO 203
  725 CONTINUE
C     BRICK ELEMENT
      E=E2
      T=T2
      POIS=POIS2
  203 EE(NNN)=E
      DO 10 I=1,200
      IF (NNN.NE.MC(I))GO TO 10
      EE(NNN)=0.0001
      E=.0001
   10 CONTINUE
      G=E/(2.*(1.+POIS))
C     ELEMENT STIFFNESS MATRIX
      DO 205 I=1,8
      DO 205 J=1,8
      ZN1(I,J)=0.0
      ZN1T(I,J)=0.0
      ZB(I,J)=0.0
  205 BDB(I,J)=0.0
      DO 770 J=1,7,2
      ZN1(1,J)=TXINT*TYINT*0.25
  770 ZN1(2,J+1)=TXINT*TYINT*0.25
      DO 771 J=1,5,4
      ZN1(3,J)=-TYINT*0.5
  771 ZN1(4,J+1)=-TYINT*0.5
      DO 772 J=3,7,4
      ZN1(3,J)=TYINT*0.5
  772 ZN1(4,J+1)=TYINT*0.5
      DO 773 J=1,3,2
      ZN1(5,J)=-TXINT*0.5
  773 ZN1(6,J+1)=-TXINT*0.5
      DO 774 J=5,7,2
      ZN1(5,J)=TXINT*0.5
  774 ZN1(6,J+1)=TXINT*0.5
      DO 775 J=1,7,6
      ZN1(7,J)=1.0
  775 ZN1(8,J+1)=1.0
      DO 776 J=3,5,2
      ZN1(7,J)=-1.0
  776 ZN1(8,J+1)=-1.0
       DO 206 I=1,8
      DO 206 J=1,8
  206 ZN1(I,J)=ZN1(I,J)/(TXINT*TYINT)
      DO 207 I=1,8
      DO 207 J=1,8
  207 ZN1T(I,J)=ZN1(J,I)
      PX=1.-POIS*POIS
      GX=(1.-POIS)/2.
      BDB(3,3)=1.0
      BDB(6,6)=1.0
      BDB(3,6)=POIS
      BDB(6,3)=POIS
      DO 777 I=1,2
      DO 777 J=1,2
  777 BDB(3+I,3+J)=GX
      BDB(7,7)=(TYINT/2.)**2*PX/3.
      BDB(8,8)=(TXINT/2.)**2*PX/3.
      CONS=E*(TXINT*TYINT)/PX
      DO 208 I=1,8
      DO 208 J=1,8
  208 BDB(I,J)=BDB(I,J)*CONS
      DO 209 I=1,8
      DO 209 J=1,8
      ZB(I,J)=0.0
      DO 209 K=1,8
  209 ZB(I,J)=ZB(I,J)+ZN1T(I,K)*BDB(K,J)
      DO 210 I=1,8
```

```
      DO 210 J=1,8
      SK(I,J)=0.0
      DO 210 K=1,8
  210 SK(I,J)=SK(I,J)+ZB(I,K)*ZN1(K,J)
      DO 211 I=1,8
      DO 211 J=1,8
  211 SK(I,J)=SK(I,J)*T
C     INSERT BEAM FLANGES
C      ADJACENT FLANGES
      FT=(AF*0.5*E1)/TXINT
      DO 201 I=1,NX1
      IF(J1.NE.NOD1(I)) GO TO 200
      SK(1,1)=SK(1,1)+FT
      SK(1,3)=SK(1,3)-FT
      SK(3,1)=SK(3,1)-FT
      SK(3,3)=SK(3,3)+FT
  200 IF(J3.NE.NOD1(I)) GO TO 201
      SK(5,5)=SK(5,5)+FT
      SK(5,7)=SK(5,7)-FT
      SK(7,5)=SK(7,5)-FT
      SK(7,7)=SK(7,7)+FT
  201 CONTINUE
      CALL ASSMBL(NNN,SK)
  110 CONTINUE
      RETURN
      END



      SUBROUTINE ASSMBL(NNN,SK)
      DIMENSION APL(8),KROW(8),V(60),SK(8,8)
      COMMON NJ,NM,NS,NCD,NPD,NL,NLC,KS,NB,KSMAX,NBMAX,NEQCOR,TW,TH
      COMMON/ONE/NX,NY,APLOD(1000),AJ(500,2),JNUM(450,4),NODCON(1000)
      COMMON/TWO/E1,E2,POIS1,POIS2,SKE(8,8),NOD1(50)
      COMMON/FILE/MSTIF,LOSOL
      COMMON/SIX/JNL,LCL,STRSF(3,450),MC(200),EE(450),STRES(3,450),
     1STREC(3,450),PSTR(2,450),ANG(450),JCJ
      DO 6 I=1,8
         APL(I)=0.0
    6    KROW(I)=0.0
      DO 10 J=1,4
         KROW(2*J)=2*JNUM(NNN,J)
         KROW(2*J-1)=KROW(2*J)-1
   10 CONTINUE
C CHECK IF ANY DISPLACEMENTS CONSTRAINED
      IF(NCD.EQ.0)GO TO 35
C ADJUST KROW FOR CONSTRAINTS
      DO 15 J=1,8
         KR=KROW(J)
      IF(NODCON(KR).LT.0)KROW(J)=-NODCON(KR)
   15 CONTINUE
C CHECK IF TWO DISPLACEMENTS SAME FOR THIS ELEMENT
      DO 30 J=1,7
      JJ=J+1
      DO 30 I=JJ,8
      IF(KROW(I).NE.KROW(J))GO TO 30
      DO 20 II=1,8
         SK(J,II)=SK(J,II)+SK(I,II)
   20    SK(I,II)=0.0
      DO 25 II=1,8
         SK(II,J)=SK(II,J)+SK(II,I)
   25    SK(II,I)=0.0
   30 CONTINUE
C CHECK FOR PRESCRIBED DISPLACEMENTS
   35 IF(NPD.EQ.0)GO TO 55
      DO 45 J=1,8
         KR=KROW(J)
      IF(NODCON(KR).NE.2)GO TO 45
      DO 40 I=1,8
         SK(J,I)=0.0
      JJ=J+1
      DO 41 L=JJ,8
         KRL=KROW(L)
      IF(NODCON(KRL).EQ.2)SK(L,J)=0.0
   41 CONTINUE
      APL(I)=APL(I)-SK(I,J)*APLOD(KR)
         SK(I,J)=0.0
   40 CONTINUE
   45 CONTINUE
      DO 50 I=1,8
         KR=KROW(I)
   50    APLOD(KR)=APLOD(KR)+APL(I)
   55 CONTINUE
C MODIFY ELEMENT STIFFNESS MATRIX FOR ZERO DISPLACEMENTS
      DO 65 J=1,8
         KR=KROW(J)
      IF(NODCON(KR).NE.1)GO TO 65
         APLOD(KR)=0.0
      DO 60 I=1,8
      SK(J,I)=0.0
   60 SK(I,J)=0.0
   65 CONTINUE
      DO 70 J=1,8
         KR=KROW(J)
      IF(NODCON(KR).NE.0)KROW(J)=0
   70 CONTINUE
C ADD IN MODIFIED ELEMENT STIFFNESS MATRIX
      DO 80 J=1,8
         KR=KROW(J)
      IF(KR.EQ.0)GO TO 80
      READ(1'KR)(V(K),K=1,NB)
      DO 75 I=1,8
```

```
      KE=KROW(I)-KR+1
      IF(KE.GT.NB)GO TO 85
      IF(KE.LT.1)GO TO 75
      V(KE)=V(KE)+SK(J,I)
   75 CONTINUE
      WRITE(1'KR)(V(K),K=1,NB)
   80 CONTINUE
      RETURN
   85 WRITE(3,90)
   90 FORMAT(1X,'BANDWIDTH EXCEEDS NB')
      RETURN
      END



      SUBROUTINE LOADS
      DIMENSION ND(65),SLD(65,2)
      COMMON NJ,NM,NS,NCD,NPD,NL,NLC,KS,NB,KSMAX,NBMAX,NEQCOR,TW,TH
      COMMON/ONE/NX,NY,APLOD(1000) ,AJ(500,2),JNUM(450,4),NODCON(1000)
      COMMON/FILE/MSTIF,LOSOL
      COMMON/SIX/JNL,LCL,STRSF(3,450),MC(200),EE(450),STRES(3,450),
     1STREC(3,450),PSTR(2,450),ANG(450),JCJ
      READ(6'1)(APLOD(J),J=1,KS)
      DO 450 I=1,KS
  450 APLOD(I)=0.0
      IF(NL.EQ.0)GO TO 421
      WRITE(3,400)
  400 FORMAT(///20X,'LOAD INFORMATION',/12X,'JOINT NUMBER',11X,'X LOAD',
     113X,'Y LOAD')
      IF(LCL.NE.0)GO TO 420
C     READ IN INCREMENTAL APPLIED LOAD VALUES
      DO 420 I=1,NL
      READ(2,411)NODE,XF,YF
  411 FORMAT(I3,1X,2(F10.0))
      ND(I)=NODE
      SLD(I,1)=XF
      SLD(I,2)=YF
  420 CONTINUE
      DO 452 I=1,NL
      NODE=ND(I)
      LCON1=(NODE-1)*2+1
      LCON2=LCON1+1
      XF=SLD(I,1)
      YF=SLD(I,2)
      APLOD(LCON1)=XF
      APLOD(LCON2)=YF
      JCL=LCL+1
      IF(JCJ.EQ.1)JCL=LCL
      XFA=XF*JCL
      YFA=YF*JCL
      WRITE(3,412)NODE,XFA,YFA
  412 FORMAT(16X,I3,7X,2(5X,F10.0))
  452 CONTINUE
  421 CONTINUE
      DO 425 I=1,NLC
  425 WRITE(6'I)(APLOD(J),J=1,KS)
      LCL=LCL+1
      IF(JCJ.EQ.1)LCL=LCL-1
      RETURN
      END



      SUBROUTINE GSOLVE(NODCON)
      DIMENSION AK(60,60),SOL(1000,1),NODCON(1000),CPL(1)
      COMMON NJ,NM,NS,NCD,NPD,NL,NLC,KS,NB,KSMAX,NBMAX,NEQCOR,TW,TH
      COMMON/FILE/MSTIF,LOSOL
      COMMON/SIX/JNL,LCL,STRSF(3,450),MC(200),EE(450),STRES(3,450),
     1STREC(3,450),PSTR(2,450),ANG(450),JCJ
      ICORE(I)=I-((I-1)/NEQCOR)*NEQCOR
      NRS=KS-1
      READ(1'1)((AK(I,J),J=1,NBMAX),I=1,NEQCOR)
      READ(6'1)((SOL(I,J),I=1,KSMAX),J=1,NLC)
      NEQINC=NEQCOR
      DO 20 N=1,NRS
      IF(NODCON(N).NE.0)GO TO 20
      M=N-1
      MR=MIN0(NB,KS-M)
      NCE=ICORE(N)
      PIVOT=AK(NCE,1)
      DO 1 LC=1,NLC
      CPL(LC)=SOL(N,LC)
    1 SOL(N,LC)=CPL(LC)/AK(NCE,1)
      DO 2099 L=2,MR
      CP=AK(NCE,L)/PIVOT
      I=M+L
      ICE=ICORE(I)
      IF(I.LE.NEQINC)GO TO 6
      NWAD=I-NEQCOR
      IF(ICE.GT.NCE)NW=NEQCOR+1-ICE
      IF(ICE.LT.NCE)NW=NCE-ICE
      NEQINC=NEQINC+NW
      IF(NEQINC.LE.KS)GO TO 5
      NEQINC=KS
      NW=KS-I+1
    5 NFAD=ICE+NW-1
      WRITE(1'NWAD)((AK(IW,JW),JW=1,NBMAX),IW=ICE,NFAD)
      READ(1'I)((AK(IW,JW),JW=1,NBMAX),IW=ICE,NFAD)
    6 IF(NODCON(I).NE.0)GO TO 2099
      J=0
      DO 10 K=L,MR
      J=J+1
```

```
   10    AK(ICE,J)=AK(ICE,J)-CP*AK(NCE,K)
         AK(NCE,L)=CP
      DO 8 LC=1,NLC
    8    SOL(I,LC)=SOL(I,LC)-AK(NCE,L)*CPL(LC)
 2099 CONTINUE
   20 CONTINUE
         KSE=ICORE(KS)
         NWAD=KS+1-NEQCOR
      KSS=KSE+1
      WRITE(1'NWAD)((AK(IW,JW),JW=1,NBMAX),IW=KSS,NEQCOR)
C     NOT ALL OF UPPER TRIANGLE TRANSFERRED TO DISK
C     BACKSUBSTITUTION
      DO 25 LC=1,NLC
      IF(NODCON(KS).NE.0)GO TO 26
   25    SOL(KS,NLC)=SOL(KS,NLC)/AK(KSE,1)
   26 DO 45 I=1,NRS
         N=KS-I
         M=N-1
         MR=MINO(NB,KS-M)
         NCE=ICORE(N)
      IF(NODCON(N).NE.0)GO TO 41
      DO 40 K=2,MR
         L=M+K
      DO 40 LC=1,NLC
   40    SOL(N,LC)=SOL(N,LC)-AK(NCE,K)*SOL(L,LC)
   41 IF(NCE.NE.1)GO TO 45
      IF(N.EQ.1)GO TO 45
         NRAD=N-NEQCOR
      READ(1'NRAD)((AK(IR,JR),JR=1,NBMAX),IR=1,NEQCOR)
   45 CONTINUE
      WRITE(6'1)((SOL(I,J),I=1,KSMAX),J=1,NLC)
      RETURN
      END



      SUBROUTINE RM4OUT
      DIMENSION SOL(1000),DISP(8),STR(3,8)
      COMMON NJ,NM,NS,NCD,NPD,NL,NLC,KS,NB,KSMAX,NBMAX,NEQCOR,TW,TH
      COMMON/ONE/NX,NY,APLOD(1000) ,AJ(500,2),JNUM(450,4),NODCON(1000)
      COMMON/TWO/E1,E2,POIS1,POIS2,SKE(8,8),NOD1(50)
      COMMON/FOUR/MOD1(40),MOD2(40),E3,POIS3,NZE,NBE
      COMMON/FILE/MSTIF,LOSOL
      COMMON/SIX/JNL,LCL,STRSF(3,450),MC(200),EE(450),STRES(3,450),
     1STREC(3,450),PSTR(2,450),ANG(450),JCJ
      READ(6'1)(SOL(I),I=1,KS)
      DO 501 I=1,KS
      IF(NODCON(I).EQ.2)SOL(I)=APLOD(I)
         NOD=-NODCON(I)
      IF(NOD.GT.0) SOL(I)=SOL(NOD)
  501 CONTINUE
C     PRINT HEADINGS
      WRITE(3,500)
  500 FORMAT(///20X,'TABLE OF STRESSES AT ELEMENT CENTROIDS - MPA',//)
C     CALCULATE STRESSES AT ELEMENT CENTROIDS
      DO 810 J=1,NM
      DO 810 I=1,2
      ANG(J)=0.0
  810 PSTR(I,J)=0.0
      JCJ=0
      XINT=0.0
      YINT=0.0
      DO 530 NN=1,NM
      DO 510 I=1,3
      STRES(I,NN)=0.0
  510 STREC(I,NN)=0.0
      J1=JNUM(NN,1)
      J2=JNUM(NN,2)
      J3=JNUM(NN,3)
      J4=JNUM(NN,4)
      E=EE(NN)
      DO 520 I=1,NBE
      IF(NN.NE.(MOD1(I)))GO TO 520
C     BEAM ELEMENT
      POIS=POIS1
      GO TO 525
  520 CONTINUE
      DO 521 I=1,NZE
      IF (NN.NE.(MOD2(I)))GO TO 521
C     ELEMENT IN THE OPENING
      POIS =POIS3
      GO TO 525
  521 CONTINUE
C     BRICK ELEMENT
      POIS=POIS2
  525 CONTINUE
         TXINT=AJ(J2,1)-AJ(J1,1)
         TYINT=AJ(J3,2)-AJ(J1,2)
         XINT=TXINT
         YINT=TYINT
      CALL ELSTRS(XINT,YINT,POIS,STR,E)
  515 N=(J1-1)*2+1
      M=(J2-1)*2+1
      K=(J3-1)*2+1
      L=(J4-1)*2+1
      DISP(1)=SOL(N)
      DISP(2)=SOL(N+1)
      DISP(3)=SOL(M)
      DISP(4)=SOL(M+1)
      DISP(5)=SOL(K)
      DISP(6)=SOL(K+1)
      DISP(7)=SOL(L)
```

```
      DISP(8)=SOL(L+1)
      DO 511 J=1,3
      DO 511 IK=1,8
  511 STRES(J,NN)=STRES(J,NN)+STR(J,IK)*DISP(IK)
      DO 512 J=1,3
  512 STREC(J,NN)=STRSF(J,NN)+STRES(J,NN)
      CALL PRSTRS(STREC,PSTR,ANG,NN)
  530 CONTINUE
      CALL CRACK(PSTR,ANG,NM,MC,EE,JCJ,STRSF)
      IF(JCJ.EQ.0)GO TO 600
C     OUT PUT STRESSES BEFORE INSERTION OF CRACK
      WRITE(3,531)
  531 FORMAT(//20X,'ELEMENT STRESSES BEFORE NEW CRACKS-UNITS-MPA')
      WRITE(3,532)LCL
  532 FORMAT(/20X,'LOAD INCREMENT =',2X,I2)
      WRITE(3,541)
  541 FORMAT(//2X,'ELEMENT',3X,'STRESS-X',3X,'STRESS-Y',3X,'SHEAR
     1STRESS',3X,'PRI-STRESS-1',3X,'PRI-STRESS-2',3X,'ANG',/)
      DO 543 I=1,NM
      WRITE(3,542)I,STREC(1,I),STREC(2,I),STREC(3,I),PSTR(1,I),PSTR(2,I)
     1,ANG(I)
  542 FORMAT(5X,I3,4X,F8.3,3X,F8.3,6X,F8.3,4X,F8.3,7X,F8.3,7X,F6.2)
  543 CONTINUE
      GO TO 601
  600 CONTINUE
C     OUTPUT FINAL STRESSES FOR INCREMENT
      DO 602 I=1,NM
      DO 602 J=1,3
  602 STRSF(J,I)=STREC(J,I)
      WRITE(3,546)
  546 FORMAT(/10X,'FINAL STRESSES FOR LOAD INCREMENT')
      WRITE(3,547)LCL
  547 FORMAT(/10X,'LOAD INCREMENT =2X,I2)
      WRITE(3,548)
  548 FORMAT(//2X,'ELEMENT',3X,'STRESS-X',3X,'STRESS-Y',3X,'SHEAR
     1STRESS',3X,'PRI-STRESS-1',3X,'PRI-STRESS-2',3X,'ANG',/)
      DO 545 I=1,NM
      WRITE(3,544)I,STRSF(1,I),STRSF(2,I),STRSF(3,I),PSTR(1,I),
     1PSTR(2,I),ANG(I)
  544 FORMAT(5X,I3,4X,F8.3,3X,F8.3,6X,F8.3,4X,F8.3,7X,F8.3,7X,F6.2)
  545 CONTINUE
  601 RETURN
      END



      SUBROUTINE ELSTRS(XINT,YINT,POIS,STR,E)
      DIMENSION STR(3,8)
      DO 300 I=1,3
      DO 300 J=1,8
  300 STR(I,J)=0.0
      A=XINT/2.
      B=YINT/2.
      PX=(1.-POIS)/2.
      STR(1,1)=-B
      STR(1,5)=-B
      STR(1,3)=B
      STR(1,7)=B
      STR(2,2)=-A
      STR(2,4)=-A
      STR(2,6)=A
      STR(2,8)=A
      STR(1,2)=-POIS*A
      STR(1,4)=-POIS*A
      STR(1,6)=POIS*A
      STR(1,8)=POIS*A
      STR(2,1)=-POIS*B
      STR(2,5)=-POIS*B
      STR(2,3)=POIS*B
      STR(2,7)=POIS*B
      STR(3,1)=-PX*A
      STR(3,3)=-PX*A
      STR(3,5)=PX*A
      STR(3,7)=PX*A
      STR(3,2)=-PX*B
      STR(3,6)=-PX*B
      STR(3,4)=PX*B
      STR(3,8)=PX*B
      CONS=E/(XINT*YINT*(1.-POIS*POIS))
      DO 316 I=1,3
      DO 316 J=1,8
  316 STR(I,J)=STR(I,J)*CONS
      RETURN
      END



      SUBROUTINE  PRSTRS(STREC,PSTR,ANG,NN)
      DIMENSION STREC(3,450),PSTR(2,450),ANG(450)
      STRX=STREC(1,NN)
      STRY=STREC(2,NN)
      SHST=STREC(3,NN)
      R=STRX-STRY
      RR=SQRT(R*R+(4.*SHST*SHST))/2.
      W=(STRX+STRY)/2.
      PSTR(1,NN)=W+RR
      PSTR(2,NN)=W-RR
      TANA=(PSTR(1,NN)-STRX)/SHST
      TANB=ABS(TANA)
      ANGA=ATAN(TANB)
      ANGD=ABS(ANGA*57.29)
      ANG(NN)=ANGD
```

```
      RETURN
      END


      SUBROUTINE CRACK(PSTR,ANG,NM,MC,EE,JCJ,STRSF)
      DIMENSION PSTR(2,450),ANG(450),MC(200),EE(450),STRSF(3,450)
      JCJ=0
      KN=0
      DO 51 I=1,200
   51 MC(I)=0
C     CHECK FOR PREVIOUS CRACK
      DO 900 NN=1,NM
      IF(EE(NN).LT.0.001)GO TO 70
      IF(PSTR(1,NN).LT.0.0)GO TO 900
      ANG1=ANG(NN)
      X=90.0
      IF(ANG1.GT.X)GO TO 900
      FTTHE=PSTR(1,NN)
      FTTH=ABS(FTTHE)
      FC=PSTR(2,NN)
      FCC=ABS(FC)
      Y=67.5
      IF(ANG1.GT.Y)GO TO 50
      A=0.7*EXP(-0.14*FCC)
       B=1.34*7.*ANG1/(22.*57.29)+0.02
      FT=A-B
      FTT=ABS(FT)
      GO TO 60
   50 FTT=.1
   60 IF(FTTH.LT.FTT)GO TO 900
      JCJ=1
      DO 71 I=1,3
   71 STRSF(I,NN)=0.0
   70 CONTINUE
      KN=KN+1
      MC(KN)=NN
  900 CONTINUE
      WRITE(3,61)(MC(I),I=1,200)
   61 FORMAT(//15X,'ELEMENT CRACKED',/,2X,40I3,/,2X,40I3)
      RETURN
      END
```

INPUT DATA FORMAT FOR THE COMPUTER PROGRAMME

Input Data		
1	NX,NY,NL,NLC,NS,NCD,NPD,TW,TH	7I3,2F7.1
2	XCRD(I), I = 1, NX	10F8.1
3	YCRD(I), I = 1, NY	10F8.1
4	JNL	I3
5	NODE, IX, IY	I5,3X,2I2
6	E1,E2,POIS1,POIS2,T1,T2,E3,POIS3,NZE,NBE	8F8.0,2I4
7	NODI(I), I = 1, NX1 [NX1 = 2*(NX-1)]	20I4
8	MOD1(I), I = 1, NBE	20I4
9	MOD2(I), I = 1, NZE	20I4
10	AF	F8.1
11	NODE, XF, YF	I3,1x,2F10.0